THE IDENTIFICATION OF A NEW MOLECULAR TOOL TO INVESTIGATE THE ROLE OF ACTIN AND MICROTUBULE CYTOSKELETONS IN THE ENDOCYTOSIS PATHWAY OF THE PATHOGENIC FUNGUS *USTILAGO MAYDIS*

Submitted by Natalie Clark
to the University of Exeter as a thesis for the degree of
Doctor of Philosophy in Biological Sciences
In May 2014

I certify that all material in this thesis which is not my own work has been identified and that no material has previously been submitted and approved for the award of a degree by this or any other University.

Signature: ……..

Natalie Clark

TABLE OF CONTENTS

ABSTRACT

Endocytosis is essential for the pathogenic development of *Ustilago maydis*. It has been shown that the initiation of pathogenicity relies upon the ability of the cell to recognize pheromone (a1 or a2) released from its mating partner and subsequently to form conjugated hyphae. The actin and microtubule cytoskeleton plays an essential role in all aspects of cell growth. A component of the actin cytoskeleton, the filamentous actin is required for cell-cell fusion, whereas the molecular motors, kinesin and dynein, move along microtubules and provide the long distance transport of many proteins and they are important in cell growth and pathogenicity.

In this thesis, we investigated the role of the cytoskeleton in endocytosis and a1 pheromone transport, using a fluorescently labelled derivative of the a1 pheromone. We confirmed that uptake of the a1 pheromone is also receptor-mediated. In addition, we have shown that pheromone transport towards the cellular vacuole requires the actin and microtubule cytoskeletons. Furthermore, we revealed that the microtubule-dependent motors kinesin-1 and kinesin-3 and dynein were shown to be essential in the delivery of the pheromone to vacuoles. Moreover, a mutation in the early endosomal protein Yup1 gene causes a stop in delivery of the synthetic pheromone to the vacuole. This suggests that it travels with early endosomes. Within the actin cytoskeleton, we analysed the dynamics of actin patches in the presence of the synthetic pheromone and found that the dynamics of the patches increased significantly. Additionally, in the presence of an over-expression of the tail domain of the molecular motor myosin-5, the dynamics of the patches were significantly reduced and their intensity diminished.

ACKNOWLEDGEMENTS

First and foremost, I would like to thank my two supervisors Dr Mark Wood and Professor Gero Steinberg for their encouragement, supervision and patience throughout my time as a research student. I also wish to express my gratitude to the BBSRC for funding this research project, without which, this thesis would not have been possible.

In addition, I would like to thank all members of Lab 211 past and present, for their assistance, support and friendship; notably I owe thanks to Dr Martin Schuster for his assistance with microscope techniques and Dr Ewa Bielska for her endless protocol knowledge and problem solving abilities.

I would like to give an enormous thanks to Yvonne for helping to proof read this thesis, as well as, her invaluable friendship and guidance throughout my time as a research student. Furthermore, I owe huge thanks to Charli and all members of the Residence Life Team, particularly Owen, Lottie and Steph for their pastoral care giving abilities, friendship and thesis distraction. It was the laughter and chocolate that got me through.

Finally, I wish to thank my parents, Alan and Sandra, my step parents Colin and Georgina and brother Gareth for their endless love and support as well as, gratefully received food parcels and motivational phone conversations during experimental work and thesis writing. I am also indebted to my boyfriend Mark for his friendship, love and for being patient with me during the tough periods throughout writing up my thesis.

LIST OF TABLES AND FIGURES

The author wishes to acknowledge the following for permission to reproduce copyright material in this thesis:

Figure 1.1. The endocytic pathway in yeast.
Publisher: Nature
Author: Professor Lemmon

Figure 1.2. Receptor-mediated endocytosis (RME).
Publisher: Nature
Author: Professor Ravichandran

Figure 1.3. The growth cycle of *U. maydis*.
Publisher: Nature

Figure 1.4. Developmental stages of *U. maydis.*
Publisher: Nature

Figure 1.6. Patch formation in filamentous fungi.
Publisher: Nature

Figure 1.7. Formation of microtubules.
Publisher: Nature

Figure 1.8. Bi-directional early endosome transport.
Publisher: Nature

Every effort has been made to trace rights holders, but if any have been inadvertently overlooked, the author would be pleased to make the necessary arrangements at the first opportunity.

ABBREVIATIONS

α - factor	alpha factor
aa	amino acid
ABP	actin-binding proteins
Ahx	6-aminohexanoic acid
ATP	adenosine 5’ triphosphate
a.u.	arbitrary unit
BAR	Bin-amphiphysin-Rvs proteins
bleR	phleomycin-resistance-cassette
bp	base pair(s)
cbx-locus	gene locus of the iron-sulphur subunit of the succinate dehydrogenase from *U. maydis*
cbxR	carboxin-resistance-cassette
CM	complete medium
crg - promoter	conditional arabinose induced promoter
C-terminal/ C-term	carboxy-terminal
DNA	desoxyribonucleic acid
dNTP	desoxynucleotides
Δ	deletion
EE	early endosome(s)
eGFP	enhanced green fluorescent protein
EGFR	epidermal growth factor receptor
ER	endoplasmic reticulum
5-FAM	5-carboxyfluorescein
GFP	green fluorescent protein
eGFP	enhanced green fluorescent protein
GPCR	G-protein coupled receptors
h	hour
hygR	hygromycin-resistance-cassette
KIF	kinesin superfamily proteins
kin-1	kinesin-1
kin-3	kinesin-3
LE	late endosomes

min	minute
ml	millilitre
mm	millimetre
LDLR	low-density lipoprotein receptor
ms	millisecond
MT	microtubule
MTOC	microtubule-organizing centers
N	sample size
natR	nourseothricin-resistance-cassette
nm	nanometre
N-terminal/N-term	amino-terminal
Pnar	conditional nitrate reductase promoter
ORF	open reading frame
PCR	polymerase chain reaction
P*crg*	promoter of the arabinase gene from *U. maydis*
rab5a	small endosomal Rab5-like GTPase
REM	receptor-mediated endocytosis
rpm	rounds per minute
RT	room temperature
ROX	5- carboxy-X-rhodamine
s	second
SEM	standard error of the mean
SNARE	soluble *NSF* attachment protein receptor
SPK	spitzenkörper
Tub1	α-tubulin from *U. maydis*
TS	temperature-sensitive allele
U	unit
µl	microlitre
µm	micrometre
µM	micromolar
wt	wild-type
WASP	Wiskott-Aldrich syndrome protein

CHAPTER 1 - INTRODUCTION

1.1. Endocytosis

Cells need to communicate with external stimuli in their surrounding environments in order to ensure cellular growth and multiplication. One of the cellular processes involved is endocytosis, which allows the eukaryotic cell to internalize extra-cellular compounds and recycle plasma membrane components and receptor-associated ligands (Goldstein et al., 1979, Doherty and McMahon, 2009). It provides a means to maintain plasma membrane balance by the recovery of protein and lipid components, which have been inserted into the plasma membrane by secretion (Hubbard, 1989). Furthermore, endocytosis also functions in activities involving the transmission of metabolic signals, the uptake of nutrients and the interaction of the cell with the surrounding environment (Mellman, 1996). The uptake of material into the cell was first visualised in the 1960's following the introduction of a cell fixation method using glutaraldehyde and analysis using electron microscopy (Roth and Porter, 1964, Rosenbluth and Wissig, 1964). There are a number of mechanisms for endocytosis in mammalian cells to accommodate a range of cargoes and different accessory proteins (Doherty and McMahon, 2009).

Clathrin-mediated endocytosis is known to be used by all eukaryotic cells (McMahon and Boucrot, 2011) and although other mechanisms such as clathrin-independent endocytosis (Mayor and Pagano, 2007), raft-dependant internalisation (Nabi and Le, 2003) and dynamin-independent uptake (Kumari and Mayor, 2008) exist in mammalian cells, they are extensively documented in other organisms (Doherty and McMahon, 2009). The first step of clathrin-mediated endocytosis in mammalian cells is the nucleation of the plasma membrane. This occurs when F-BAR domain only proteins are activated by phosophatidylinositol-4,5-bisphophate rich zones of the plasma membrane and recruit epidermal growth factor receptor (EGFR) protein tyrosine kinase substrate (Eps15) and intersectins such as Hip1R (Henne et al., 2010). This complex labels the site of internalisation and begins to recruit AP2, which leads onto the second step of cargo selection, whereby AP2 binds cargo specific adaptors/receptors, followed by the cargo and clathrin (Traub, 2009).

Clathrin is a heterodexameric coat protein that is thought to drive the curvature of the membrane to form a vesicle or pit (Ford et al., 2002) during both endocytic and secretory pathway events (Ungewickell and Branton, 1981). This, in turn, leads to the third step of coat assembly, whereby clathrin polymerizes to displace the edge of the forming vesicle into a curve or “pit”. As the vesicle matures, the GTPase dynamin is recruited to the neck of the forming vesicle by Bin-amphiphysin-Rvs (BAR) proteins, which are highly conserved protein dimersation domains which self-polymerise to induce vesicle scission (Hinshaw and Schmid, 1995, Warnock et al., 1996). The recruitment of actin *via* *N*-WASP and Arp2/3 proteins aids in the “pit” being internalised whereas auxilin or cyclin G-associated kinase recruit the ATPase heat shock cognate (HSC70) (Schlossman et al., 1984) to disassemble the clathrin coat and produce an endocytic vesicle (Taylor et al., 2011).

Receptors incorporated into the clathrin coated vesicle are specific to molecules being internalised and therefore, rely on this specificity for coordinated cell development (Goldstein et al., 1985). In contrast, fluorescent analysis of endocytic proteins in yeast identified that endocytosis in yeast (summarised in Figure 1.1.), begins with assembling of clathrin, Hip1R (homolog Sla2) and the Eps15 homolog Pan1 at the plasma membrane (Toret and Drubin, 2006). This is followed by the recruitment of WASP/myosin-1, along with yeast homologues of actin capping protein, fimbrin sac6 and Arp2/3 complex which polymerise actin and provide force generation for the invagination of vesicles (Jonsdottir and Li, 2004). Finally, amyphiphysin homologues Rvs161 and Rvs167 are recruited to the plasma membrane, in order to separate the vesicle from the plasma membrane (Breton et al., 2001). Internalised molecules travel to early endosomes (EE), where they are sorted to multiple locations such as the plasma membrane or transported to lysosomes for degradation. In mammalian cells, several groups of proteins are required to confer specificity and regulation during endocytic sorting and membrane trafficking. One of them is the soluble *N*-ethylmaleimide-sensitive factor accessory protein receptors [SNAREs] which plays a crucial role in intracellular membrane fusion (Rothman and Warren, 1994). They are related membrane-anchored proteins that contain a coiled-coil domain, the so-called

"SNARE" motif. This interaction is thought to draw membranes into close contact and initiate membrane fusion (Jahn and Sudhof, 1999).

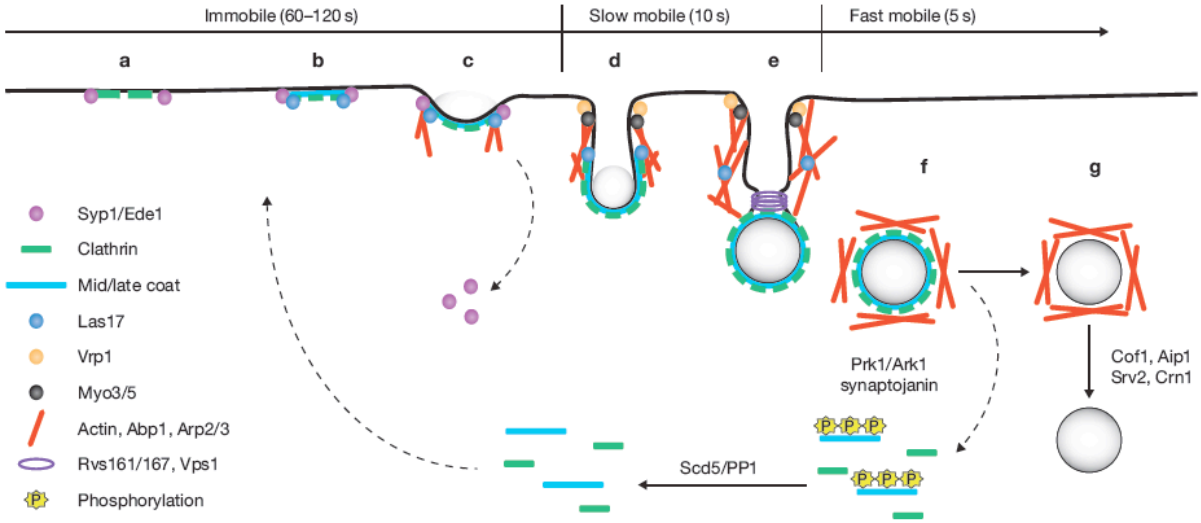

Figure 1.1. The endocytic pathway in yeast.
Early factors including clathrin, Syp1 and Ede1 are recruited during the immobile phase (a). Assembly of mid/late coat proteins including Sla2, Pan1 and Sla1 and Las17 occurred next (b). Before the patch becomes mobile Syp1 and Ede1 depart from the cortex and WASP/myosin/actin are recruited (c, d). Once the extended tubule forms, the vesicles scission apparatus RVS161/RVS167 narrows the neck of the vesicle forming at the invagination tip to promote scission (e). After release from the plasma membrane, the vesicle is uncoated by synaptojanin and Prk1/Ark1 activity (f) and moves rapidly inwards, shedding its actin shell through the action of Cof1, Aip1, Srv2, Crn1 (g). Image taken from (Boettner et al., 2012).

The majority of membrane-traffic components in the endocytic pathway of eukaryotes, recognize the correct organelle by binding to either specific lipids, such as phosphoinositides, or to activated forms of Rab GTPases (Behnia and Munro, 2005). Both lipids and GTPases provide each organelle with a unique identity that will be recognized by many proteins that act on its cytosolic surface, allowing it to be sorted to the correct organelle. Once inside the sorting endosome, the acidic environment causes the ligands to dissociate from their receptors (Mukherjee et al., 1997). Receptors can be directly routed

back to the plasma membrane or delivered to the endocytic-recycling compartment before their return to the plasma membrane (Hopkins, 1983, Yamashiro et al., 1984). Ligands are degraded as the sorting endosomes mature the ligands and a subset of membrane proteins migrate to multi-vesicular bodies and develop into late endosomes (LE) (Katzmann et al., 2002). They are finally converted into lysosomes/vacuoles by fusion with hydrolase-bearing transport vesicles from the *trans*-Golgi network (Geuze et al., 1985, Geuze et al., 1988). It is thought that such a recycling of components is essential to maintain the proper composition of various organelles and for the return of molecules with essential functions at the appropriate compartments (Maxfield and McGraw, 2004).

1.1.1. Receptor-mediated endocytosis

Clathrin-mediated endocytosis can also be referred to as receptor-mediated endocytosis (RME). RME is a process that is relatively similar between animal cells (Geli and Riezman, 1998, Girao et al., 2008) and yeast (reviewed in Geli and Riezman, 1998). The various pathways of receptor-mediated endocytosis share a feature in the recruitment of receptors to coated pits. However, there are differences in the mechanisms that trigger this recruitment as well as differences in the routes which ligands and receptors follow after entering the cell (Hopkins et al., 1985). In *Saccharomyces cerevisiae,* the *trans*-membrane bound G-protein coupled pheromone receptors Ste2 and Ste3 show two different modes of receptor-mediated endocytosis. First, a constitutive uptake, which appears to be ligand-independent and second the ligand-dependent, uptake. It has been shown that constitutive endocytosis is quick and the Ste2 and Ste3 receptors are directly delivered to the vacuole upon internalisation (Davis et al., 1993, Roth and Davis, 1996, Roth et al., 1998, Roth and Davis, 2000). During constitutive receptor endocytosis, the internalisation is triggered by ubiquitin, an internalisation signal that is located on the cell surface (Roth and Davis, 1996, Roth et al., 1998, Roth and Davis, 2000). In comparison, ligand-induced receptor endocytosis occurs after binding of the yeast mating pheromone to its corresponding receptor. An internalisation signal encoded by the receptor, which is specific to its cargo, is exposed after binding and

induces receptor-ligand internalisation (Chen and Davis, 2000). In higher eukaryotic systems, the ligand-induced mode of receptor endocytosis is described. Prominent examples for this mode are the EGFR, the low-density lipoprotein receptor (LDLR) and the transferrin receptor (Mellman, 1996).

Following clustering, the internalisation of components requires the action of a large number of proteins (summarized in D'Hondt et al., 2000). It has been shown that the initial steps of endocytosis are actin-dependent and result in budding of clathrin-coated, and membrane-bound vesicles into the cytoplasm (Kaksonen et al., 2003, Huckaba et al., 2004, Lakadamyali et al., 2006, Toshima et al., 2006a). Subsequently, the vesicles, which contain receptor complexes lose their clathrin coats (Bonifacino and Lippincott-Schwartz, 2003) and become part of the endosomal pathway by fusion with each other and with the early endosomes (EEs) (the process of RME is summarised in Figure 1.2.) In mammalian cells, EEs are known to form a sorting compartment with two populations (Sheff et al., 1999, Lakadamyali et al., 2006). Each has its own distinct mobility and maturation kinetics and they provide links between sorting for degradation and recycling compartments within the cell. However, in yeast, no evidence has been provided to suggest that sub-populations of EEs exist for sorting of cargoes, for degradation or recycling (Prescianotto-Baschong and Riezman, 1998, Mulholland et al., 1999, Pelham and Chang, 2001).

1.1.2. Endocytosis in filamentous fungi

Filamentous fungi are found throughout the world and have been shown to enter into symbiotic relationships with animal as well as plant parasites. They invade host tissues by directed invasive growth of fungal hyphae (Gow et al., 2002). Hyphae expand at their apex which has shown to be similar to that of tip growing plant cells, such as pollen tubes in *Lilium formosanum* (Geitmann and Emons, 2000, Vidali et al., 2001). Fungal filamentous growth is supported by polarised exocytosis at the hyphal tip (Gow et al., 1995), and accumulation of peroxisomes and secretory vesicles. The spitzenkörper which is present at the growth region is thought to consist of secretory vesicles, that aid in hyphal growth (Bartnicki-Garcia et al., 1995). Hyphal tips expand quickly and at rates

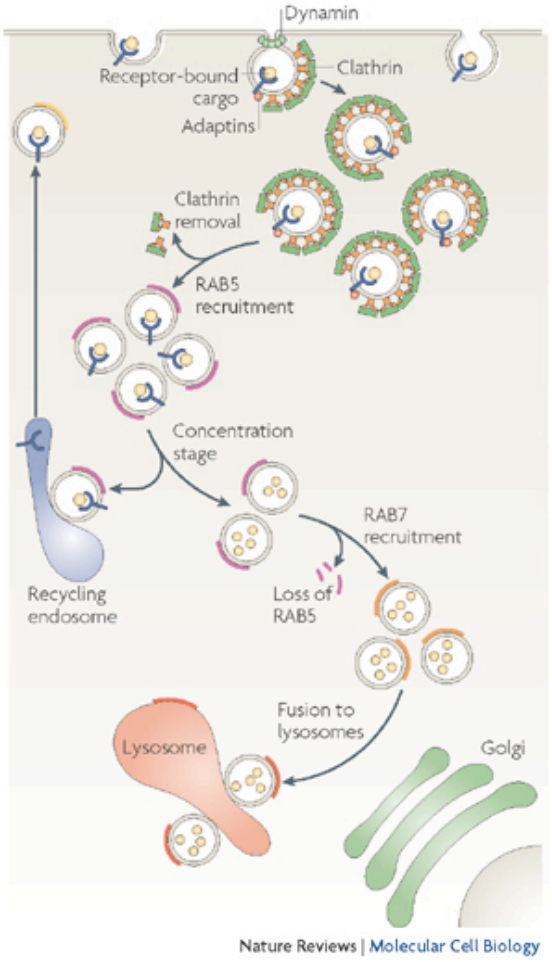

Figure 1.2. Receptor-mediated endocytosis (RME).
The activated receptor is internalised via a clathrin-coated pit. Clathrin is removed from the vesicle after dynamin-mediated scission from the membrane. Receptors are then trafficked to the recycling endosome, where they are eventually sorted back to the cell surface. Endocytosed vesicles acquire the GTPase Rab5, to allow heterotypic fusion with Rab4-positive recycling endosomes. Rab5 is then exchanged for Rab7 through the HOPS (homotypic fusion and vacuole protein sorting) complex, resulting in fusion with acidic lysosomes. Image taken from (Kinchen and Ravichandran, 2008).

which suggest that rapid, polarised growth requires the endocytic uptake and recycling of wall-components, such as synthetic enzymes (Wessels, 1986) and chitin synthases (Lenardon et al., 2010). The first indications for endocytosis in fungi were found in *Uromyces fabae* (Hoffmann and Mendgen,

1998), hyphae of *Neurospora crassa*, *Trichoderma viride* (Read et al., 1998) and *S. cerevisiae* (Chuang and Schekman, 1996) where they saw the uptake of the endocytic marker FM4-64 by germ tubes and in *U. maydis* where uptake was observed in cell wall-less protoplasts (Wedlich-Söldner et al., 2000). Additionally, studies in other fungal species such as *Magnaporthe oryzae*, *N. crassa,* and *Aspergillus nidulans,* have suggested that endocytosis is common in filamentous fungi (Fischer-Parton et al., 2000, Atkinson et al., 2002, Read and Kalkman, 2003, Peñalva, 2005). This was contradicted by ultra-structural and light microscopy techniques applied in *N. crassa*, which did not show any evidence of endocytosis. (Torralba and Heath, 2002). However, the first genomic evidence for endocytosis was provided in *Ustilago maydis,* where conditional mutants of *yup1*, an early endosome marker, showed defective uptake of FM4-64 (Wedlich-Söldner et al., 2000). This was supported by work carried out in *Aspergillus oryzae*, where the internalisation and transport of the eGFP-fused plasma membrane-bound purine transporter *AoUapC* was analysed (Higuchi et al., 2006). Furthermore, the existence of homologous proteins involved in yeast endocytosis, appeared in screens of fungal genomes in *N. crassa* (Read and Kalkman, 2003) and *U. maydis* (Fuchs and Steinberg, 2005) which provided support for endocytosis in filamentous fungi. Studies have also shown a necessity for endocytosis in various cellular processes, including polar growth and indirectly through action of the EEs on pathogenicity (Hoffmann and Mendgen, 1998, Wedlich-Söldner et al., 2000, Atkinson et al., 2002). The presence of homologues suggests a similar endocytic pathway to that in yeast, whereby clathrin-coated pits internalize cellular components with the aid of the actin cytoskeleton; however more detailed analysis in filamentous fungi is yet to be established.

1.2. The model organism *Ustilago maydis*

U. maydis is a dimorphic basidiomycete fungus and is the causative agent of corn smut disease (Christensen, 1963). Its ability to switch from a yeast-like budding to a filamentous hyphal growth (Banuett and Herskowitz, 1994b), is very important for its pathogenicity (Snetselassr et al., 1993, Banuett, 1995).

The yeast-like form (sporidia) is non-pathogenic and haploid, whereas the hyphal form is pathogenic and dikaryotic (Klosterman et al., 2007, Banuett, 1995). The cell cycle of *U. Maydis* is summarised as a whole in Figure 1.3 and starts with growth of haploid sporidia, where two different mating-types exist, namely a and b. The a and b mating-type loci regulate cell fusion, filamentous growth and pathogenicity. Whereas, the a locus (a1 or a2) encodes a mating factor precursor (Mfa1 or Mfa2) as well as the pheromone receptor (Pra1 or Pra2) (Bölker et al., 1992). The b locus two homeodomain proteins (bE and bW) which are required for formation of conjugated hyphae (Kämper et al., 1995) (Figure 1.4. A). Cells respond to the pheromone secreted by cells of opposite mating-type and form conjugation tubes which fuse at their tips, (Snetselassr et al., 1993, Banuett and Herskowitz, 1994b, Spellig et al., 1994) (Summarised in Figure 1.4. B). Upon recognition of two compatible sporidia, a cascade of regulatory events is induced by the pheromone, which leads to a cell cycle arrest in the G2 phase (García-Muse et al., 2003). This in turn, increases expression of the pheromone receptor as well as the pheromone itself. This series of events allows the cell to switch from budding to filamentous growth (Diagrammatically represented in Figure 1.4.C) (Feldbrügge et al., 2004). The fusion of two hyphae is accompanied by the formation of a heterodimeric transcription factor, which is encoded by the *b*-mating-type loci of both cells and creates stable *b*-dependent hyphae (Wahl et al., 2010). These hyphae invade the host plant tissue, where they are able to form tumours and diploid spores. A summary of the developmental stages of *U. maydis* can be seen in Figure 1.5. The spores germinate and form a promycelium, which undergoes meiosis and generates sporidia again (Banuett and Herskowitz, 1996). It has been found that *U. maydis* is able to induce tumours at the stem, leaves and corncobs of the maize plants (Banuett and Herskowitz, 1996). With the life cycle of *U. maydis* in mind, it becomes obvious that cell–cell communication is necessary for pathogenicity and polarised hyphal growth. Pathogenicity is accompanied by a yeast–hyphal transition, similar to other fungal pathogens such as *Candida albicans* and *Histoplasma capsulatu*

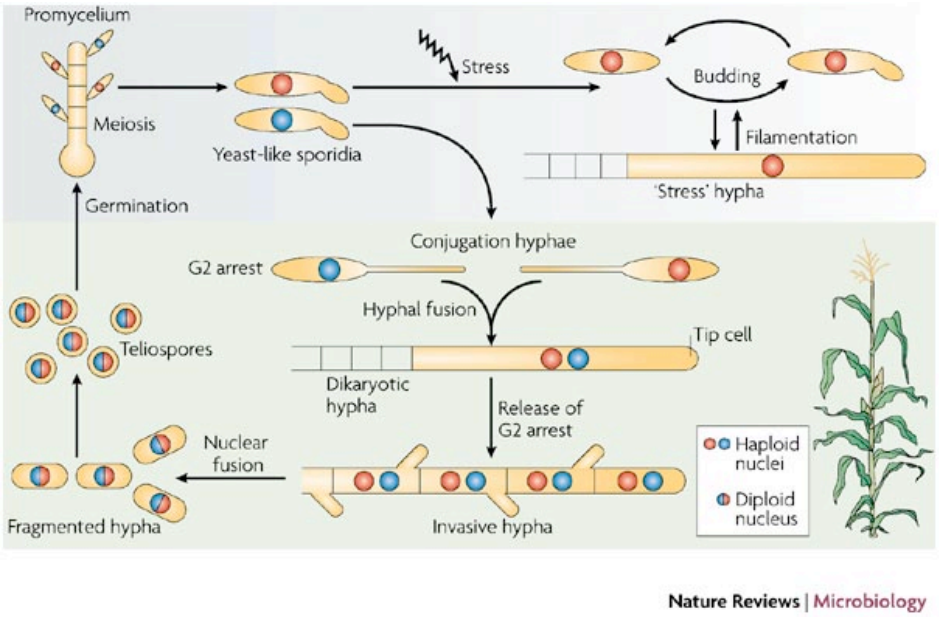

Figure 1.3. The growth cycle of *U. maydis*.

The growth cycle starts with haploid yeast-like sporidia. These cells grow by polar budding and under stress conditions switch to filamentous growth. On the surface of the plant, compatible cells (different colour nuclei), are able to recognize each other by the exchange of pheromone signals and grow towards each other. This leads to the formation of conjugation hyphae that fuse giving rise to dikaryotic hyphae, which invade the plant tissue. Inside the plant, the long hyphae colonizes the plant and induce the formation of large tumours. When proliferation occurs, nuclear fusion causes the hyphae to fall apart and teliospores are formed. Finally these teliospores germinate to form promycelium which after meiosis produces the yeast-like sporidia and the cycle begins again (Image taken from (Steinberg, 2007b).

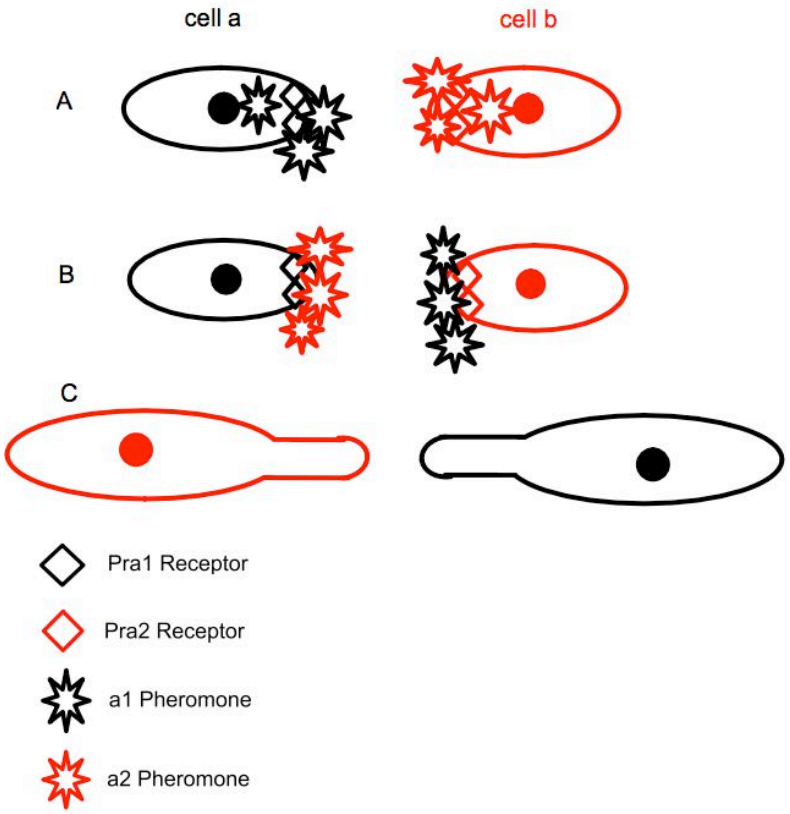

Figure 1.4. Diagrammatical representation of the pheromone signalling in *U.maydis* cells

A) Cell a1 contains the mating precursor Mfa1, the pheromone receptor Pra1 and the pheromone a1 whereas cell a2 contains the mating precursor Mfa2, the pheromone receptor Pra2 and the pheromone a2. The cells release these pheromones in search of ones with the opposite mating type.

B) Once one of the cells encountered the pheromone of its opposing mating type this is taken in by the pheromone receptor and the cells arrest in G2.

C) The arrest in G2 allows the cell to grow in the direction of the pheromone source in search of its opposing mating type, where if the b loci homeodomain proteins are different conjugation hyphae will form and invasion of host plant tissue can occur.

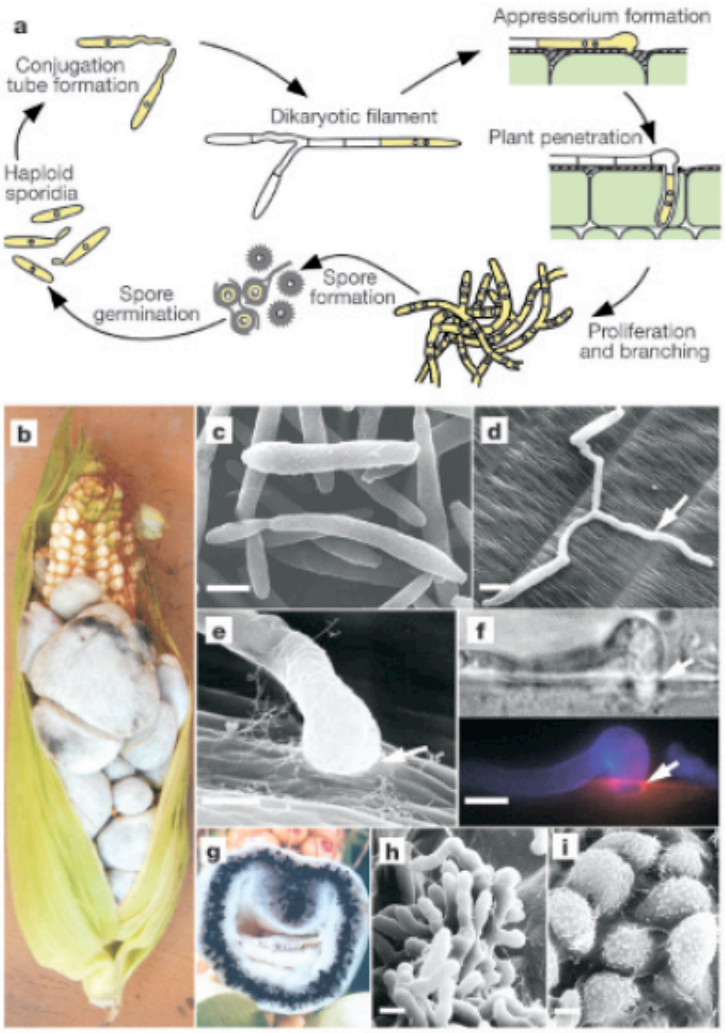

Figure 1.5. Developmental stages of *U. maydis.*

(a) Summary of the life cycle of *U.maydis.* (b) tumour formation on maize. (c) haploid sporidia from a scanning electron microscopy (SEM) image. (d) SEM image of mated sporidia on plant epidermis; arrow denotes dikaryotic filament growth. (e) SEM image of appressorium; arrow marks entry point into plant tissue. (f) DIC image of appressorium (top panel); image of fungal cell wall stained with calcofluor (blue) and endocytotic vesicles stained with FM4-64 (red) (bottom panel). (g) tumour section showing visible black teliospores. (h), SEM image of sporogenous hyphae and early stages of spore development. (i) SEM image of ornamented teliospores. Scale bars, 5 mm. Image taken from (K*ä*mper et al., 2006).

1.2.1. Pheromone structure and function

The importance of pheromones and their receptors for mating initiation was demonstrated in sterile mutants in *S. cerevisiae* (Steden et al., 1989) as well as in filamentous fungi such as *U. maydis* (Bölker et al., 1992) and *Ustilago hordei* (Anderson et al., 1999). In yeast, it has been established that the alpha factor pheromone receptor, encoded by the *STE2* gene is a G-protein-coupled receptor and is required for mating of a and α haploid cell types (Schrick et al., 1997). The α pheromone is secreted and binds to receptors on the surface of haploid cells. The a cells respond to the α-factor by arresting division in the G1 phase and inducing proteins required for mating and fusion. Previous studies using genetic and biochemical approaches in yeast, have indicated that pheromone receptors activate a heterotrimeric GTP-binding regulatory protein which, upon activation, induces a protein cascade that regulates cell division and expression of pheromone-responsive genes (Overton et al., 2005). Sequence elements in the *C*-terminus cytoplasmic domain of the a-factor receptor show that it is essential for both ligand-induced (Roth and Davis, 1996) and constitutive endocytosis (Hopkins et al., 1985), whereas the *C*-terminal domain of the α-factor receptor has been shown only to be necessary for constitutive endocytosis (Davis et al., 1993). In *U. maydis,* two pheromones are known, the tridecapeptide a1 (mfa1) and the nonapeptide a2 (mfa2). Each is different in its structure, summarised in Figure 1.6; the a1 is composed of 13 amino acids whereas a2 is composed of 9 aa. However they are conserved in their farnesylated *C*-terminal cysteine residue, which is essential for specific binding to receptor elements (Spellig et al., 1994). Numerous fungi have been shown to have this type of farnesylated *C*-terminus including, *Rhodosporidium toruloides* (Kamiya et al., 1978), *Tremella mesenterica* (Sakagami et al., 1981), *Schizophyllum commune* (Wendland et al., 1995), *U. hordei* (Anderson et al., 1999), and *S. cerevisiae* (Anderegg et al., 1988) and *Schizosaccharomyces pombe* (Davey, 1992). The pheromone receptors in *U. maydis* also belong to the family of seven trans-membrane receptors that are coupled to heterotrimeric G proteins. Additionally, a short DNA sequence, termed the pheromone response element, is found in the vicinity of all pheromone-inducible genes in *U. maydis* making it both necessary and sufficient for pheromone induction (Urban et al.,

1996a). Previous work suggests the pheromone signal is transmitted by a MAP kinase cascade, whose complete set of components remains to be identified in *U. maydis* (Banuett and Herskowitz, 1994a). The switch from yeast-like to filamentous growth associated with dikaryon formation, requires autocrine stimulation of the pheromone response pathway (Bölker et al., 1992, Spellig et al., 1994). The regulation of this pathway and the recycling of the receptor are therefore very important.

a1

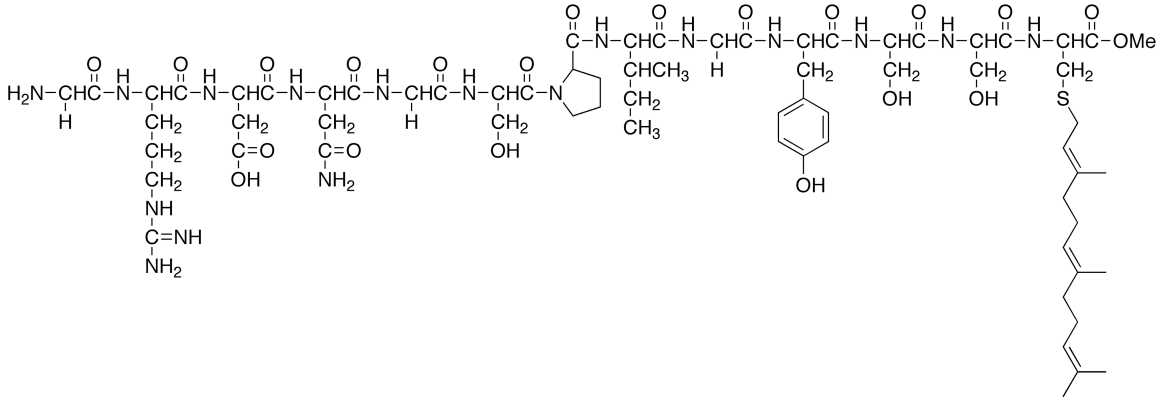

a2

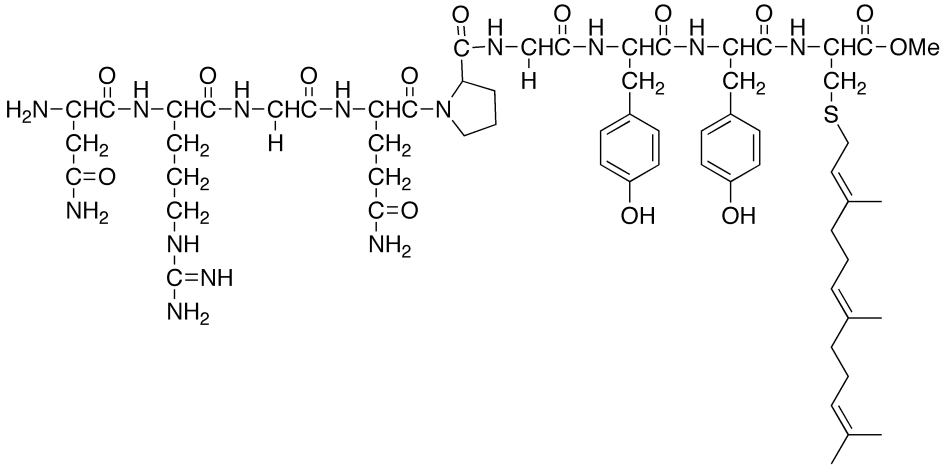

Figure 1.6. *Ustilago maydis* pheromone structure.

Expanded view of the naturally occurring tridecapeptide a1 pheromone consisting of 13 aa's and the a2 nonopeptide consisting of 9 aa's.

1.3. Endocytic receptor recycling

The endocytosis of many signalling receptors is stimulated through ligand binding activation (Lakadamyali et al., 2006). The recycling of these internalised receptors allows multiple rounds of ligand binding and internalisation (Ciechanover et al., 1983, Goldstein et al., 1985). After internalisation, receptors are sorted to recycling endosomes where the low pH leads to dissociation of ligand from receptor. Following disassociation, the presence of certain sequence motifs leads to differential recycling. In mammals, two methods of receptor recycling have been suggested (Li et al., 2012). If the receptor does not bear a cytoplasmic signal for sorting to the late endosomes (LEs), it is directly recycled back to the plasma membrane through coordinated activity of Rab4 and Rab15, Rab14 GTPases (Van Der Sluijs et al., 1991, Van der Sluijs et al., 1992). However, if a signal is detected or the receptor has undergone ubiquitylation, whereby a 76 aa protein called ubitquitin is added, and slower route of recycling occurs, involving the activity of Rab11, Rab15 and Rab22a GTPases (Wilcke et al., 2000). For some receptors, such as the LDLR receptor and the transferrin receptor, the fast route of recycling is always applied (Grant and Donaldson, 2009). However for others such as the EGF receptor, the recycling fate is undetermined with some of the receptors being reused via recycling and some being degraded through transport to lysosomes (Xie et al., 2004). It has been shown that recycling receptors concentrate in specific domains of sorting endosomes, suggesting an interaction of a undetermined sorting signals with an endosome-associated complex (Geuze et al., 1987). In *U. maydis*, the pheromone receptor Pra1 accumulates at the cell membrane in the presence of the a2 pheromone. It has also been shown to co-localize with two Rab GTPases, namely Rab4 and Rab5a, which both have links to the endocytic/recycling pathways (Fuchs and Steinberg, 2005, Fuchs et al., 2006).

1.4. Cytoskeleton

In eukaryotic cells, the transport of vesicles and motility of endosomes along the cytoskeleton is an essential feature of the endocytic pathway. It is

composed of three major components: actin filaments, microtubules (MTs) and intermediate filaments (Gow et al., 1995). In skin melanocytes, the bi-directional MT-dependent transport system provides a way of transporting the melanosomes to the cell periphery, where the acto-myosin system acts to ensure that the mature melanosomes are captured and stay in position to be transferred to keratinocytes. Overall, several models have been proposed to describe the cooperation between MT-based motors and their tracks. Most recently, the 'tug-of-war' model proposes a competition between MT-based motors and myosins (actin-based motors). In *Xenopus*, myosin-V contributes to the dispersion of melanosomes by counteracting the action of dynein, particularly shortening the length of dynein-driven runs, and by ensuring the regular motion of melanosomes towards the MT plus-end (Wollert et al., 2002). This leads to the speculation that the productive association of myosins with organelles might be coordinated with the inactivation of MT motors. In *S. pombe*, the MT cytoskeleton delivers formin For3 to the cellular tip where it assembles actin cables (Martin et al., 2005). Genetic evidence in yeast suggests that the kinesin-related protein, Smy1, stabilizes the protein complex, which is formed by Sec4, and Myo2. In filamentous fungi, the cytoskeleton, co-ordinates hyphal growth through the function of membrane trafficking along MT and/or actin tracks. In *N. crassa* MTs extend into the Spitzenkörper (SPK) (Freitag et al., 2004), a vesicle supply centre, that is essential for targeted secretion of new plasma membrane and cell wall synthesizing enzymes. Whereas, actin localises just to the core of the SPK and also forms a collar of endocytic patches which associate with the plasma membrane (Berepiki et al., 2010). The different distribution of MTs and actin at hyphal tips suggest that the SPK acts as a 'bridge' between the two cytoskeletons i.e. from long distance transport along MTs to short-distance along actin to mediated targeted vesicle delivery to the apical plasma membrane of the hyphal tip (Harris et al., 2005). In *U. maydis*, the interaction of both the actin and microtubule cytoskeleton with the SPK, aids in tip growth expansion (Steinberg, 2007a).

1.5. The actin cytoskeleton

Actin is an abundant, highly conserved polymer found in all eukaryotes and occurs in a monomeric and filamentous form. The monomeric form (globular or G-actin), consists of a 43-kDa single polypeptide chain which is formed by two major domains that form a deep cleft and participates in adenosine 5' triphosphate (ATP) binding (Dominguez and Holmes, 2011). Furthermore, the self-assembling of actin is a dynamic process with individual filaments continually growing and shrinking, which is regulated by ATP hydrolysis and an enormous range of actin-binding proteins (ABPs) (Robertson et al., 2009a). This process gives rise to microfilaments (F-actin) with structural polarity. These filaments consist of two parallel filaments with a diameter of 7 nm and a loop repeating every 37 nm (Galletta and Cooper, 2009). In *S. cerevisiae,* actin structures such as patches, cables and rings were first described with the use of fluorescently labelled phalloidin and actin antibodies (Adams and Pringle, 1984, Kilmartin and Adams, 1984). Actin patches and cables were found within growing buds, which suggested a role for both in polarised growth. The discovery of patches, cables and rings in fission yeast was confirmed shortly after (Marks et al., 1986). In fungi, components of the actin cytoskeleton, specifically patches and actin rings, have been visualised using immunofluorescent microscopy in the hyphae of *A. nidulans*, *N. crassa*, and *C. albicans* (Yokoyama et al., 1990, Barja et al., 1991, Torralba et al., 1998b, Suei and Garrill, 2008). Imaging any form of actin in living cells provided a problem for many years. Therefore, in order to generate a suitable fluorescently labelled probe, Abp140 of *S. cerevisiae* was truncated to a 17 aa peptide (called lifeact) and fused to GFP (Riedl et al., 2008). The truncated peptide showed the same staining pattern as the full length Abp140, and was used to image the actin cytoskeleton in yeast (Yang and Pon, 2002). It has been used to visualise actin cytoskeleton dynamics in a range of organisms such as mice, plants, and filamentous fungi (Riedl et al., 2008, Vidali et al., 2009, Berepiki et al., 2010, Delgado-Álvarez et al., 2010, Ueda et al., 2010). In filamentous fungi, the presence of three higher-order F-actin structures has been identified and shown to have distinct cellular roles, localisation patterns, methods of assembly and dynamics (Berepiki et al., 2010, Berepiki et al., 2011).

1.5.1. Actin patches and their dynamics

Actin patches are accumulations of F-actin, which interact with over 60 different proteins to mediate endocytosis in yeast (Kübler and Riezman, 1993, Mulholland et al., 1994, Munn et al., 1995, Robertson et al., 2009b). They have been assigned a role as a marker of the sites of endocytosis (Harris et al., 1994, Torralba et al., 1998a, Pruyne et al., 1998, Huckaba et al., 2004, Ayscough, 2005). Their formation is initiated by the accumulation of clathrin and endocytic adaptor proteins like Ede1, Eps15/Pan1, Sla1 and Sla2 at the plasma membrane which, in turn, triggers the recruitment of the Arp2/3 complex to this site (Kaksonen et al., 2003, Kaksonen et al., 2005). Activation of this complex by the Wiskott-Aldrich syndrome protein (WASP), Las17 (Li, 1997, Madania et al., 1999), and class I myosin-1 (Jonsdottir and Li, 2004, Sun et al., 2006) stimulates actin assembly within patches to generate an F-actin network which is cross-linked by fimbrin (Kaksonen et al., 2005). In order to sever away from the plasma membrane and provide force to invaginate endocytic vesicles, amphiphysin BAR proteins and myosin-I motor activity has been suggested (Ayscough et al., 1997, Ayscough, 2000, Jonsdottir and Li, 2004, Sun et al., 2006, Aghamohammadzadh and Ayscough, 2009, Robertson et al., 2009a). The components of patches and the details of their assembly in filamentous fungi, are thought to be similar to those found in *S. cerevisiae*, based on the high degree of ABP conservation between *S. cerevisiae*, *N. crassa* and *A. nidulans*. The formation and re-organisation of cortical actin patches are regulated by cortical patch-like protein structures, including the Arp2/3-complex and several of its activators, as well as endocytic adaptors and scaffolds (Pruyne et al., 2002). A summarized version of events is depicted in Figure 1.7. Emphasis on the actin cytoskeleton being required for the internalisation step of endocytosis (Sun et al., 2006) has been strengthened by studies which found that actin binding proteins stabilize actin filaments (Karpova et al., 1998) and without their correct functioning lead to smaller patches. Such as in *sac6* (yeast homolog of fimbrin) mutants in *S. cerevisiae* (Adams et al., 1991, Kübler and Riezman, 1993) and *fimA* (fimbrin mutants) in *A. nidulans* (Upadhyay and Shaw, 2008). Additionally,

endocytosis of the dye FM4-64 is affected in *fimA* mutants. This is consistent with what is found in mutants of *act1-1*, *act1-2* and *sac6* mutants of *S. cerevisiae* (Adams et al., 1991, Kübler and Riezman, 1993). In *U.maydis*, actin patches and cables have been visualised *in vivo* but as yet, nothing is known about their function and whether indeed they are required for endocytosis.

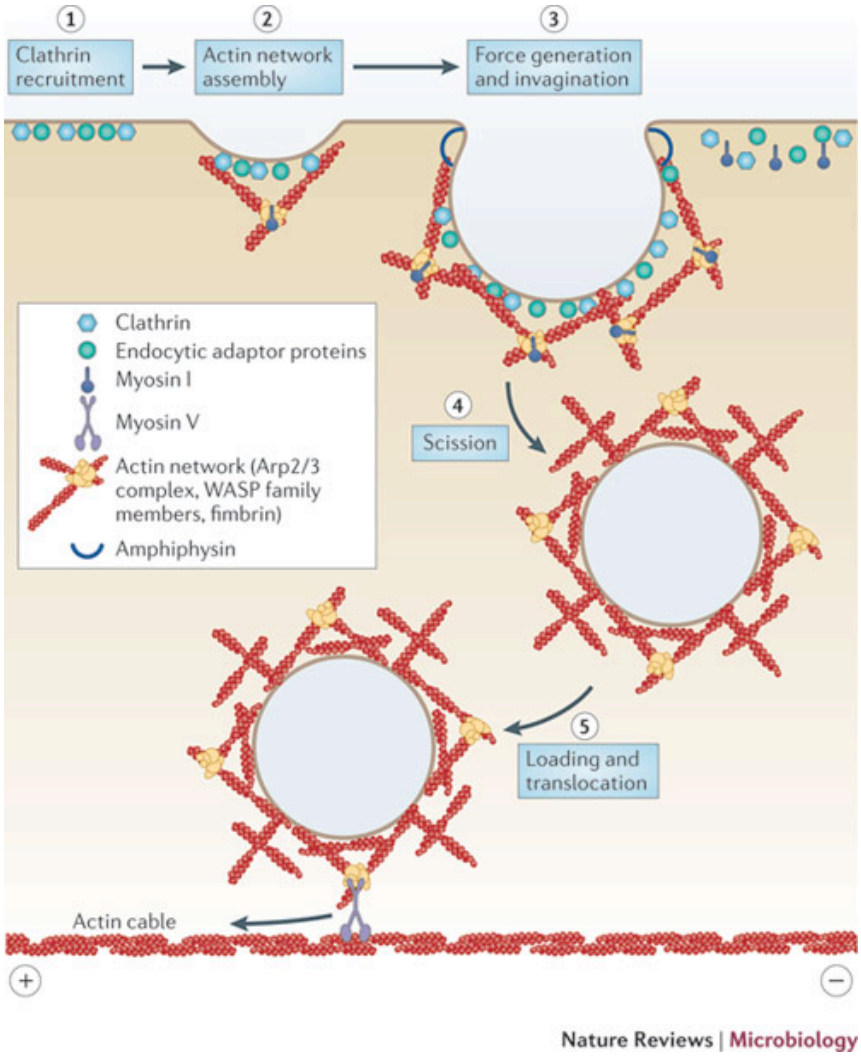

Figure 1.7. Patch formation in filamentous fungi.

(1) clathrin is accumulated at the plasma membrane. (2) Arp2/3-complex, WASP and myosin-1 catalyse the formation of a filamentous-actin network. (3) Continuation of actin assembly through the recruitment of endocytic adaptor proteins such as Sla1 and Sla2 promote the invagination and scission of the endocytic vesicle. (4) This is also promoted by the function of amphiphysin bar proteins alongside myosin-1. (5)

Upon internalisation, the clathrin coated pit loses its coat and is loaded onto actin cables (Image taken from (Berepiki et al., 2011).

1.5.2. Actin cables and their dynamics

Actin cables are long bundles of actin filaments, which contain fimbrin and tropomyosin. These cables are randomly distributed in non-dividing yeast cells and in dividing cells, they originate from polarised sites such as the bud tip and extend throughout the mother cell along the cellular axis from late G1 to M phase (Evangelista et al., 2002, Moseley and Goode, 2006). The first visualization of actin cables was in *S. cerevisiae* cells, using an Abp140-GFP fusion construct (Heath, 2000). The assembly of actin cables occurs first in the bud, where cables are polarising along the mother-bud axis and through a process of assembly and elongation, cables undergo retrograde flow into the mother cell (Chesarone et al., 2010). Studies with tropomyosin mutants (a protein known to stabilise cables; (Liu and Bretscher, 1989), show a loss of actin cables and implicate actin cables in polarised growth and polarised localisation of actin patches, secretory vesicles, and the mitotic spindle (Pruyne et al., 1998). Furthermore, mutations in Sac6 lead to defects in internalisation of alpha factor receptor suggesting it is also responsible for the stabilization and organisation of cables (Kübler and Riezman, 1993). In *N. crassa* germlings, long actin cables between 5-10 µm have been observed and suggest a role for actin cables in organelle/vesicle transport (Berepiki et al., 2010). Surprisingly, cargoes of actin cables, like secretory vesicles and chitin synthases, differ between species. In *A. nidulans,* transport of secretory vesicles is actin dependant whereas in *N. crassa,* it is transported via MTs (Fuchs et al., 2002, Suelmann and Fischer, 2000).

1.5.3. Actin rings

Cytokinesis in many eukaryotes requires a contractile ring of actin and myosin, which is formed between two daughter cells and cleaves the cell in two separated cells (Pollard and Wu, 2010). In *S. cerevisiae*, myosin-1 a class

II myosin, forms a ring at a bud site shortly before bud emergence. It remains until the end of anaphase, when a ring of F-actin is formed around it and the acto-myosin ring contracts. After ring contraction, actin patches congregate in the growth region and septum formation, as well as, cell separation follows quickly. In fungi the most likely explanation of actin cable condensation into rings is the search, capture, pull, and release mechanism found in studies of *S. pombe* (Lord et al., 2005, Vavylonis et al., 2008, Wu and Pollard, 2005). In addition, class-II myosins localise to the acto-myosin ring in both *N. crassa* and *A. nidulans* (Calvert et al., 2011, Taheri-Talesh et al., 2008).

1.5.4. Myosin motors and the actin cytoskeleton

Myosins are molecular motors that are found in almost all eukaryotes and grouped into 35 classes. Four classes of myosins (I, II, V and VI) have been implicated in the dynamics of a large variety of organelles such as endoplasmic reticulum, recycling endosomes, lysosomes, secretory granules and melanosomes in mammalian cells (Warrick and Spudich, 1987, Hammer and Wagner, 2013, Korobova et al., 2014, Calvert et al., 2011) as well as secretory vesicles, vacuoles, Golgi, endoplasmic reticulum and mitochondria in yeast (Win et al., 2001, Yasushi, 2003, Geli and Riezman, 1996, Hill et al., 1996). They are dimers, which share a common structure comprising of three domains, motor head, neck region and tail domain. The motor head, is thought to comprise the motor domain, which hydrolyses ATP to induce movement along actin filaments (Wu et al., 2000). The neck region binds regulatory light chains such as calmodulin and finally the tail region, a specific domain that is different among the classes of myosins, acts to bind to cargos. Evidence has shown that although the domain structure of different myosins is similar, their regulation of kinetics in association with ATP can differ (Lodish et al., 2000). Some move along actin filaments without dissociating from the tracks whereas others induce tension between actin filaments causing them to fall off the actin track along with their cargoes (Seabra and Coudrier, 2004). They are implied in various functions and the differences in the tail domains of myosins were thought to contain crucial information to target myosins to different cellular compartments. In mammalian cells, studies in mice alluded to

an essential role in the tail region of myosin-5 in binding melanophilin in skin melanocytes (Barral and Seabra, 2004). It has also been suggested for a role in capturing melansomes alongside cortical actin (Wu et al., 1998). The mammalian genome encodes three myosin-5 related genes, myosin 5a, myosin 5b and myosin 5c (Berg et al., 2001), which have been implicated in transport of melanosomes, plasma membrane recycling trafficking and regulating of the cellular distribution of endocytic compartments respectively (Wu et al., 1997, Lapierre et al., 2001, Rodriguez and Cheney, 2002).

Myosin-5 may be ideally suited for organelle transport, as it is an efficient, processive motor which works in 37 nm steps and corresponds to the structure of the actin filament (Mehta et al., 1999). Indeed, several class-V myosins have been shown to be involved in organelle trafficking (Desnos et al., 2007). Furthermore, myosin-5 driven motility of an organelle is differentially controlled during the cell cycle, as shown for the endoplasmic reticulum in Xenopus egg extracts (Wollert et al., 2002). Another well established myosin in mammalian cells are class-II myosins. They have been shown to be essential for muscle contraction and particularly, cytokinesis (Satterwhite and Pollard, 1992, Fishkind and Wang, 1995), where they are involved in constriction of the contractile ring (Mabuchi and Okuno, 1977, Bezanilla and Pollard, 2000). In mammalian systems, myosin-XI has been broadly implicated in endocytosis events and the presence of a 53 aa insert, proximal to the motor domain, allows it to travel towards the minus ends of actin filaments (Wells et al., 1999, Park et al., 2007). Whereas, class-I myosins have been shown to have a role in endocytosis and actin organisation in *S. cerevisiae* (Geli and Riezman, 1996), in particular, roles have been identified in the assembling of actin patches (Lee et al., 2000) and scission of endocytic vesicles (Jonsdottir and Li, 2004). Other notable examples in yeast include class-V myosins, where one of two class-V myosins, Myo2, delivers various organelles to the bud tip during cell division (Pruyne et al., 1998, Wagner and Hammer, 2003, Rossanese et al., 2001, Itoh et al., 2002, Hill et al., 1996), suggesting a role in polar growth during budding (Johnston et al., 1991). In filamentous fungi, the class-I myosin homologues in *C. albicans* are essential during hypha formation (Oberholzer et al., 2002) and in *A. nidulans,* MYOA was essential in polar growth and secretion (McGoldrick

et al., 1995, Osherov et al., 1998). This suggests a role in exo- and endocytosis as shown in yeast. In *N. crassa,* cells were found to divide using an acto-myosin ring and depletion of myosin-2 leads to lower rate of ring constriction (Calvert et al., 2011). In *U. maydis*, class-V myosin Myo5 does not appear to be essential but is needed for normal cell separation, mating, hyphal growth and pathogenicity (Weber et al., 2003). Similarly, in *C. albicans* and *A. nidulans*, class-V myosins are not essential for cellular viability but are required for correct polarisation of the actin cytoskeleton, efficient secretion and normal hyphal growth (Taheri-Talesh et al., 2008, Woo et al., 2003, Zhang et al., 2011). The available experimental evidence suggests that there is great complexity in myosin-driven organelle dynamics. The same class-V myosin isoform can transport multiple organelles, all with unique destinations. Therefore, the interaction of myosin with organelles needs to be further researched and understood.

1.6. The microtubule cytoskeleton

Long-range organelle transport via microtubules organizes eukaryotic cells and enables communication over large distances (Gross, 2004, Welte, 2004) The MTs are hollow cylinders consisting of 13 to 16 protofilaments, composed of α- and β-tubulin dimmers (Job et al., 2003). *In vivo*, MT formation (summarised in Figure 1.8.) usually begins at microtubule-organizing centers (MTOCs). The MTOCs contain a third MT subunit, the γ–tubulin (Oakley and Oakley, 1989, Oakley, 2000), which is thought to be involved in recruitment of tubulin dimers for MT nucleation (Job et al., 2003, Oakley, 2004). The polymer is elongated by polymerisation of tubulin subunits at the plus end, where β-tubulin is exposed at their plus-end; the opposite MT minus end remains in contact with the MTOC. In mammalian cells, studies have shown that MT's can switch from elongation to rapid disassembly, termed dynamic instability (Carminati and Stearns, 1997, Drummond and Cross, 2000, Steinberg et al., 2001, Finley and Berman, 2005). Microtubule assembly and dynamics are regulated by microtubule assembly-promoting factors, microtubule stabilizing factors (such as structural or classical microtubule-associated proteins

(MAPs)), microtubule destabilizing factors, microtubule severing proteins and microtubule-based motors of the kinesin and dynein superfamilies. (Howard and Hyman, 2007). Treatment of the cytoskeleton with MT depolymerizing agents (e.g., nocodazole) slows defects in adsorptive and fluid-phase endocytosis, suggesting that receptor-mediated endocytosis could be affected (Pratten and Lloyd, 1979, Piasek and Thyberg, 1980, Gekle et al., 1997). In fungi, MTs are found to grow with their plus ends towards the cell tip in order to facilitate organelle transport to this site. MTs are important for a wide range of cellular processes such as maintaining the polarization of fungal hyphae, forming the apical SPK and are required for directed transport of membranous organelles and vesicles to the hyphal tip (Gow et al., 1995). Molecular motors drive long-range intracellular movement or trafficking within cells, an example of which, being kinesin motors. They are known to move cargoes towards MT plus-ends, but they can also modify MT dynamics, leading to organisation of the cellular MT (Konzack et al., 2005, Wu et al., 2006, Steinberg, 2007c). Thus, MT motors, and in particular kinesins, participate in a broad spectrum of functions in the fungal cell, including membrane transport, spindle elongation in mitosis and regulation of MT dynamics. Another molecular motor known to utilize MT for transport is the molecular motor dynein. This motor, alongside kinesin, uses ATP-hydrolysis to "walk" along MTs and aid in nuclear migration in *A. nidulans* (Xiang et al., 1994). In mammalian cells, kinesin motors undertake steps towards the plus-end, whereas dynein transports its "cargo" towards the minus-end of the MT (Gross, 2004).

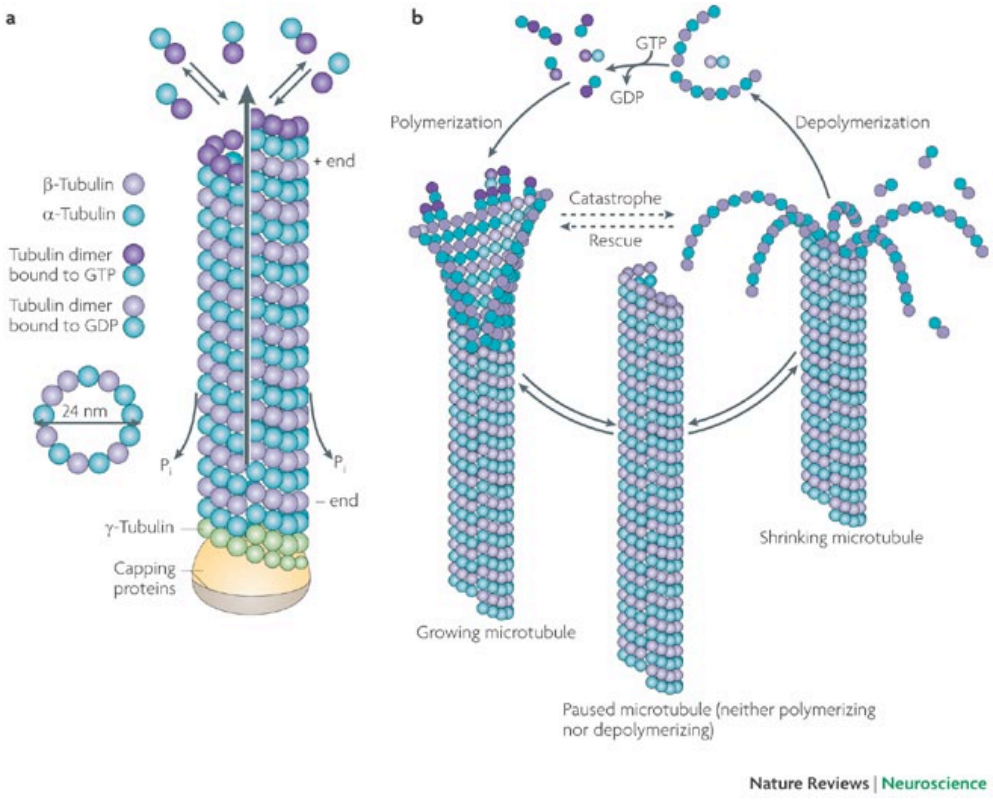

Figure 1.8. Formation of microtubules.

a) Microtubules are composed of alpha- and beta-tubulin subunits assembled into linear protofilaments. A single microtubule contains 10 to 15 protofilaments (13 in mammalian cells) that wind together to form a 24 nm wide hollow cylinder. b) Microtubules are structures that can rapidly grow (*via* polymerization) or shrink (*via* depolymerization) in size, depending on how many tubulin molecules they contain (Image taken from (Conde and Caceres, 2009).

1.6.1. Role of molecular motors

Eukaryotic cells use molecular motors to transport molecules and organelles along cytoskeletal tracks. In mammalian cells, molecular motors known as the kinesin superfamily proteins (KIFs), have been shown to transport organelles, protein complexes and mRNAs to specific destinations along MT whilst hydrolyzing ATP for energy (Hirokawa et al., 1998). KIFs also participate in chromosomal and spindle movements during mitosis and meiosis (Hirokawa, 1998). In eukaryotes, 14 families of kinesin motor proteins are known with various functions but a large number of plus-end-directed kinesins use MTs to support anterograde (tip-directed) transport (Hirokawa and Takemura, 2004).

Kinesin-1, -3 and dynein motor proteins, are often found in a wide range of organisms to provide bidirectional organelle transport (Gross et al., 2002, Muller et al., 2008, Ally et al., 2009, Hendricks et al., 2010). Kinesin-1 proteins, formerly called conventional kinesin, was first identified in animals and considered the founding member of the kinesin superfamily (Brady, 1985, Vale et al., 1985, Scholey et al., 1989). It is known to be involved in organelle and vesicle transport (Hirokawa et al., 1998, Hirokawa, 1998, Wozniak and Allan, 2006, Wozniak et al., 2009). Conventional kinesin and Unc104/Kif1A-like motors (Hall and Hedgecock, 1991, Aizawa et al., 1992), renamed kinesin-3 (Lawrence et al., 2004), are known in mammalian cells for their role in organelle transport (Okada et al., 1995, Yonekawa et al., 1998). The other bi-directional transport motor protein, dynein, is a large complex of polypeptides that mediates intracellular transport towards minus-ends of MTs. It is known that two types of dynein exist in cells, namely the axonemal and the cytoplasmic dynein, each with distinct function (Gibbons et al., 1994). Axonemal dynein regulates the movement of cilia and flagella (Gibbons and Rowe, 1965), whereas cytoplasmic dynein is known for its role in retrograde transport (Allan, 2011). Cytoplasmic dynein was first identified in neuronal cells (Paschal and Vallee, 1987) and it has since been ascribed a wide range of functions in a variety of cells including organelle positioning (Corthesy-Theulaz et al., 1992, Allan, 1995, Harada et al., 1998), vesicle transport (Traer et al., 2007, Banks et al., 2011) and more recently, neuronal migration (Tsai et al., 2007). In *S. cerevisiae,* which is used as a model for cellular function, it does not contain any member of the kinesin-3 family. In yeast, dynein has been shown to rescue de-polymerising MTs by generating pulling forces at the cellular cortex (Laan et al., 2012a, Laan et al., 2012b) and its deletion results in reduced MT growth and shrinking rates, as well as a decrease of catastrophe frequency (Carminati and Stearns, 1997). In *U. maydis*, kinesin-1 and kinesin-3 are known to cooperate in hyphal growth alongside myosin-5 (Schuchardt et al., 2005) and kinesin-3 has been shown to support roles in organelle transport (Wedlich-Söldner et al., 2000, Wedlich-Söldner et al., 2002b). Additionally, kinesin-3 has been shown to cooperate with dynein in long-range reterograde endosome motility (Schuster et al., 2011b).

1.6.2. Kinesin-1

The kinesin-1 complex consists of two heavy chains, which form a dimer via a coiled coil region in the neck region and a tail domain. Additionally, in animal cells, there are two light chains for specific cargo binding (Kuznetsov et al., 1989). The head of kinesin forms the motor domain and binds to tubulin, cleaving ATP and performing what has evolved to be termed the 'hand-over-hand' or 'alternating site mechanism' movement along MTs (Howard et al., 1989, Hackney, 1994, Schief and Howard, 2001). The tail of kinesin-1 supports cargo binding (Seiler et al., 2000) but has also been found, in the absence of cargo, to fold back to the motor head, to inactivate the motor protein (Cai et al., 2007, Dietrich et al., 2008, Hackney and Stock, 2008). In order to activate the motor, the cargo must bind to the kinesin-1 tail, thereby freeing the motor domains for ATP-driven motility. In animal cells, the presence of the two light chains allows the specific binding to intermediate filaments (Prahlad et al., 1998) and mRNA (Brendza et al., 2000). Surprisingly in fungal species such as *U. maydis,* kinesin-1 light chains are not found (Steinberg and Schliwa, 1996, Steinberg, 1997, Steinberg et al., 1998). However, it is known that kinesin-1 participates in a number of processes, including vacuole formation during hyphal growth (Steinberg et al., 1998) and organelle motility (Wedlich-Söldner et al., 2002b). In the absence of kinesin-1, accumulations of EE's at the MT plus-ends are lost (Lehmler et al., 1997). This evidence suggests that kinesin-1 participates in transport of secretory vesicles and is therefore, essential for polarised hyphal growth (Konzack et al., 2005, Schuchardt et al., 2005). Additionally, a role for kinesin-1 in the delivery of cytoplasmic dynein to the MT plus ends was established (Zhang et al., 2003, Lenz et al., 2006). This delivery mechanism prepares the cell for retrograde movement and is essential in polarised growth. Furthermore, kinesin-1 has been suggested for a role in endocytosis, as deletions of it led to a defect in the transport of lucifer yellow to vacuoles (Steinberg et al., 1998).

1.6.3. Kinesin-3

Kinesin-3 is not found in *S. pombe*, and *S. cerevisiae* lacks both kinesin-1 and kinesin-3, suggesting that long-distance transport is only a requirement in

mammalian systems and filamentous fungi (Steinberg and Perez-Martin, 2008). In fungal cells, the kinesin-3 motor family has been characterized in *U. maydis*, and *N. crassa* (McCaffrey and Vale, 1989, Schuchardt et al., 2005, Fuchs and Westermann, 2005). In *N. crassa,* the kinesin-3 motor, Kin2, is responsible for mitochondrial distribution (Fuchs and Westermann, 2005) and in *U. maydis*, kinesin-3 is required for endosome movement (Wedlich-Söldner et al., 2002b, Lenz et al., 2006, Schuster et al., 2011b). A deletion of kinesin-3 causes a reduction in endosome motility and abolishes endosome clustering at the distal cell pole and septa (Wedlich-Söldner et al., 2002b). Indeed, another study provided evidence that kinesin-3 is required for exocytosis (Schuchardt et al., 2005) as in its absence, acid phosphate secretion was dramatically impaired. It is proposed that dynein and kinesin-3 counteract each other in the movement of EE in *U. maydis* in order to arrange them throughout the cell (Wedlich-Söldner et al., 2002b). Furthermore, it is suggested that they counteract each other as they are bound to the same organelle and participate in a 'tug of war' to determine the direction of motility (Muller et al., 2008, Soppina et al., 2009, Hendricks et al., 2010). Interestingly, it was found that kinesin-3 is permanently bound to EEs and is therefore, found in both anterograde and retrograde movement of EEs (Schuster et al., 2011b). However, it is suggested that in the retrograde movement it is only a passive cargo to the retrograde motor protein dynein (Schuster et al., 2011a).

1.6.4. Dynein

Cytoplasmic dynein consists of two heavy chains, intermediate chain, light intermediate chain and three types of light chains (LC8, Tctex1 and Roadblock) (Vallee et al., 2004, Palmer et al., 2009). It has been shown that the heavy chain forms the globular motor domain responsible for MT binding, whereas the tail domain contains homodimerization interaction sites for the dynein intermediate (DIC) and dynein light intermediate chain (DLIC) (Habura et al., 1999, King, 2000, Tynan et al., 2000). In *S. cerevisiae,* elongating MT plus-ends take dynein to the cortex, where it becomes 'activated' and 'offloaded' in order to migrate toward minus ends to mediate spindle positioning (Lee et al., 2003, Sheeman et al., 2003). In fungi, dynein has been

shown to direct the positioning of the spindle in mitosis, as well as nuclear migration (Plamann et al., 1994, Xiang et al., 1994, Bloom, 2001, Straube et al., 2001, Tsujikawa et al., 2007, Finley et al., 2008, Roca et al., 2010), motility of EEs (Wedlich-Söldner et al., 2002b, Zhang et al., 2010) and endoplasmic reticulum (ER) (Wedlich-Söldner et al., 2002a). In *U. maydis* no direct link has been made between dynein and endocytosis, however its role in bi-directional transport and organizing the EE (Wedlich-Söldner et al., 2002b, Lenz et al., 2006) could suggest that without its presence, endocytosis will be inhibited.

1.6.5. Endosomes - cargoes transported along microtubules

Trafficking in the reverse direction or endocytosis, is essential to ensure the cells receive information from the external environment and that endocytosed trans-membrane receptors are transported to the correct organelle for sorting (Prescianotto-Baschong and Riezman, 1998, Soldati and Schliwa, 2006). The main function of the endocytic pathway is to sort internalised ligands and receptors to different destinations (Trowbridge et al., 1993, Mellman, 1996, Mellman and Warren, 2000, Gruenberg, 2001). Ligands such as transferrin, LDL receptors, and certain G protein-coupled receptors (GPCR) are recycled back to the plasma membrane (Anderson et al., 1982, Marchese et al., 2003) to continue with multiple rounds of internalisation. In comparison, EGF's (Carpenter and Cohen, 1979) are transported to late endosomes and lysosomes for degradation (Goldstein et al., 1985). In mammalian cells, two different populations of endosomes have been identified and termed early and late endosomes (Hubbard, 1989, Rodman et al., 1990). EEs have been considered as the initial sorting stations for the aforementioned proteins, in order to separate which cargoes are for plasma membrane recycling and which are for degradation (Maxfield and Yamashiro, 1987, Mellman, 1996, Gruenberg, 2001). The late endosomal compartment is also known as the pre-lysosomal compartment, because of its function in the delivery of lysosomal enzymes to lysosomes (Griffiths et al., 1988). The EE compartment is involved in dissociating ligands from their receptors and is characterized by several markers such as EEA1 (Ramanathan et al., 2013), PI(3) Kinase,

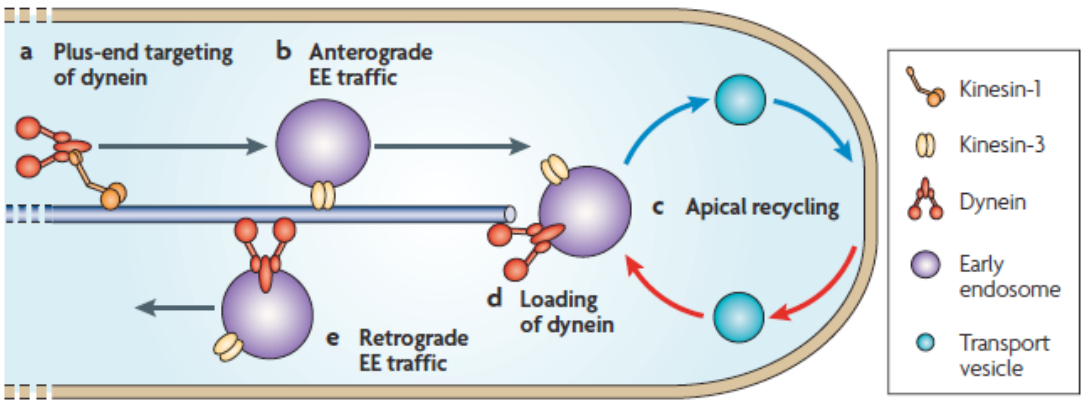

Figure 1.9. Bi-directional early endosome transport
kinesin-3 moves early endosomes to the hyphal tip (a, b), where membrane exchange with the plasma membrane occurs (c). Endosomes are loaded onto dynein (d), which is activated and moves the early endosomes back to the sub-apical regions with the kinesin-3 still attaches for another round of motility (e). The accumulation of dynein at MT plus ends is mediated by kinesin-1, which either, directly or indirectly binds the dynein-dynactin complex and targets it to the MT. Image taken from (Steinberg, 2007b).

VPS34 (Li et al., 1995) and the GTPase Rab5 (Christoforidis et al., 1999). Rab5 is already found at the plasma membrane on a subset of endocytic structures (Bucci et al., 1992, Sato et al., 2005) and therefore its localisation to EEs is not surprising. It has also been linked to EE fusion (Gorvel et al., 1991) and the regulation of EE motility along MT (Nielsen et al., 1999). In order to maintain the polarization of fungal hyphae and formation of the SPK, transport of membranous organelles and vesicles needs to be directed to hyphal tips (Gow, 1995). A genetic mutational approach led to the identification of *yup1*, a target-soluble *N*-ethylmaleimide-sensitive fusion protein attached to protein receptor (t-SNARE). It is known for its localisation on EEs in eukaryotic cells (Behnia and Munro, 2005), and shown to impair endocytosis in *U. maydis* (Wedlich-Söldner et al., 2000). Specifically, it was found that a temperature-sensitive mutant to the *yup1* gene led to the t-SNARE's dissociation from the endosomal membrane and the GFP-fused Pra1 pheromone receptor was no longer able to be constitutively endocytosed

and instead, remained trapped at the plasma membrane (Wedlich-Söldner et al., 2000). Additionally, Yup1 was found to co-localise with Rab-5 (Fuchs et al., 2006), a known marker of EEs. This gave the first evidence of early endsomes in fungi, which was confirmed by the visualization of EE compartments in *A. nidulans* (Peñalva, 2005) and their bi-directional movement in hyphae along MT's in *U. maydis* (Lenz et al., 2006). This motility of EEs has been shown to be regulated by the plus-end directed kinesin-3 and minus-end directed dynein motor proteins, summarised in Figure 1.9. (Wedlich-Söldner et al., 2002a, Lenz et al., 2006) and is also required for fungal secretion, endocytosis and ultimately, plant infection (Wedlich-Söldner et al., 2000).

1.7. Objectives

In *U. maydis,* it is understood that endocytosis does occur but the exact mechanism is not understood. Extensive studies in yeasts such as *S. cerevisiae* and *S. pombe* have shown that the actin cytoskeleton is essential, whereas the microtubule cytoskeleton is impartial. However it can be assumed that differences between structure and organisation of both the actin and microtubule cytoskeletons may exist, as filamentous fungi undergo longer periods of polarised growth in order to aid in pathogenicity (Fuchs et al., 2005, Basse and Steinberg, 2004) as well as other functions. We know in *U. maydis* that the pathogenic response is initiated by the interaction of the signalling pheromone and its receptor however, despite structure-function studies (Szabo et al., 2002) carried out on the *a1* and *a2* peptides, little is known about their localisation or transport within *U. maydis*. Visualization of the vesicles during endocytosis has relied on the vacuole dye FM4-64 and only the Pra1 receptor has been localized via GFP fusion within the cell. The use of dyes such as FM4-64 and lucifer yellow has allowed researchers to follow endocytic transport from the plasma membrane to the vacuole in real-time. However, induction with them does not inform on specific pathways of endocytosis such as receptor-mediated. In this thesis, we aim to produce a viable fluorescently labelled pheromone that can be used *in vivo* as a probe to

study receptor-mediated endocytosis in filamentous fungi. A similar approach was adopted in *S. cerevisiae* (Toshima et al., 2006b) and provided evidence that endocytosis in yeast is mediated by the actin cytoskeleton. In using the fluorescently labelled pheromone we aimed to identify the pathway taken from internalisation and binding to its corresponding receptor, to its eventual degradation in the cell vacuole. In order to address the role of the cytoskeleton in this process, the role of actin patches and cables will be investigated. Furthermore, tests will be carried out to establish whether a clathrin-mediated endocytosis pathway similar to that, observed in yeast and mammalian cells, is present in *U. maydis*. Additionally, we wish to analyse which molecular motors in particular, kinesin-1, kinesin-3, dynein and myosin are required for the pheromone's transport within the cell and whether it is sorted *via* EEs.

2. CHAPTER 2 – MATERIALS AND METHODS

2.1. Growth Conditions

2.1.1. Escherichia coli

E. coli was grown in liquid dYT medium (Sambrook et al., 1989). Antibiotics were added, as required, at the following concentrations; ampicillin (100 µg/ml; Sigma Aldrich, Dorset, United Kingdom), kanamycin (40 µg/ml; Invitrogen Life technologies, Paisley, UK) and X-Gal (40 µg/ml; Carl Roth, Mühlberg, Germany). Liquid cultures of *E. coli* were induced at 37 °C with shaking (200 rpm). Glycerol stocks were made from exponentially growing cultures and mixed with dYT-Glycerol at a ratio of 1:1 (v/v) and stored at -80 °C. To grow cultures from glycerol stocks they were placed straight into liquid media and grown overnight.

dYT Medium

12.8 g (1.6 % w/v) tryptone (Sigma Aldrich, Dorset, UK)
8.0 g (1.0 % w/v) yeast extract (Sigma Aldrich, Dorset, UK)
4.0 g (0.5 % w/v) sodium chloride (Fisher, Loughborough, UK)
10.0 g agar (1.3 % w/v) (LabM, Lancashire, UK)
Deionised H_2O added to 800 ml and autoclaved for 20 minutes at 121 °C

2.1.2. Ustilago maydis

All *U. maydis* strains, except temperature sensitive and mutants containing the promoter of the arabinose gene from *U. maydis* (p*CRG*), were grown in complete medium, supplemented with 1 % glucose (CM-GLU) at 28 °C, with shaking (200 rpm). DynTS and Yup1TS mutants, along with their control strains, were grown overnight at 22 °C before transferring 5 ml of the cultures to new flasks at 32 °C, with shaking (200 rpm) and fresh media. Microscopic analysis was conducted after at least 2 hours at the restrictive temperature. The P*crg* mutants were grown overnight in CM-GLU, where the promoter is

repressed, before being centrifuged at 3000 rpm and transferred to fresh CM-ARA media, where the *CRG* promoter over expresses genes when the only carbon source is arabinose (Bottin et al., 1996). For light microscopic observation, cultures with an OD_{600} 0.6-0.8 were selected. Glycerol stocks were produced from exponentially growing overnight cultures and mixed with NSY-Glycerol at a ratio of 1:1 (v/v) and stored at -80 °C. In order to grow cultures from glycerol stocks, strains were placed on solid medium, where agarose was added to the CM medium, to a final concentration of 2 %. Selective CM plates used for screening transformants, contained carboxin (2 µg/ml; Sigma Aldrich, Dorset, United Kingdom), nourseothricin/ClonNAT (150 µg/ml; Werner Bioagents, Jena, Germany), hygromycin (200 µg/ml; Roche, West Sussex, UK) or phleomycin (40 µg/ml; Source Biosciences, Nottingham, UK).

The following media and additives were used to cultivate *U. maydis*:

CM Medium (Holliday, 1975)
2.5 g (0.25 % w/v) casamino acids **(**Melford, Ipswich, UK)
1.0 g (0.1 % w/v) yeast extract (Sigma Aldrich, Dorset, UK)
10.0 ml (1.0 % w/v) vitamin solution
62.5 ml (6.25 % w/v) salt solution
0.5 g (0.05 % w/v) DNA (from herring sperm) (Sigma Aldrich, Dorset, UK)
1.5 g (0.15 % w/v) ammonium nitrate (Fisher, Loughborough, UK)
Deionised H_2O added to 1 litre, pH set to 7.0 with sodium hydroxide (Fisher, Loughborough, UK)
Autoclave for 20 min at 121 °C
Supplement with 1 % with glucose (50% w/v stock; Fisher, Loughborough, UK) or 1 % arabinose (25% w/v stock; Fisher, Loughborough, UK))

YEPS light (modified Tsukuda *et al.*, 1988)
10.0 g (1.0 % w/v) yeast extract (Sigma Aldrich, Dorset, UK)
4.0 g (0.4 % w/v) peptone (Fisher, Loughborough, UK)
4.0 g (0.4 % w/v) sucrose (Fisher, Loughborough, UK)

Deionised H_2O added to 1 litre

Autoclave for 20 min at 121 °C

Vitamin Solution (Holliday, 1975)

100 mg (0.1% w/v) thiamine hydrogen chloride (Serva Electrophoresis, Heidelberg, Germany)

50 mg (0.05 % w/v) riboflavin (Sigma Aldrich, Dorset, UK)

50 mg (0.05 % w/v) pyridoxine hydrochloride (Sigma Aldrich, Dorset, UK)

200 mg (0.2 % w/v) D-pantothenic acid hemicalcium salt (Sigma Aldrich, Dorset, UK)

50mg (0.2 % w/v) 4-aminobenzoic acid (Sigma Aldrich, Dorset, UK)

200 mg (0.2 % w/v) nicotinic acid (Sigma Aldrich, Dorset, UK)

200 mg (0.2 % w/v) choline chloride (Sigma Aldrich, Dorset, UK)

1 g (1.0 % w/v) *myo*-inositol (Sigma Aldrich, Dorset, UK)

Deionised H_2O added to 1 litre and 40ml aliquots frozen at -20 °C

Trace Elements (Holliday, 1975)

60 mg (0.06 % w/v) boric acid (Carl Roth, Mühlberg, Germany)

100 mg (0.01 % w/v) ferric acid.$6H_2O$ (Sigma Aldrich, Dorset, UK)

40 mg (0.4 % w/v) sodium molybdate.$2H_2O$ (Sigma Aldrich, Dorset, UK)

400 mg (0.04 % w/v) zinc chloride (Carl Roth, Mühlberg, Germany)

140 mg (0.14 % w/v) manganese (II) chloride.$4H_2O$ (Sigma Aldrich, Dorset, UK)

40 mg (0.04 % w/v) copper(II) sulphate.$5H_2O$ (Sigma Aldrich, Dorset, UK)

Deionised H_2O added to 1 litre and filter sterilized

Salt Solution (Holliday, 1975)

16 g (16 % w/v) monopotassium phosphate (Carl Roth, Mühlberg, Germany)

8 ml (8.0 % w/v) trace elements

1.32 g (1.32 % w/v) calcium chloride.$2H_2O$ (Sigma Aldrich, Dorset, UK)

4 g (4.08 % w/v) magnesium sulphate.$7H_2O$ (Sigma Aldrich, Dorset, UK)

8 g (8.0 % w/v) potassium chloride (Sigma Aldrich, Dorset, UK)

4 g (4.0 % w/v) sodium sulphate (Sigma Aldrich, Dorset, UK)

Deionised H_2O added to 1 litre and filter sterilized

NSY Glycerol

5 g (0.5 % w/v) sucrose (Fisher, Loughborough, UK)

8 g (0.8 % w/v) bacto Nutrient Broth (LabM, Lancashire, UK)

1 g (0.1 % w/v) yeast Extract (Sigma Aldrich, Dorset, UK)

800 ml (80.0% w/v) 87% glycerol (final concentration 69.6 %) (Fisher, Loughborough, UK)

Deionised H_2O added to 1 litre

Autoclave for 20 min at 121 °C

2.2. Strains and Plasmids

All *U. maydis* strains and plasmids used in this study are listed in Table 1. All plasmids were generated using standard techniques or *in vivo* recombination in *Saccharomyces cerevisiae,* following published protocols (Raymond et al., 2002). *U. maydis* strains FB1, FB2 (Banuett and Herskowitz, 1989) AB33 (Brachmann et al., 2001), SG200 (K*ä*mper et al., 2006), Lifeact GFP (Schuster et al., 2011c) and Yup1TS (Wedlich-Söldner et al., 2000) were described previously. Strains ΔKin-1 (Christine Lehmler, unpublished), ΔKin-3 (Tina Müller, unpublished) and DynTS (Irene Schulz, unpublished) were not previously published but checked *via* microscope for correct phenotype as expected from published strains with the same deletion. To allow the actin dynamics to be studied alongside the pheromone uptake and transport dynamics, Potef_lifeact_GFP was transformed into FB2 wild-type cells. Positive colonies were viewed under a microscope to visualise whether the GFP was expressed, showing both actin patches and cables. In order to visualise the effect of myosin tail over-expression on pheromone uptake and transport, plasmids pP*crg*-HA-Myo1, pP*crg*-HA-Myo2 and pP*crg*-HA-Myo5 were digested, precipitated and transformed into FB2_lifeact_nat and confirmed via cbx Southern blot, western blot and microscopic analysis.

Table 1: Strains and plasmids used in this study

Strain	***Genotype***	**Established**
FB1	*a1b1*	(Banuett and Herskowitz, 1989)
FB2	*a2b2*	(Banuett and Herskowitz, 1989)
AB33	*a2 Pnar-bW2 Pnar-bE1, ble*	(Brachmann et al., 2001)
SG200	*a1 mfa2 bW2 bE, ble*	(Kämper et al., 2006)
Lifeact-GFP	*a2 Pcrg:bW2,bE1, ble, Potef-Lifeact-*	(Schuster et al., 2011c)
FB2 Lifeact	*a2b2, Potef-egfp-Lifeact, nat*	This study
FB2 myo1tail	*a2b2, Pcrg-HA-myo1tail_cbx*	This study
FB2 myo2tail	*a2b2, Pcrg-HA-myo2tail_cbx*	This study
FB2 myo5tail	*a2b2, Pcrg-HA-myo5tail_cbx*	This study
Lifeact-GFP myo1tail	*a2 Pcrg:bW2,bE1, ble, Potef-Lifeact-egfp, cbx, Pcrg-HA-myo1tail_HygoR*	This study
Lifeact-GFP myo2tail	*a2 Pcrg:bW2,bE1, ble, Potef-Lifeact-egfp, cbx, Pcrg-HA-myo2tail_HygoR*	This study
Lifeact-GFP myo5tail	*a2 Pcrg:bW2,bE1, ble, Potef-Lifeact-egfp, cbx, Pcrg-HA-myo5tail_NatR*	This study
FB2 Dkin-1	*a2b2 ∆kin-1::cbx*	Christine Lehmler
FB2 Dkin-3	*a2b2 ∆kin-3::hyg*	Tina Müller
FB2 DynTS	*a2b2 dyn2ts, nat*	Irene Schulz
FB2 Yup1TS	*a2b2 yup1ts*	(Wedlich-Söldner et al., 2000)
Plasmid Name	***Genotype***	**Established**
pLifeact-egfp	*Potef-lifeact-egfp_cbx_amp*	(Steinberg and Schuster, 2011)
pLifeact NatR	*Potef-egfp-Lifeact_nat*	This study
pMyosin 1 tail	*p123-Pcrg-HA_myo1tail_cbx_amp*	Steffi Treitschke
pMyosin 2 tail	*p123-Pcrg-HA_myo1tail_cbx_amp*	Steffi Treitschke
pMyosin 5 tail	*p123-Pcrg-HA_myo1tail_cbx_amp*	Steffi Treitschke
pMyosin 1 tail_hyg	*Pcrg-HA_myo1tail_hyg_amp*	This study
pMyosin 2 tail_hyg	*Pcrg-HA_myo2tail_hyg_amp*	This study
pMyosin 5 tail_nat	*Pcrg-HA_myo5tail_nat_amp*	This study

a, *b*, mating-type loci; *E1, W2*, genes of the b mating-type locus; P, promoter; *wt,* wild-type; -, fusion; *::*, replacement; *hyg*, hygromycin resistance; *ble*, phleomycin resistance; *nat*, nourseothricin resistance; *cbx*, carboxin resistance; *amp*, ampicillin; resistance Δ, deletion; /, ectopically integrated; *otef*, constitutive promoter; *nar*, conditional nitrate reductase promoter; *crg,* conditional arabinose-induced promoter; *lifeact*, 13 aa peptide; *egfp*, enhanced green fluorescent protein; *dyn2*: C-terminal half of the dynein heavy chain; *yup1*TS, temperature-sensitive allele of the endosomal t-SNARE *yup1; Rab*, small Rab GTPase; *p123*, standardised *E. coli* expression vectors

pLifeact_nat – In order to change the resistance cassette of the pPotef-Lifeact-egfp plasmid so that it could be used alongside other plasmids with cbx resistance, pPotef-Lifeact-egfp was digested with *Not*I/*Bsr*GI, to obtain a 1649 bp region containing the otef promoter and GFP signal, *Bsr*GI/*Bgl*I to obtain a stop codon and *Bgl*I/*Not*I to obtain a *S. cerevisiae URA3* marker, 2 µm *ori*, and an *E. coli* origin of replication. Finally the nat resistance sequence was amplified through digestion with *Not*I from laboratory standardized plasmid pNEB_nat (New England Biolabs (NEB), Ipswich, UK) and all fragments were ligated using T4 DNA ligase (New England Biolabs (NEB), Ipswich, UK), before being transformed into competent *E. coli* cells. All colonies were screened *via* restriction digests and screened via PCR for correction integration. The primers used for the PCR were NC53 (GTATCATATGATACACAGACAACATCATC; stock concentration 100 pmol/µl; New England Biolabs (NEB), Ipswich, UK) and NC54 (CTATGACCATGGTTACCGATGAATTCTC; stock concentration 100 pmol/µl; New England Biolabs (NEB), Ipswich, UK).

pMyosin1tail_hyg, pMyosin2tail_hyg and pMyosin5tail_nat – To investigate the effect of over-expression of myosin tails on actin patch dynamics, the pP*crg*-HA-Myo1 plasmid was digested with *Mlu*I/*Hind*III-HF to give a 7780 bp fragment containing the *crg* promoter, myosin-1 tail, HA tag and *E. coli* plasmid backbone. This was ligated with the hygromycin resistance cassette of laboratory plasmid pNEB-hyg (New England Biolabs (NEB), Ipswich, UK), which was digested with *BssH*II/*Hind*III-HF to give a 2807 bp fragment. Additionally, the pP*crg*-HA-Myo2 plasmid was digested with *Bsi*WI/*Hind*III-HF, to give a 9203 bp fragment which contained the *crg* promoter, myosin-2 tail, HA tag and a background vector for *E. coli* replication. The hygromycin resistance cassette was taken from a laboratory standardized plasmid pSL-Hyg (New England Biolabs (NEB), Ipswich, UK), which was digested, to give a 2850 bp fragment with *Bsr*GI/*Hind*III-HF. Furthermore, pP*crg*-HA-Myo5 was digested with *Ssp*I and calf intestinal alkaline phosphatase (CIP; New England Biolabs (NEB), Ipswich, UK), which prevents re-ligation of linearized plasmids, to give a 9276 bp fragment containing the *E. coli* origin of replication, *crg* promoter, myosin-5 tail and HA tag. This fragment

was ligated with the resistance cassette nourseothricin/ClonNAT (Werner Bioagents, Jena, Germany), digested from laboratory standardized plasmid pNEB-Nat (New England Biolabs (NEB), Ipswich, UK) with *Pvu*II to give a 1832 bp fragment. All fragments were ligated with T4 DNA ligase (New England Biolabs (NEB), Ipswich, UK) and transformed into competent *E. coli* cells. In order to confirm the correct ligation, positive colonies were screened and digested with restriction enzymes to check for different banding patterns. In order to confirm over-expression of myosin tails, the proteins for each strain were extracted and western blotted.

2.3. Methods for strain construction

2.3.1. Transformation of plasmid DNA into E. coli

The DNA suspension was then introduced into *E. coli* strain DH5α (Stratagene XL ultra-competent cells; Stratagene, California, USA) by thermo-transformation. This was achieved by adding 8 µl to 50µl of defrosted *E. coli* competent cells. This was then mixed by pipetting and incubated on ice for 30 mins. The tubes were transferred to a 42 °C thermomixer (Eppendorf, Hamburg, Germany) for 30 seconds, before being returned on ice for 5 mins. 200 µl of dYT media was then added and the tubes transferred to a 37 °C thermomixer (Eppendorf, Hamburg, Germany) to shake at 1,000 rpm for 30 mins. Next the entire content of the tube was plated onto dYT + ampicillin plates and incubated overnight at 37 °C. DNA restriction digest screening of *E. coli* clones and confirmation of the correct vectors by DNA sequencing, was carried out where appropriate and all confirmed plasmids were frozen at -80 °C as part of the Steinberg plasmid collection.

2.3.2. U. maydis transformation

Transformation of *U. maydis* was carried out as previously described (Schulz et al., 1990). *U. maydis* cells were grown overnight in YEPS light medium at 28 °C (or 22 °C for temperature sensitive strains) to a cell density of OD_{600} 0.6 – 0.8. Cells were centrifuged (10 min, 3000 rpm, RT) and washed in 25 ml

SCS before re-suspension in 2 ml SCS, containing 3.5 mg / ml lysing enzymes (Sigma Aldrich, Dorset, UK). Cells were incubated for 10 min at RT to digest the cell wall material. This process was followed under the microscope. After proto-plasting of the elongated *U. maydis* cells, they were washed three times with ice-cold SCS and centrifuged at 2400 rpm for 10 min at 4 °C (Thermo Scientific, Massachusetts, USA). This was followed with an additional wash with ice-cold STC. Finally, the protoplast pellet was re-suspended in 0.5 ml STC and aliquots of 50 µl were used immediately or stored at – 80 °C. For transformation of protoplasts, linearised DNA (5 µg) and 1 µl heparin (Sigma Aldrich, Dorset, UK) were added to the protoplast aliquot and the sample was incubated for 10 min on ice. Subsequently, 500 µl STC/40%PEG was added and the protoplast mix was incubated for another 15 min on ice. The transformation mix was plated onto regeneration-agar. Transformed colonies appeared after 3-7 days and were singled-out and grown on CM agar plates, containing the appropriate antibiotic. Single colonies were picked and saved on CM plates. Media and solutions used for transformations were as follows:

SCS

Solution 1:

5.9 g (0.6% w/v) sodium citrate.2H_2O (final concentration 20 mM) (Carl Roth, Mühlberg, Germany)

182.2 g (18.2% w/v) sorbitol (final concentration.1M) (Melford, Ipswich, UK)

Deionised H_2O added to 1 litre

Solution 2:

4.2 g (0.4% w/v) citric acid.H_2O (final concentration. 20 mM) (Carl Roth, Mühlberg, Germany)

182.0 g 18.2% w/v) sorbitol (final concentration. 1 M) (Melford, Ipswich, UK)

Deionised H_2O added to 1 litre

add solution 2 to solution 1 until pH of 5.8 was reached (ratio 1:2 is 5:1)

STC - buffer

50 ml (50 % w/v) sorbitol (Melford, Ipswich, UK)

1.0 ml (1.0% w/v) 1 M tris-HCl pH 7.5 (Carl Roth, Mühlberg, Germany)
10.0 ml (10.0% w/v) 1 M calcium chloride (Sigma Aldrich, Dorset, UK)
Deionised H_2O added to 100 ml
Autoclave for 20 mins at 121 °C

STC/40%PEG

90 ml (60.0 % w/v) STC buffer
60 g (40 % w/v) PEG 4000 (Fisher, Loughborough, UK)
Deionised H_2O added to 150 ml and filter sterlized before use.

Regeneration (REG) Agar

8.0 g (1.0 % w/v) yeast extract (Sigma Aldrich, Dorset, UK)
16.0 g (2.0% w/v) peptone (Fisher, Loughborough, UK)
16.0 g (2.0% w/v) sucrose (Fisher, Loughborough, UK)
145.76 g 18.22% w/v) sorbitol (Melford, Ipswich, UK)
Deionised H_2O added to 800 ml
6.0 g agar (1.5% w/v) per 400 ml media (LabM, Lancashire, UK)
Autoclave for 20 mins at 121 °C

2.3.3. Identification of positive transformants

In order to check for the presence of the correct plasmid construct in *U. maydis* transformants, individual colonies were plated onto CM-plates containing the antibiotic and then allowed these to grow for 2-3 days. With those that successfully grew, part of the *U. maydis* colony using a yellow tip and placed it into 5 ml of TE. The TE suspensions were then vortexed to allow for the breakdown of the cell walls and the release of the cell's DNA. 1 ml of the 5 ml cell suspension was then used as template DNA for 20 ml Dream Taq PCR (Fermentas, Thermo Scientific, Massachusetts, USA). However the first step of the PCR program was extended in time in order to allow the genomic DNA to be denatured but the rest of the PCR was performed as detailed below.

2.4. Microbiological laboratory methods

2.4.1. DNA isolation from U. maydis

For this method, (modified from Hoffmann and Winston, 1987)), 2 ml of *U. maydis* cell suspension was grown overnight in $YEPS_{LIGHT}$, and was pelleted in 2 ml Eppendorf tubes by centrifugation (1 min, 13000 rpm; Thermo Scientific, Massachusetts, USA). The supernatant was discarded and 0.3 g glass beads (Fisher, Loughborough, UK), 400 µl lysis buffer and 500 µl phenol-chloroform (1:1 v/v; Sigma Aldrich, Dorset, UK) were added. The samples were incubated for 10 min on a Vibrax-VXR shaker (IKA; Sigma Aldrich, Dorset, UK) at full speed. After phase separation for 15 min at 13,000 rpm, 400 µl of the upper phase of the supernatant was transferred to a new 1.5 ml Eppendorf tube and mixed with 1 ml ethanol. Subsequently, the samples were washed twice with ethanol and finally centrifuged for 2 min at 13,000 rpm and the pellet was re-suspended in 50 µl TE/RNAse A at 55 °C and stored at –20 °C. 20 µl of DNA suspension was used for Southern blotting.

Lysis Buffer

5.85 g (5.85 % w/v) sodium chloride (Fisher, Loughborough, UK)
10 ml (10 % w/v) 1M tris-HCl (pH 8.0) (Carl Roth, Mühlberg, Germany)
20 ml (20 % w/v) triton X (Carl Roth, Mühlberg, Germany)
50 ml (50% w/v) 20% SDS (Fisher, Loughborough, UK)
2 ml (2 % w/v) 0.5 M EDTA (Carl Roth, Mühlberg, Germany)
Deionised H_2O added to 1 litre and filter sterilized

TE

4 ml (1.0 % w/v) 1 M tris (Melford, Ipswich, UK)
800 µl (0.8 % w/v) 0.5 M EDTA (Carl Roth, Mühlberg, Germany)
Deionised H_2O added to 400 ml
pH adjusted to 8.0 with 0.4 M sodium hydroxide

2.4.2. Protein extraction and immuno-detection

Protein extraction and immuno-detection were performed as described (Straube et al., 2001). Whole cell extracts were prepared from overnight cultures of wild-type FB2 and AB33 strains along with the over-expression tail mutants of myosin-1, myosin-2 and myosin-5, grown to an OD_{600} 0.60 - 0.80 in both CM-GLU or CM-ARA media. The cells were harvested by centrifugation at 3000 rpm for 10 min (Thermo Scientific, Massachusetts, USA). After one wash in extraction buffer (100 mM PIPES, pH 6.9, 5 mM MgSO4, 1 mM EDTA, 1 mM EGTA), cells were re-suspended in extraction buffer (50 mM Tris-HCl, 50 mM NaCl, pH 7.5) supplemented with complete protease inhibitor (1 tablet / 10 ml buffer; Roche Applied Sciences, Penzberg, Germany). The cell suspension was then frozen using liquid nitrogen and disrupted in a mixer mill MM200 (Retsch, Haan, Germany), for 2 x 5 min at full speed. After thawing, the solution was centrifuged for 30 min at 24,000 rpm to clear the supernatant of cellular debris and large organelles. Protein content of the supernatant was then analysed using the Bradford test. A reference graph was constructed with known concentrations of bovine serum albumin (BSA New England Biolabs (NEB), Ipswich, UK), against which the samples were analysed. Equal amount of proteins from the different samples were subsequently loaded onto a gel for a western blot.

Proteins were separated on 10 % polyacrylamide gels and transferred to nitrocellulose membranes for 1 hr at 400 mA in a semi-dry blot chamber. In order to detect HA-labelled proteins, a monoclonal anti-HA antibody (1:1,000; Roche) was used. Anti α-tubulin antibody (1:1,000; Oncogene Research Products, La Jolla, CA, USA) was used as a loading control. For each anti-rat (1:5,000; Invitrogen, Frederick, MD, USA) or anti-mouse immunoglobulin G (H+L), horseradish peroxidise-conjugated antibodies (1:5,000; Promega, Madison, WI, USA) were used for secondary antibody reaction. Detection was carried out using ECL plus western blot detection reagent following the manufacturer's instruction (GE Healthcare Life Science, Buckinghamshire, UK) and visualised on medical X-ray films (Fuji Film, Kanagawa, Japan).

2.4.3. Standard PCR reactions

For construction of plasmids and PCR-based analysis of knockout strains, Phusion Polymerase (New England Biolabs (NEB), Ipswich, UK) was used. Primer stocks were ordered at 100 µM. Standard PCR reactions were performed according to the following protocol:

Template DNA	4 µl (100 ng)
Primer 1	4 µl (final concentration. 10 µM)
Primer 2	4 µl (final concentration. 10 µM)
dNTPs	4 µl (final concentration. 20 mM)
5x GC Buffer	20 µl
Phusion	1 µl

Deionised H_2O add to total volume of 100 µl

Standard PCR programs were carried out under these conditions:

1. Denaturing	98 °C	(30 s)
2. Denaturing	98 °C	(10 s)
3. Annealing	60 °C	(20 s)
4. Elongation	72 °C	(15-30 s per kb)
5. Final Elongation	72 °C	(10 min)

Steps 2. to 4. were repeated 35-40 times.

2.4.4. Restriction digests

In order to confirm the correct ligations of plasmids in *E. coli*, DNA was extracted from cells and digested by three different restriction enzymes. All restriction enzymes were acquired from NEB (New England Biolabs (NEB), Ipswich, UK) and used as per the manufacturer's instructions. 1 µl of DNA was mixed with 0.5 µl of the chosen restriction enzyme, 2 µl of the specific

buffer (New England Biolabs (NEB), Ipswich, UK) provided with the restriction enzyme (or the one suggested on the NEB website for multiple restriction enzyme digestions), 2 µl of 0.1 M BSA (New England Biolabs (NEB), Ipswich, UK) if required to stabilize proteins during incubation and deionised water to a final volume of 20 µl. The digestion mixture was then incubated at 37 °C (or higher if NEB instructions for enzymes indicated so) for at least two hours or overnight if restriction enzymes were being used for ligations. A 5 µl sample of the digestion mix was then run on a 1 % agarose gel to check that banding patterns were correct.

2.4.5. Gel electrophoresis

In order to visualise DNA from PCR digestion or ligations, 1 µl samples were mixed with a DNA loading buffer (bromophenol-blue and sucrose) and water and then loaded into a TAE 1 % agarose gel that had been stained with ethidium bromide (4 µl per 100 ml; Fisher, Loughborough, UK). Samples were also loaded with a 1 kb ladder (Fermentas, Thermo Scientific, Massachusetts, USA) to provide a reference for the sizes of the bands seen. Gels were run for up to 1 hour, depending on the size of bands required. The gel was viewed with an ultraviolet (UV) transilluminator (UV solo TS imaging system; Biometra, Göettingen, Germany) and the picture taken could be used as proof of correct band sizes for ligations and PCR confirmation of transformants. The illuminated gel slice could also be cut out and dissolved, in order to recover the DNA.

2.4.6. Recovery of DNA from agarose gels

First the gel slice containing the DNA band was cut out, avoiding prolonged periods of UV exposure, to ensure integrity of the DNA. The gel slice was placed into an Eppendorf tube and weighed (1 g approximately equal to 1 ml). Three volumes of binding solution (6 M sodium iodide; Fisher, Loughborough, UK) was added to one volume of gel and incubated for 5 min at 55 ^{o}C to dissolve agarose. Next, re-suspended silica powder suspension (40 µl per tube) was added to the dissolved gel, followed by incubation for 5 min at 55 ^{o}C, with mixing (by vortex) every 2 min to keep the silica powder in

suspension. The silica powder/DNA complex was then spun at 13,000 rpm for 15 sec to form a pellet and the supernatant was removed. 500 µl of ice-cold wash buffer was added, the solution was mixed (by vortex) and then placed at room temperature for 5 min. The solution was again spun at 13,000 rpm for 15 sec and the supernatant discarded, before adding 500 µl of ice-cold wash buffer. The aforementioned step was repeated twice more. After the last wash, the tube was spun again and the remaining liquid removed with a pipette. The pellet was then re-suspended in 10 – 20 µl of water and incubated at 55 ^{o}C for 5 – 8 min. Finally the tube was spun and the supernatant was transferred into a new tube. An aliquot of the suspension was run on an agarose gel to determine the amount of DNA.

Wash Buffer

2.922 g (0.5 % w/v) sodium chloride (Fisher, Loughborough, UK)
1.211 g (0.1 % w/v) tris-HCl (Carl Roth, Mühlberg, Germany)
730.6 mg (0.025 % w/v) EDTA (Carl Roth, Mühlberg, Germany)
Ethanol added to total volume of 500 ml (50 % w/v) (Fisher, Loughborough, UK)
Autoclave for 20 mins at 121 °C
500 ml ethanol added before use with storage at 4 °C.

2.4.7. DNA precipitation

In order to precipitate DNA straight from digestion, without the need for gel electrophoresis, 1/10th volume of 3 M sodium acetate (pH 4.8; Carl Roth, Mühlberg, Germany) was added to the digestion mix of plasmid DNA, 10x NEB buffer (New England Biolabs (NEB), Ipswich, UK), bovine serum albumin (BSA; New England Biolabs (NEB), Ipswich, UK), restriction enzyme and water. 1 ml of ethanol (Fisher, Loughborough, UK) was also added and the mixture was then incubated at -20 ^{o}C for 10 minutes. This was then spun down for 10 mins at 13,000 rpm (Thermo Scientific, Massachusetts, USA) and the supernatant discarded. The pellet was washed with 500 µl of 70% ethanol (Fisher, Loughborough, UK) and re-spun twice before being air-dried. Finally

the pellet was re-suspended in 45 µl of deionised water for use in Southern blotting or in 20 µl for *U. maydis* DNA transformation.

2.4.8. Southern blotting

In addition to PCR-based confirmation, Southern blots were carried out on Rab deletion strains to confirm the correct integration of the deletion cassette and to demonstrate that the deletion cassette had not been integrated ectopically elsewhere in the genome. In addition, a Southern blot involving the carboxin (CBX) resistance cassette was used to establish the integration of the P*crg* myosin tail constructs into wild-type cells. Before transformation, the plasmids were digested with restriction enzyme *Ssp*I (New England Biolabs (NEB), Ipswich, UK) and for Southern blotting, restriction enzymes were chosen that did not cut in the wild-type cbx locus but would cut in the insert of the mutant. Additionally, an enzyme was chosen that would cut closer to one end of the insert than the other, in order to check for tandem, as well as homologous, integration. The restriction enzymes and predicted fragment sizes for all Southern blots are summarised in Table 2. Genomic DNA was isolated as previously mentioned for *U. maydis* DNA extraction. Probes were generated using DIG probe labelling mix (Roche, West Sussex, UK) as per the manufacturer's instruction. The following parameters were used as a guide for probe amplification; initial denaturation at 98 °C for 45 s, followed by 30 cycles of 98 °C for 10 s, 60 °C for 10 s, and 72 °C for 60 s, and then a final extension at 72 °C for 60 s. The probe was then purified by gel extraction and precipitation. Following isolation and digestion of genomic DNA, DNA fragments were separated on an agarose gel with a xylene cyanol loading buffer (6x loading buffer = 0.1% xylene cyanol, 30% glycerol). The gel was then depurinated in 0.25 M hydogren chloride for 15 mins and neutralised in 0.4 M sodium hydroxide, before being transferred to an Amersham Hybond - NX membrane (GE Healthcare, Buckinghamshire, UK) for a minimum of 4 hours. The membrane was then UV cross-linked to ensure complete transfer and incubated with hybridization buffer and probe at 68 °C overnight. The following day, the membrane was washed, blocked and then detected using streptavidin-IRDye 800CW conjugate (LiCOR; GE Healthcare,

Buckinghamshire, UK) as per the manufacturers instructions. It was then developed onto X-ray film (Fisher, Loughborough, UK) using a LiCOR Odtssey scanner.

Table 2: Predicted DNA fragment sizes and restriction enzymes for Southern blots

Strain	Restriction enzyme/s	Fragment size (kb) for WT control	Fragment size for cbx Southern
FB2 myo1tail	*Bam*HI	5661 bp	3589, 5445, 6442 bp
FB2 myo2tail	*Bam*HI	5661 bp	2376, 3589, 4302, 6442 bp
FB2 myo5tail	*Bam*HI	5661 bp	3589, 5789, 6442 bp

Hybridization buffer

500 ml (50 % w/v) 1 M sodium phosphate

350 ml (35 % w/v) 20 % SDS

Deionised H_2O added to 1 litre and store at 28 °C

2.4.9. Preparation of thermo-competent E. coli cells

The preparation of thermo-competent cells was carried out by standard procedures (Sambrook et al., 1989). Overnight starter cultures (3 ml LB broth) were inoculated with single colonies of DH5α (Stratagene, California, USA) and grown at 37 °C. The next day, 250 ml of SOB in a 1 L flask was inoculated with 1 ml of overnight culture, and incubated at 37 °C in a rotary shaker (Thermo Scientific, Massachusetts, USA) at 200 rpm until an of OD_{600} = 0.6 was reached. The cells were transferred to culture tubes and placed on ice for 10 minutes, before being spun at a low speed of 2500 g for 5 min, at 4 °C. The cells were re-suspended in 80 ml of TB and rested on ice for 10 minutes, before being spun again as before. While spinning, 1.4 ml dimethyl sulfoxide (DMSO; Carl Roth, Mühlberg, Germany) was added to 18.6 mL of ice-cold TB and 20 ml of the TB-DMSO (7 % DMSO in TB) was used to re-suspend the pellet, once spinning had concluded. Cells were placed on ice for a further 10 minutes, before being aliquoted into 50 or 100 µl batches on ice (in pre-cooled tubes on ice) and frozen immediately in liquid nitrogen. The

competent cells were then stored at –80 °C and defrosted when required. Media and solutions used in this method were as follows:

SOB media

20 g (20 % w/v) tryptone (Sigma Aldrich, Dorset, UK)

5 g (5.0 % w/v) yeast extract (Sigma Aldrich, Dorset, UK)

2 ml (2.0 % w/v) 5 M sodium choride (Fisher, Loughborough, UK)

2.5 ml (0.25 % w/v) 1 M potassium chloride (Sigma Aldrich, Dorset, UK)

10 ml (1.0 % w/v) 1 M magnesium chloride (Sigma Aldrich, Dorset, UK)

10 ml (1.0 % w/v) 1 M magnesium sulphate (Sigma Aldrich, Dorset, UK)

Deionised H_2O added to 1 litre

Autoclave for 20 mins at 121 °C

LB Broth

10 g tryptone (Sigma Aldrich, Dorset, UK)

5 g yeast extract (Sigma Aldrich, Dorset, UK)

10 g sodium chloride (Fisher, Loughborough, UK)

Deionised H_2O added to 800 ml

Autoclave for 20 mins at 121 °C

2.5. Cell Biological Methods and Imaging

2.5.1. Determination of optical density

The cell density of liquid *U. maydis* cultures was measured at 600 nm wavelength (OD_{600}) in a photometer (UVUB spectrophotometer; Jenway, London, UK) against fresh medium as reference. If the density of the culture exceeded 1, the culture was diluted to allow accurate measurements. A value of OD_{600} = 1 corresponds to approximately 1.5×10^7 cells/ml.

2.5.2.a1 pheromone construction and stimulation

In collaboration with Enzo Life Sciences (Exeter, Devon UK) the synthetic pheromone was derived from previous research (Szabo et al., 2002). In collaboration with BIOMOL research laboratories we modified the C-terminal from the wild-type *S*-farnesylated cysteine methyl ester to contain a primary amide, the *N*-terminus was modified to contain an AHX (6-aminohexanoic acid) linker and a 5FAM (5-carboxyfluorescein) fluorophore which binds to receptor and triggers response. The resulting pheromone was 5-FAM-Ahx-GRDNGSPIGYSSC-(farnesyl)-NH_2. Figure 2.1 shows an expanded view of the a1-5FAM pheromone highlighting the positioning of the linker and 5FAM fluorophore The synthetic pheromone was found to be functional and cells were assayed for their ability to form conjugation hyphae. Overnight cultures of cells were induced by the addition of 0.5 µl synthetic pheromone (a1, stock 2.5 µg/µl in dimethyl sulfoxide (DMSO; Carl Roth, Mühlberg, Germany)), final concentration 2.5 x 10^{-3} µg/µl; (Szabo et al., 2002) to a 500 µl cell suspension in a 2 ml reaction tube and incubated for up to 8 hours at 22 °C, 200 rpm.

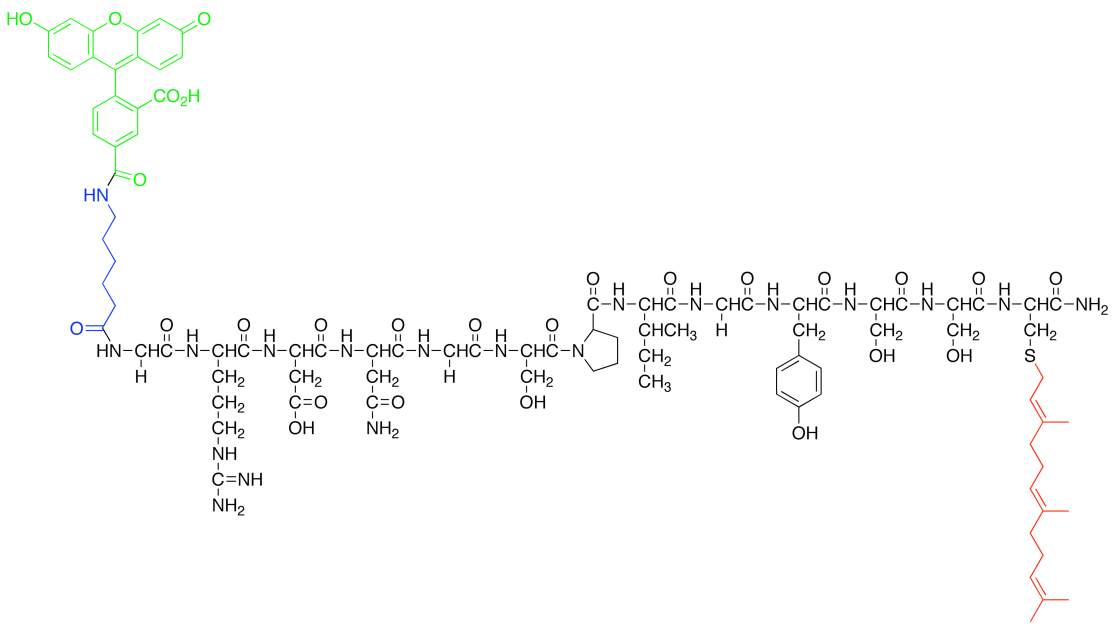

Figure 2.3. Expanded view of a1-5FAM pheromone

Image showing the expanded view of the synthesised fluorescent pheromone including, the 5FAM fluorophore (green), ahx linker (blue) and farnesyl side chain (red).

2.5.3. Inhibitor studies

For all inhibitor studies, yeast-like cells were aliquoted in 500 µl suspensions, and incubated in 2 ml reaction tubes. These were supplemented with either benomyl at 0.1-20.0 µM (stock 10 mM in DMSO, Sigma Aldrich, Steinhelm, Germany), latrunculin A (latA) at 0.1-10.0 µM (stock 20 µM in DMSO, Enzo Life Sciences, Exeter, UK) or for control strains, DMSO (Carl Roth, Mühlberg, Germany). The cells were then incubated for 1-3 hours with gentle shaking. In order to investigate the role of these inhibitors on hyphae, cells were treated with synthetic pheromone for 3 hours before the inhibitors benomyl, latrunculin A or control solvent DMSO (Carl Roth, Mühlberg, Germany) were added, followed by incubation for an additional 3 hours. Cells were sampled every hour and cell vacuole average intensity was measured and quantified by MetaMorph ® (Life Science Imaging Ltd, Buckinghamshire, UK).

2.5.4. Phenotypic analysis

To test whether mutants of myosin tails were affected in their ability to form conjugated hyphae, they were spotted onto minimal medium charcoal plates. All *U. maydis* strains myosin tail mutant strains were crossed with wild-type FB1 cells with which they would switch to filamentous growth. Both strains were plated, starting at a concentration of 10^6 cells/ml and then a series of 10-fold dilutions were spotted (5 µL per spot) on charcoal nutrient medium containing either CM-GLU or CM-ARA as the sole carbon source, to regulate the over-expression. Plates were incubated at 28 °C and the induction of hyphae was monitored after 24 and 48 h using a SMZ800 stereoscopic microscope (Nikon, Toyko, Japan).

2.5.5. Membrane and vacuole staining

In order to determine whether the cell vacuoles remain intact in the control and mutants (FB2, Myo1tail, Myo2tail, Myo5tail), the cells were incubated with 1 mg/ml of FM4-64 (N-(3-triethylammoniumpropyl)-4-(*p*-diethylaminophenyl-hexatrienyl)-pyridinium dibromide; Life technologies Ltd, Paisley, UK) in PBS (phosphate-buffered saline, pH 7.2; Roche, West Sussex, UK). Cells were

incubated for 30 minutes at RT, with shaking of 200 rpm, before being washed twice with fresh media and returned to the shaker for 30 mins and then being visualised on the microscope.

2.5.6. HBO- based epi-fluorescent microscopy

In order to visualise fluorescent proteins in a live cell, an IX81 inverted motorized microscope (Olympus, Hamburg, Germany), equipped with an UplanSApo 100x / 1.40 oil objective (Olympus, Hamburg, Germany), was used. Cells were placed on a 2 % agarose pad and observed using a 0.17 µm cover slip and Immersol TM 581F (Carl Zeiss, Jena, Germany). In order to excite the GFP tagged constructs, a USH-1030L mercury bulb (Olympus, Hamburg, Germany) was used. All images were taken using a charged-couple device camera (photometric Cool SNAP HQ, Roper Scientific, Germany). The software package MetaMorph® (Molecular Devices, Downingtown, USA) controlled all parts of the system.

2.5.7. Laser- based epi-fluorescent microscopy

The fluorescently labelled proteins were excited using a VS-LMS laser-merge-system with solid state lasers (488 nm/50 W/70 mW and 561 nm/50 mW/70 mW, Visitron System, Munich Germany). Laser intensity was controlled by a VS-AOTF100 system and coupled into the light path by using a VS-20 laser-lens-system (Visitron System, Munich, Germany). In order to avoid oxygen depletion in the samples, they were observed for no longer than 15 minutes. All measurements and image processing were carried out using MetaMorph ® (Life Science Imaging Ltd, Buckinghamshire, UK), and graphs were created using Prism4 (GraphPad, Calfornia, USA).

2.5.8. Analysis of actin patch dynamics

In order to analyse actin patches in cells, we estimated the total patch number per cell using an ellipsoid equation (Thomsen, 2014). In brief, Z-stack images of entire cells were acquired with 2 µm depth difference between images and laser intensities of 488 nm at 100 %. These images were then analysed with

MetaMorph, where the cell length (a), cell width (b) and depth (c) were taken to gauge the surface area in both mother and daughter cells, with the surface area ellipsoid equation ($SA = 4\pi[(a^pb^p + a^pc^p + b^pc^p)/3]^{1/p}$). The actin patches were then counted by hand in each frame of the Z stack, to approximate numbers of actin patches in each area. Furthermore, the dynamics of the actin patches were measured. Movies taken of wild-type and myosin tail mutant strains, with laser intensities of 488 nm at 100 %, were analysed and kymographs were drawn across the entire length of the cell. Additionally patch behaviour was split into two events (formation / scission) whereby lines were drawn on kymographs to analyse timings for each event and the raw data were stored in excel before statistical testing in Prism4 (GraphPad, Calfornia, USA).

2.5.9. Analysis of actin patch intensity data

To facilitate the experimental work in order to analyse the intensity of actin patches in the wild-type and myosin tail mutants, multiple calculations were required. In brief, movies of all strains were taken at 150 ms exposure time and image binning 1 with laser intensities of 488 nm at 80 %. In MetaMorph® (Life Science Imaging Ltd, Buckinghamshire, UK) each movie was analysed and each patch signal, which was clearly separated from the adjacent signals, was measured for average intensity for the duration of the movie. Each measurement was corrected for the adjacent background of the cell (taking a measurement from immediately adjacent to the actin patch and subtracting it), as well as a general correction to account for the bleaching of signals throughout the duration of the movie.

3. CHAPTER 3 – SYNTHETIC PHEROMONE - A NOVEL TOOL TO INVESTIGATE ENDOCYTOSIS IN *USTILAGO MAYDIS*

3.1. Introduction

The importance of small, secreted oligopeptides for intracellular communication has been described in many eukaryotic cells (Scott, 2000). In fungi, diffusible peptide hormones, known as pheromones are involved in sexual development (Bölker and Kahmann, 1993), fungal pathogenicity (Hartmann et al., 1996) and determination of cell morphology (Bölker et al., 1995). The most well-described example of these pheromones is found in the model system of *S. cerevisiae* (Wessels et al., 1994), in which the pheromones, a and α factor, are released from the two mating-types. Mating-types a and α bind to trans-membrane receptors, of which there are 800 examples in the mammalian genome and around 70 in filamentous fungi. They elicit a signalling cascade that leads to cell cycle arrest, cell morphological changes and altered gene expression (Leberer et al., 1997, Elion, 2000).

In order for some fungal pathogens to invade and colonize host tissues, it is required to make the transition from yeast-like to filamentous growth (Gow et al., 2002). In the basidiomycete *U. maydis,* this is initiated by cell fusion of two compatible yeast-like sporogenous which recognize each other by the exchange and recognition of two different peptide pheromones from the *a1* and *a2* alleles (Bölker et al., 1992). Each sporidium or sporicidal cell has a specific receptor *(Pra1 or Pra2)* for the peptide pheromone precursor *(mfa1 or mfa2)* from its partner cell (Hartmann et al., 1996). The pheromone-receptor interaction triggers a signalling cascade, which increases the production of the pheromones (Urban et al., 1996b), causing a morphological switch from yeast cells to conjugated hyphae that grow towards the pheromone source, fuse and form a dikaryon (Spellig et al., 1994, Snetselaar et al., 1996). If the

resulting dikaryon carries different alleles of the *a* and *b* locus, it is termed an infectious dikaryon, which can invade and colonize the host tissues. In *U. maydis*, both the a1 and a2 pheromones have been purified (Spellig et al., 1994) and synthetic alternatives made (Koppitz et al., 1996). Amino acid sequencing has revealed that the tri-decapeptide *a1,* (GlyArgAspAsnGlySerProIleGlyTyrSerSerCys(Farnesyl)-OMe) does not share sequence similarity with its nonapeptide counterpart *a2,* (AsnArgGlyGlnProGlyTyrTyrCys(Farnesyl)-OMe) (Spellig et al., 1994). Moreover, structure-function studies have revealed the residues essential for triggering the response for initiating filamentous growth (Szabo et al., 2002). The incorporation of *S*-farnesylated residues at the carboxy termini of both the *a1* and *a2* (Spellig et al., 1994), places them in the class of lipopeptide mating factors, similar to the aforGmentioned examples reported in *S. cerevisiae,* as well as other notable examples in *S. pombe* and *Rhodosporidium toruloides* (Akada et al., 1989). The pheromone signal has been shown to be transmitted by a mitogen-activated protein kinase (MAPK) cascade. Both pheromones a1 and a2, and their receptors, Pra1 and Pra2*,* are important in initiating the dimorphic switch to filamentous growth (Urban et al., 1996b). Previous research has shown that the pheromone receptors of *U. maydis* belong to a family of G- protein coupled receptors (GPCR) (Dohlman et al., 1991). GPCR's have been studied in depth in *S. cerevisae* and have been shown to play a role in many aspects of metabolism and signal transduction mechanisms. Manipulation of the G protein α subunit Gpa1 in *S. cerevisae* has allowed coupling of a range of mammalian GPCRs (Dowell and Brown, 2009), and their highly specific ligand recognition system, has made them a target for therapeutic agents (Wolff, 1996, Balakin et al., 2002, Klabunde and Hessler, 2002). In *U. maydis,* research done on the pheromone receptors has shown that the binding of the pheromone ligand to the receptor induces an exchange of GDP for GTP in the α subunit, specifically Gpa3. Disruption of this gene leads to mutant strains that are unable to detect the pheromone (Regenfelder et al., 1997).

The use of live cell imaging has enhanced our knowledge of endocytic events and has shown mechanistic principles of endocytic internalisation (Merrifield et al., 2002, Kaksonen et al., 2003, Sekiya-Kawasaki et al., 2003, Huckaba et

al., 2004, Kaksonen et al., 2005, Newpher et al., 2005). However, endocytosis in filamentous fungi until recently was still a matter of debate. The first indications for the existence of endocytosis came from the uptake of the endocytic marker FM4-64 by germ tubes of *Uromyces fabae* (Hoffmann and Mendgen, 1998), hyphae of *Neurospora crassa*, *Trichoderma viride* (Read et al., 1998) and cells of *S. cerevisiae* (Chuang and Schekman, 1996) and in cell wall-less protoplasts of *U. maydis* (Ayscough et al., 1997) and then later in the uptake of the amphipathic dye FM4-64 into small vesicles (Wedlich-Söldner et al., 2000). Therefore, in *U. maydis,* FM4-64 has been used to stain parts of the endocytic pathway which provided indirect evidence that endocytosis is important in polar fungal growth (Hoffmann and Mendgen, 1998, Wedlich-Söldner et al., 2000, Atkinson et al., 2002). Markers for endocytosis and vesicle trafficking both in yeast (Vida and Emr, 1995) and filamentous fungi (Read, 2000) have been identified and the specific mode of endocytosis, studied in *S. cerevisiae,* using synthetic, biologically active fluorescent mating pheromone derivatives demonstrated that receptor-mediated endocytosis occurs via a clathrin and actin-mediated endocytosis pathway. However, little is known about the pheromone uptake mechanisms or how they and the receptor are recycled within *U. maydis* cells.

The aim of the work described in this chapter is therefore

- To establish the use of modified fluorescent pheromones in *U. maydis*, specifically the a1 pheromone with a 5-carboxyfluorescein (5- FAM) marker

  (5-FAM-Ahx-GRDNGSPIGYSSC(Farnesyl)-NH_2) as a tool to investigate the endocytosis pathway
- To study the pheromone uptake
- To provide evidence for the route of endocytosis
- To determine whether it is dependent on the receptor and the cellular cytoskeleton

3.2. Results

3.2.1. Ustilago maydis synthetic peptide pheromone synthesis

The structures of both the a1 and a2 *U. maydis* pheromones are known (Figure 3.1. A). The a1 pheromone is a C-terminal methyl ester consisting of 13 amino acids (GlyArgAspAsnGlySerProIleGlyTyrSerSerCys(Farnesyl)-OMe) and the a2 pheromone contains 9 amino acids (AsnArgGlyGlnProGlyTyrTyrCys(Farnesyl)-OMe). Both pheromones are farnesylated at the sulfur atom of their C-terminal cysteine residues (Spellig et al., 1994) and previous research has shown which residues are essential for function (Koppitz et al., 1996). Thanks to a collaboration with BIOMOL, we were able to obtain synthetic pheromones, prepared using standard solid phase techniques, (as described in (Frank and Gausepohl, 1988). The farnesyl group on the C terminus of both pheromones was added after cleavage of the peptide from the solid support to prevent degradation during cleavage. We decided to concentrate on the a1 pheromone, as it proved to be easier to synthesize and had never been visualised in living cells prior to the start of this project. During discussions with BIOMOL it was decided that the ester on the C-terminal could cause some problems for synthesis. This is because of the available method for synthesis, in which the carboxyl-terminal amino acid is anchored to a solid support and then the remaining amino acids are added one at a time, lends itself to cleaving off the peptide as a primary amide. It is considerably more difficult to cleave off the peptide as an ester, so it was decided that the first peptide made would be a switch from an ester to an amide at the C-terminus (Figure 3.1. B). The second peptide to be considered was one that changed a glycine at position five for lysine towards the centre of the amino acid sequence. This change would allow for the amino group in the side chain of the lysine to be used as an anchor for a fluorophore in additional experiments (Figure 3.1. C). In order to label the pheromone with a fluorescent tag for tracking the movement of the pheromone during endocytosis and also its eventual recycling, three fluorophores were considered (Figure 3.1. D). 5-carboxy-X-rhodamine (ROX) (Figure 3.1. F) and sulforhodamine 101 acid chloride (TEXAS RED) (Figure 3.1. G) were used because of their widespread use as fluorescent probes, which can be excited

at 615 nm (red wavelength). 5-Carboxyfluorescein (5-FAM) (Figure 3.1. H) was used for excitation at 492/517 nm (green wavelength) and as it is similar in structure to ROX and TEXAS RED and therefore will retain its stability (Eaton, 1980). In order to attach the Texas Red and 5-FAM fluorophores, a 6-aminohexanoic acid (Ahx) linker was used so that the fluorophore was kept a reasonable distance from the *N*-terminus of the peptide itself. This was done in order to inhibit any inference with the biological activity of the peptide and to make sure that none of the amino acid side chains reacted with it (Figure 3.1. E).

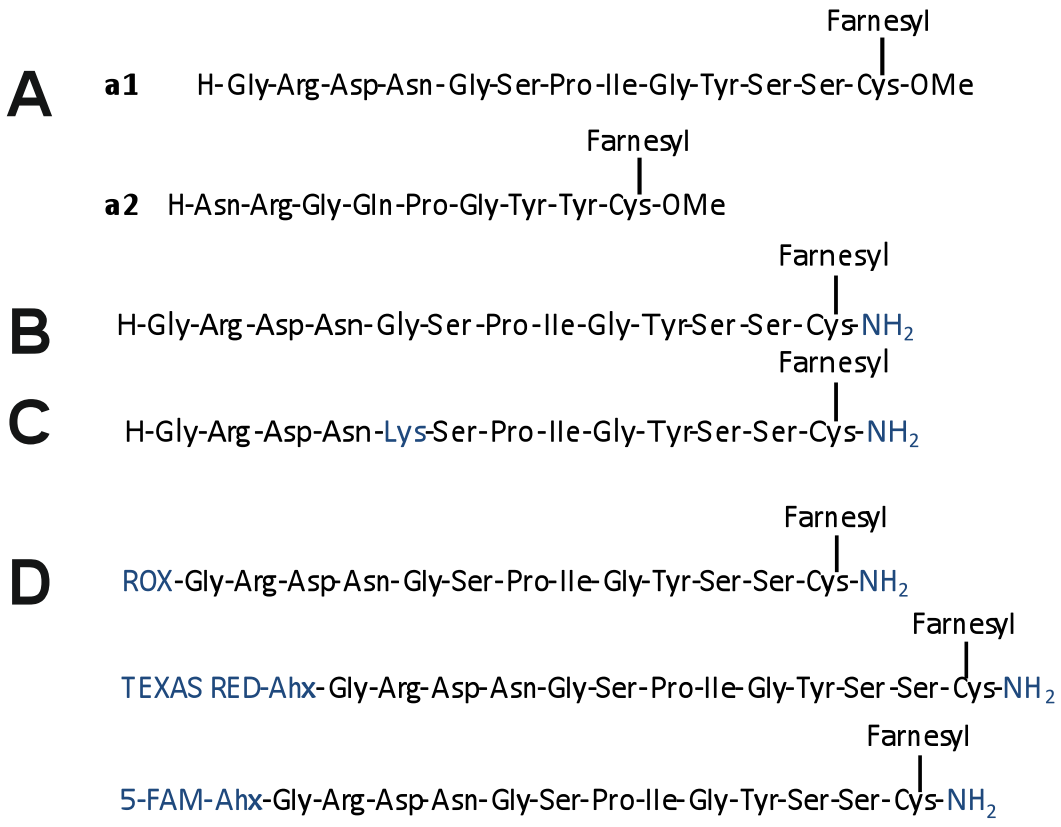

Figure 3.1. Wild-type *U. maydis* mating factor pheromone structure and proposed synthetic additions.

A. Amino acid sequences of naturally occurring *Ustilago maydis* a1 and a2 pheromones. The abbreviations listed above relate to the following aa's, Gly; glycine, Arg; arginine, Asp; aspartic acid, Asn; asparagine, Ser; serine, Pro; proline, Ile; isoleucine, Tyr; tyrosine, Cys; cysteine, Gln; glutamine, OMe; methyl ester.
B. Proposed addition to C terminus of the a1 pheromone, an amide group (blue) in exchange for the natural methyl ester
C. Proposed change in amino acid between a glycine at position 5 (blue) for a lysine
D. Proposed additions of fluorescent fluorphores (blue) to C terminus of a1 pheromone

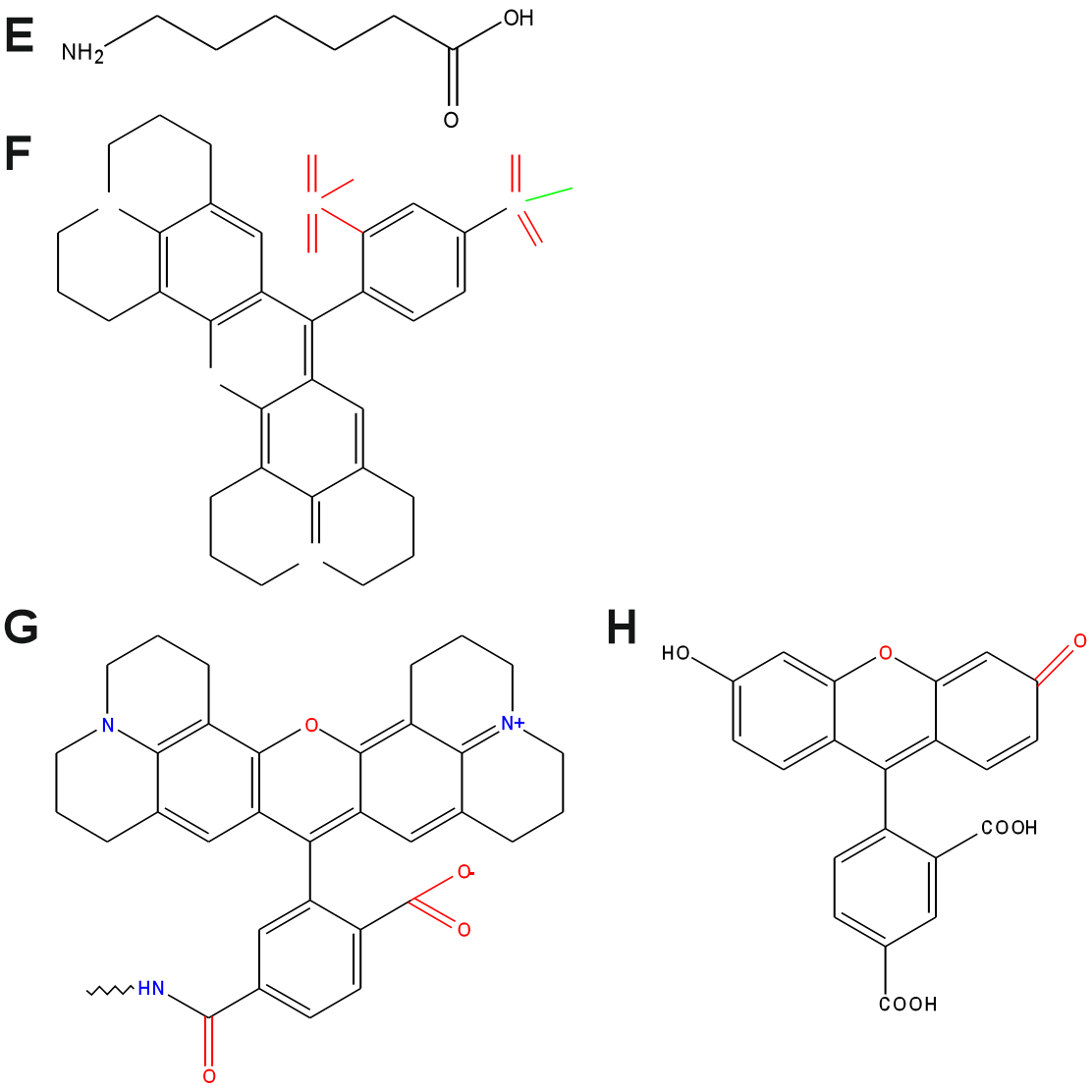

E. Schematic of amino-hexanoic acid linker (Ahx)

F. Chemical structure of ROX fluorophore attached to the a1 peptide

G. Chemical structure of TEXAS RED fluorophore attached to the a1 peptide

H. Chemical structure of 5-FAM fluorophore attached to the a1 peptide

3.2.2. The synthetic a1 amide and a1-5FAM pheromones are able to induce filamentous growth of U. maydis

The first morphological alteration observed in response to the pheromone in wild-type cells is the production of conjugation hyphae, which are tail-like structures formed preferentially at one tip of the cell (Snetselaar and Mims, 1992, Spellig et al., 1994). The cells form these conjugation hyphae as a result of arresting their cell cycle at the G2 checkpoint, so that the cytoskeletal growth machinery such as dynein, is present to help in polar growth towards the pheromone source (García-Muse et al., 2003). We tested the ability of the synthetically produced pheromones to initiate the switch from yeast-like to filamentous growth and their ability to form conjugated hyphae. Wild-type FB2 cells (Figure 3.2. A) were incubated with 2.5 µg/µl of each synthetic pheromone (dissolved in DMSO) and observed after 24 hours under the microscope (control for DMSO shown in Figure 3.2. B). We compared each of the synthetically produced pheromones with the control a1 pheromone (Figure 3.2. C), which typically shows conjugation hyphae of 40-50 µm in length. It was found that the change from ester to amide on the C terminus of the a1 pheromone (Figure 3.2. D) and the incorporation of a 5-FAM fluorophore (Figure 3.2. E) still induced a switch to filamentous growth and the formation of hyphae with comparable lengths to that of the natural pheromone. However, the change of amino acid from glycine to lysine (Szabo et al., 2002) (Figure 3.2. F) and the incorporation of the fluorophores, ROX (Figure 3.2. G) and TEXAS RED (Figure 3.2. H), meant that the cells remained yeast-like and continued to bud after 24 hours incubation, suggesting they had not entered cell cycle arrest at the G2 checkpoint and had not begun to grow towards the pheromone source.

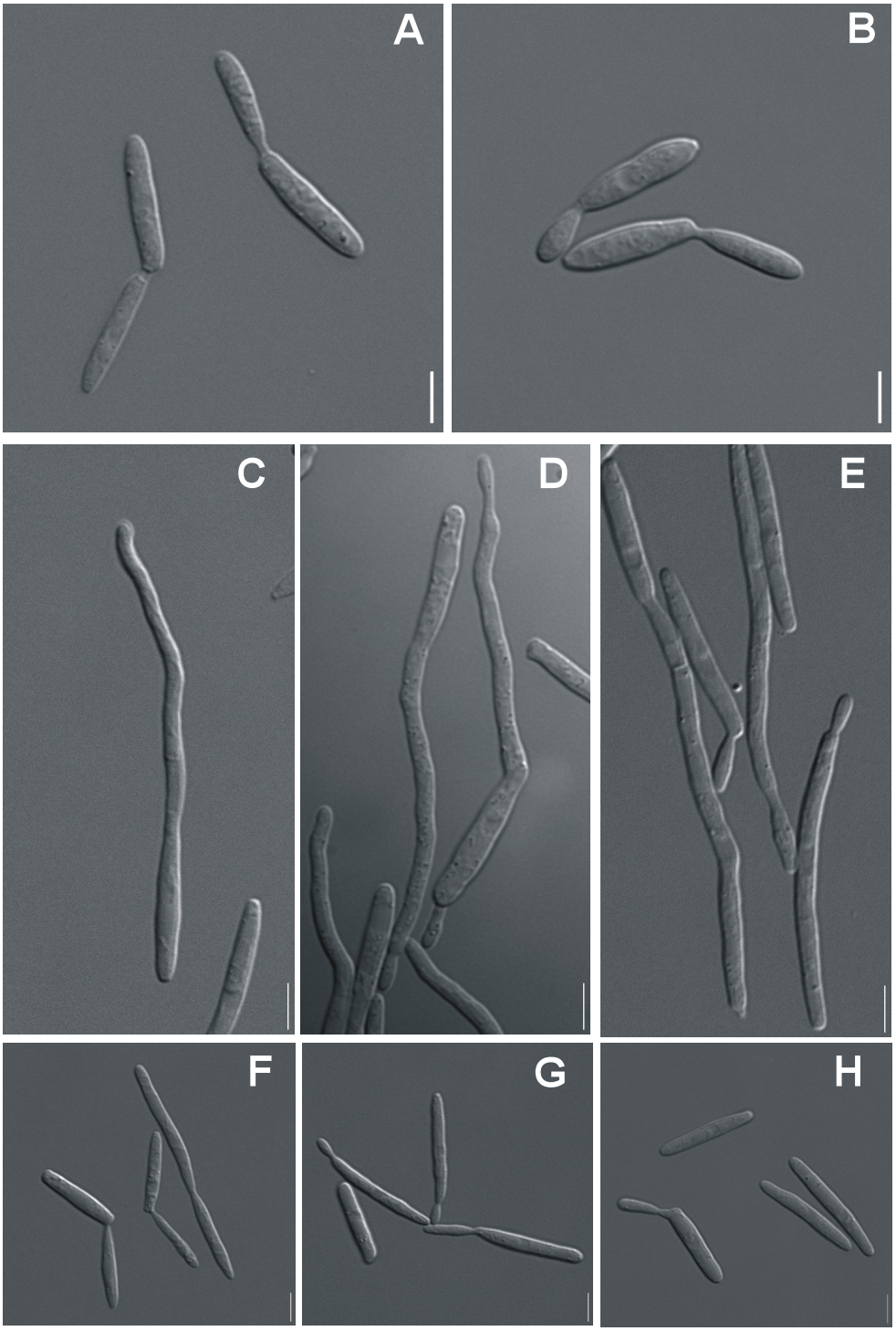

Figure 3.2. Incubation of synthetic pheromones with wild-type FB2 cells.

A. Wild-type FB2 cells incubated in CM-GLU media for 24 hours.
B. Wild-type FB2 cells incubated in CM-GLU + DMSO (concentration 2.5 µg/µl) for 24 hours to show no difference to wild-type FB2 cells incubated in just CM-GLU for 24 hours (A).
C. Wild-type FB2 cells incubated with natural a1 pheromone at a concentration of 2.5 µg/µl for 24 hours.

D. Wild-type FB2 cells incubated with synthetic amide a1 pheromone at a concentration of 2.5 µg/µl for 24 hours.
E. Wild-type FB2 cells incubated with synthetic 5-FAM a1 pheromone at a concentration of 2.5 µg/µl for 24 hours. Cells shown in (C), (D) and (E) show normal switch to filamentous growth.
F. Wild-type FB2 cells incubated with synthetic gly/lys a1 pheromone at a concentration of 2.5 µg/µl for 24 hours.
G. Wild-type FB2 cells incubated with synthetic ROX a1 pheromone at a concentration of 2.5 µg/µl for 24 hours.
H. Wild-type FB2 cells incubated with synthetic TEXAS RED a1 pheromone at a concentration of 2.5 µg/µl for 24 hours.

3.2.3. The a1 5-FAM synthetic pheromone displays a similar working concentration to that of wild-type a1 pheromone.

Synthetic alternatives to the naturally occurring pheromones for *S. cerevisiae* have been proposed and shown biological activity (Fujimura et al., 1982, Sherrill et al., 1995). In *U. maydis* modified pheromones have been isolated and these have shown a specific sequence motif deemed to be the response element (Spellig et al., 1994, Urban et al., 1996b). However, with all synthetic derivatives, it is necessary to compare them all with pheromone isolated from wild-type cells in terms of the lowest working concentration required to induce a response. In *U. maydis* it has been shown both in structure function studies (Szabo et al., 2002) and *in vivo* cellular assay studies (Fuchs et al., 2006) that an optimal working concentration for the wild-type a1 pheromone is 2.5 µg/µl. In order to establish the lowest working concentration of the a1-5FAM pheromone we compared it with the unlabelled a1 pheromone isolated from wild-type cells. As a control, we incubated wild-type FB2 cells with DMSO, the solvent used to dissolve the synthetic pheromone. We observed there to be no defect in cell morphology at 1.0 µg/µl (Figure 3.3. A), 2.5 µg/µl (Figure 3.3. B) and 5.0 µg/µl (Figure 3.3. c) concentrations. We then incubated FB2 cells with 1.0 µg/µl, 2.5 µg/µl and 5.0 µg/µl concentrations of both synthetic and natural pheromones for 6 hours and observed under the microscope and the percentage of the cells that formed conjugated hyphae. With the unlabelled natural pheromone at 1.0 ug/ul (Figure 3.3. D) we observed that not all cells

switched to filamentous growth whereas a concentration of 2.5 µg/µl (Figure 3.3. E), showed the most filamentous hyphae. It was found that after prolonged incubation with 5.0 µg/µl of the natural pheromone the cell vacuoles become pronounced in the DIC images suggesting that the cells were dead (Figure 3.3. F). We also noticed that some cells displayed division at both cell tips suggesting that the cells required a threshold value of the pheromone to grow normally. In comparison, the a1-5FAM pheromone does not appear to induce filamentous growth at a concentration of 1.0 ug/ul (Figure 3.3. G), whereas it did at 2.5 µg/µl (Figure 3.3. H) and again the cells showed signs of distress at 5.0 µg/µl (Figure 3.3. I) suggesting it also works better at the lower concentration.

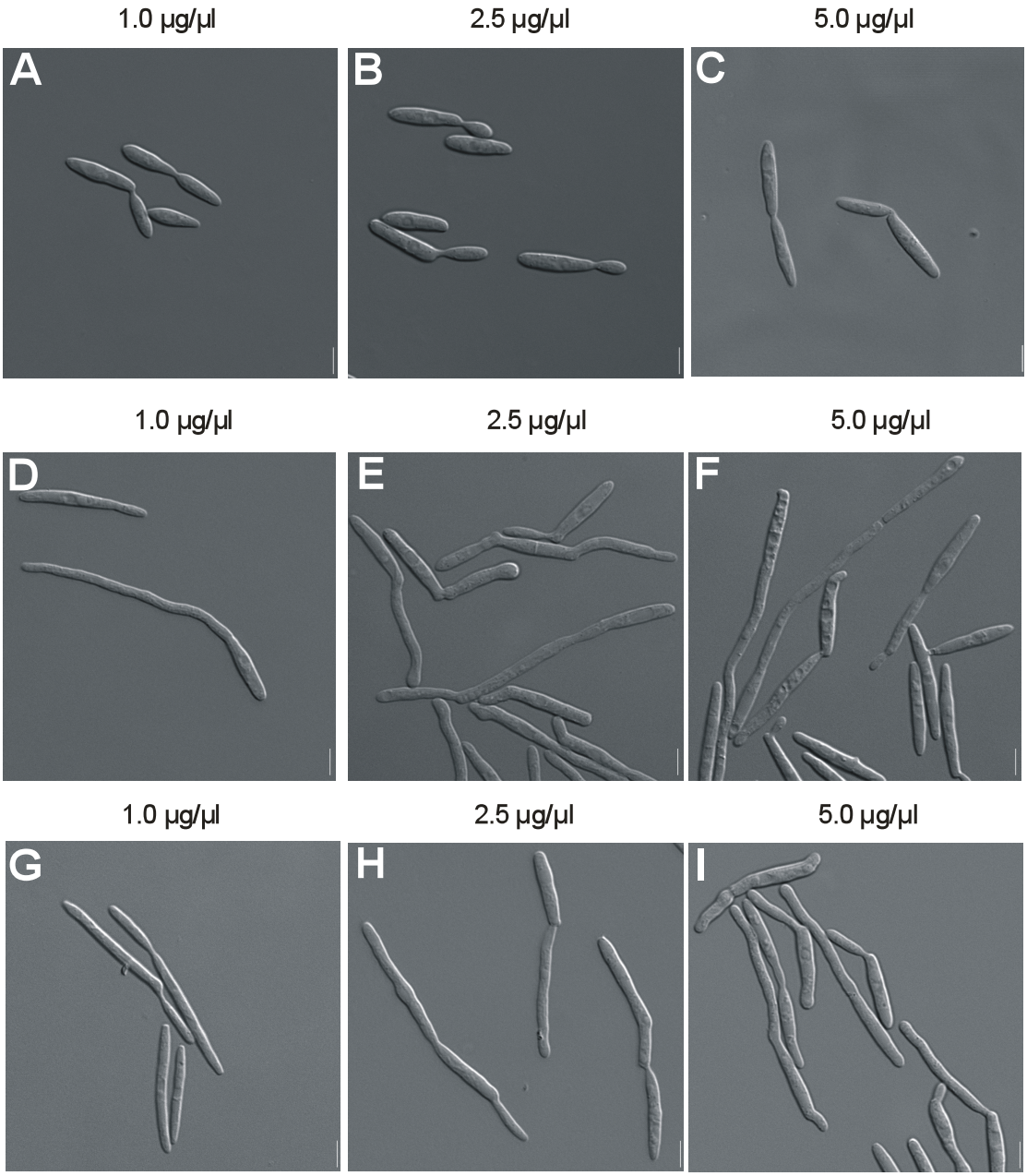

Figure 3.3. Concentration analysis of natural and synthetic a1-5FAM pheromone.

A. FB2 cells incubated for 6 hours with 1.0 µg/µl of DMSO.
B. FB2 cells incubated for 6 hours with 2.5 µg/µl of DMSO.
C. FB2 cells incubated for 6 hours with 5.0 µg/µl of DMSO.
D. FB2 cells incubated for 6 hours with 1.0 µg/µl of natural pheromone.
E. FB2 cells incubated for 6 hours with 2.5 µg/µl of natural pheromone.
F. FB2 cells incubated for 6 hours with 5.0 µg/µl of natural pheromone.
G. FB2 cells incubated for 6 hours with 1.0 µg/µl of a1-5FAM pheromone.
H. FB2 cells incubated for 6 hours with 2.5 µg/µl of a1-5FAM pheromone.
I. FB2 cells incubated for 6 hours with 5.0 µg/µl of a1-5FAM pheromone.

3.2.4. Cells treated with the a1-5FAM synthetic pheromone show filamentous growth and uptake.

Endocytosis has been shown to occur with commercially bought dyes such as FM4-64 which, when endocytosed into the cell, is transported along split pathways, with some dye entering a recycling pathway and the rest travelling to the vacuole (Wiederkehr et al., 2000). In order to fully understand the assembly and dynamics of the endocytic machinery such as cargo recruitment, concentration, internalisation and trafficking, an external fluorescently labelled cargo such as the a1 pheromone needs to be introduced into the cell. We first incubated wild-type FB2 cells with synthetic pheromones tagged with three fluorophores, (Figure 3.4. A). FB2 cells were used as they carry the Pra2 receptor, which binds to the pheromone and initiates the growth response. We used 2.5 µg/µl concentrations of each fluorescent pheromone as a starting point, as results gained in previous studies (Figure 3.3 D) indicated that it was the optimum concentration (Szabo et al., 2002). After 6 hours of incubation, we observed under the microscope, the location of the fluorescent pheromone in the cell, its intensity and the ability of the cell form conjugation hyphae. It was found that the a1-ROX (Figure 3.4. B, C) and a1-TEXAS RED (Figure 3.4. D, E) synthetic pheromones, which we had demonstrated, did not produce a filamentous response or conjugation hyphae (Figure 3.2) were internalised into the wild-type cells and showed accumulation of fluorescent signal throughout the cell (Figure 3.4. C, E). This indicated that they were not inhibited in the initial endocytic process in which they are internalised into the cell but they did not induce the morphogenetic switch to filamentous growth. In comparison, the a1-5FAM derivative was shown previously to induce a filamentous growth response (Figure 3.2) and in this experiment, the fluorescently labelled a1 pheromone was internalised into the cell (Figure 3.4. F, G). It was shown to accumulate in large compartments throughout the cell, indicating that the incorporation of the 5-FAM fluorophore did not inhibit biological function and that it remains stable in cellular assay experiments.

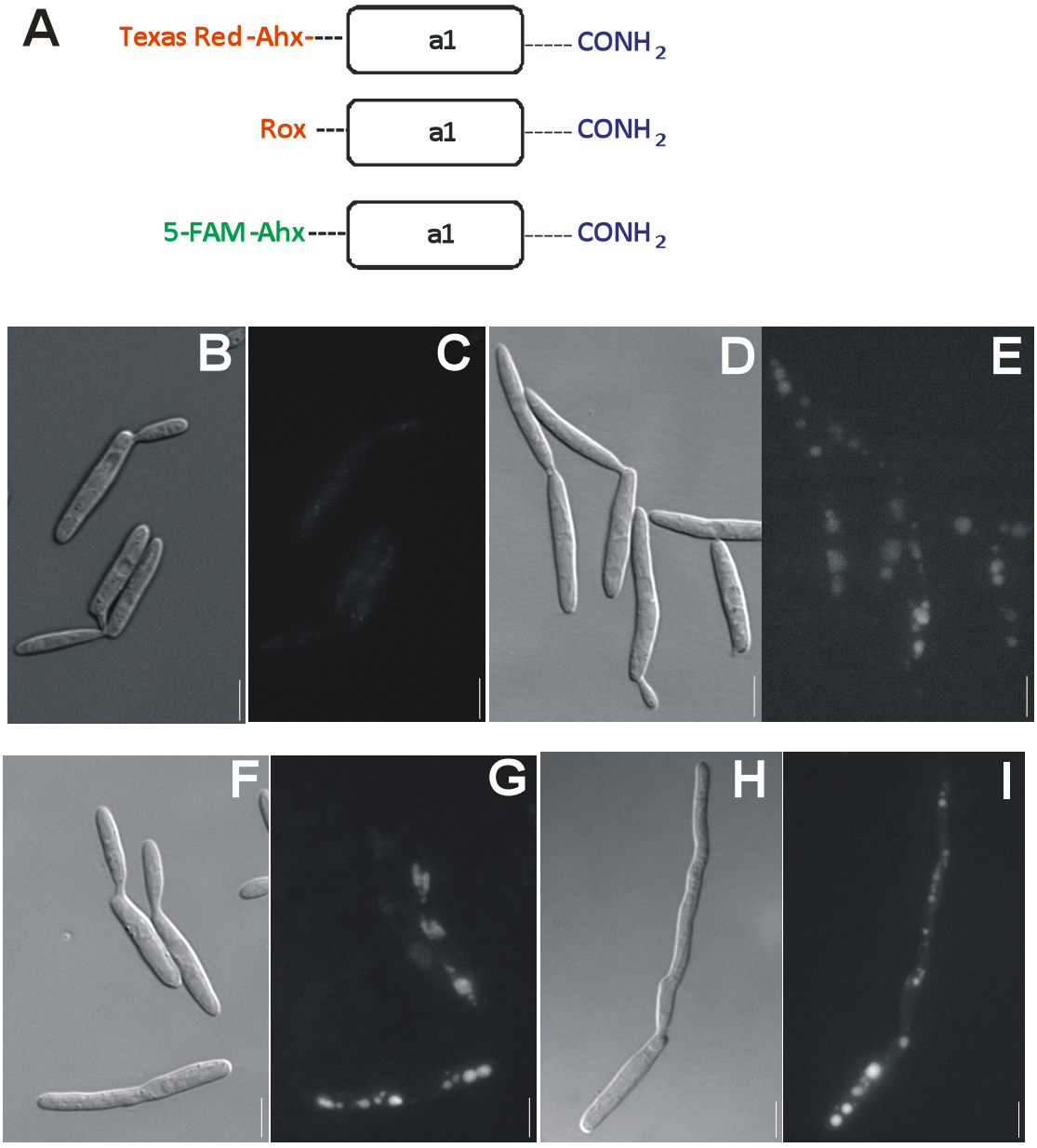

Figure 3.4. Fluorescent analyses of FB2 cells induced with tagged pheromones

A. Schematic representations of the structure of fluorescent pheromones labelled with TEXAS RED, ROX and 5-FAM-Ahx.
B. DIC image of wild-type FB2 cells incubated in CM-GLU media
C. GFP labelled image of wild-type FB2 cells incubated in CM-GLU
D. DIC image of wild-type FB2 cells incubated with ROX tagged a1 pheromone for 3 hours.
E. RFP image of wild-type FB2 cells incubated with ROX tagged a1 pheromone for 3 hours.

F. DIC image of wild-type FB2 cells incubated with TEXAS RED tagged a1 pheromone for 3 hours.
G. RFP image of wild-type FB2 cells incubated with TEXAS RED tagged a1 pheromone for 3 hours.
H. DIC image of wild-type FB2 cells incubated with 5-FAM tagged a1 pheromone for 3 hours.
I. GFP labelled image of wild-type FB2 cells incubated with 5-FAM tagged a1 pheromone for 3 hours.

3.2.5. The a1-5FAM synthetic pheromone is internalised via cell tips but is not constantly endocytosed

3.2.5.1. The initial internalisation pathway of the a1-5FAM synthetic pheromone is via cell tips

Endocytosis of cellular material is a rapid process and in response to a stimulus, yeast receptors or transporters are internalised and degraded within 20 minutes (Hicke and Riezman, 1996; Springael and Andre, 1998). In *U. maydis,* the pheromones and their receptors are responsible for triggering cellular fusion and cell cycle arrest (Spellig et al., 1994, García-Muse et al., 2003) thereby a switch between yeast-like and filamentous growth can occur. In order to establish the pathway of endocytosis for the pheromone, we incubated FB2 cells with the a1-5FAM pheromone and observed the location of the pheromone every 60 minutes. We found that the initial point of endocytosis was at the cell tips (Figure 3.5. A), with an accumulation of the pheromone leading to a 'cap-like' structure. During the remainder of the 3 hour time course, it was discovered that the pheromone fluorescent signal accumulated in a cellular compartment (Figure 3.5. B), which was perceived to be the cell vacuole, where it remained, suggesting it to be its end point.

3.2.5.2. The a1-5FAM pheromone is not constantly endocytosed

With a view to providing evidence as to whether the pheromone/receptor system present in *U. maydis* is similar to that of *S. cerevisiae*, where the Ste3

receptor is continually recycled back to the plasma membrane and the a-pheromone is continually endocytosed (Davis et al., 1993), we decided to measure the average fluorescent intensity of cell vacuoles. This was carried out at 15 minute intervals over a 3 hour time period after cells were induced with the a1-5FAM pheromone (Figure 3.5. C). It was decided that the cell vacuoles provided the best compartment to constantly view and measure the accumulation of the fluorescent pheromone. This was because a single pheromone molecule and its receptor were hard to visualise while moving and the cell vacuoles were the end point of the pheromone/receptor endocytosis pathway. The results show that the average fluorescent intensity of the cell vacuoles increased steadily for the first 150 minutes, suggesting that the pheromone is indeed continually endocytosed. However, after 150 minutes, we observed a peak of 897.00 AU and then a slight decline in average intensity to 693.85 AU suggesting that the pheromone is being degraded and therefore the decrease in fluorescent signal detected.

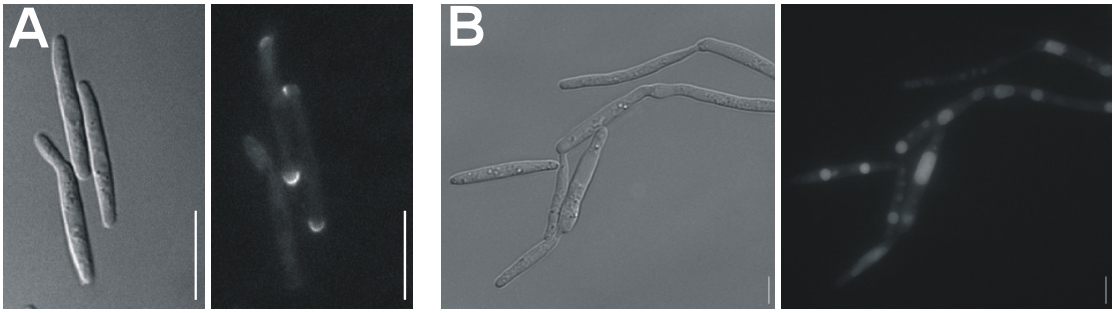

Scale bar represents 5 µm.

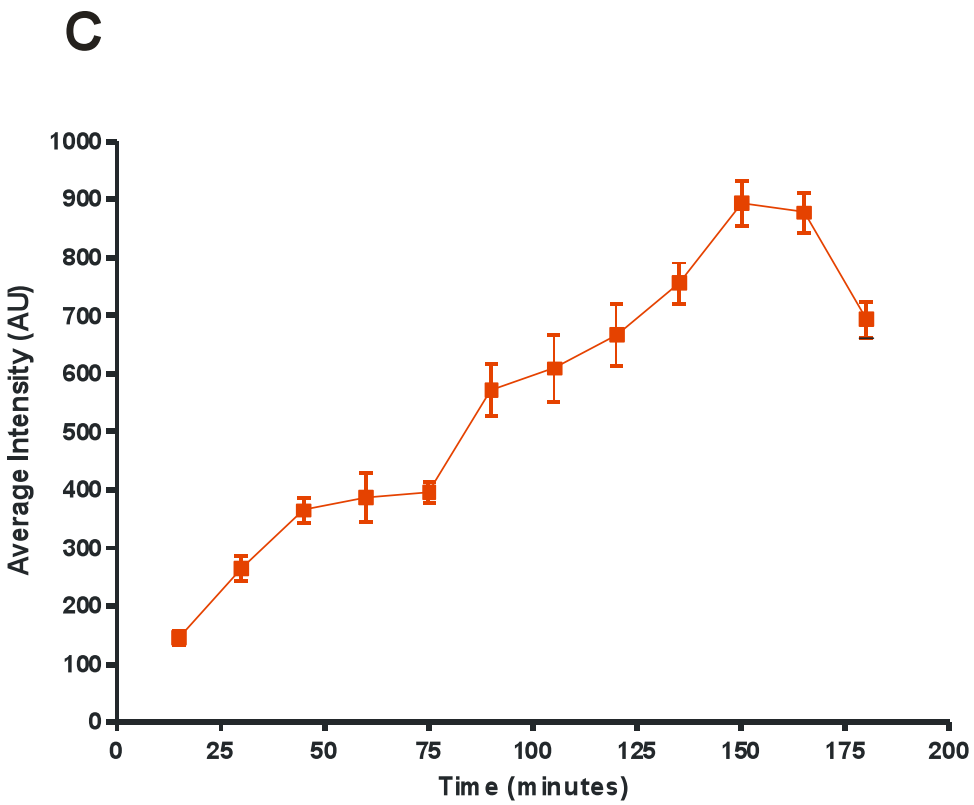

Figure 3.5. The a1-5FAM pheromone is constantly endocytosed.

A. DIC (left panel) and fluorescently 5FAM labelled (right panel) picture detailing the initial point of pheromone uptake after 15 minutes incubation with the a1-5FAM pheromone

B. DIC (left panel) and fluorescently 5FAM labelled (right panel) pictures detailing the end point of endocytosis for the pheromone in the vacuole after 3 hours incubation with a1-5FAM pheromone.

C. Quantification of the average intensity of cell vacuoles, following incubation with the a1-5FAM pheromone over 3 hours. Bars are given as ± standard error of the mean; the sample size ranges from 120 -140 cells per bar.

3.2.6. The a1-5FAM pheromone is recycled to the cell vacuole

In yeast, single internalisation and transport steps can be studied using the pheromone α-factor, which is internalised by receptor-mediated endocytosis. Once inside the cell, the α factor pheromone passes sequentially through two distinct compartments, called early and late endosomes, before it reaches the vacuole to be degraded (Singer-Krüger et al., 1994). The yeast vacuole is regarded as being very similar to lysosomes from mammalian cells; both are acidic compartments which contain a variety of hydrolytic enzymes involved in degradation and nutrient recycling processes (Dulic and Riezman, 1990). In *S. cerevisiae,* mutants lacking a functional vacuole are defective for aspects of the pheromone response (Raths et al., 1993). To investigate whether the cell vacuoles were the end point for the internalised a1-5FAM pheromone, we incubated the cells for three hours with a1-5FAM before adding, 0.5 µg/µl of CellTracker™ Blue CMAC (7-amino-4-chloromethylcoumarin) for 30 minutes. The addition of CMAC, a fluorescent cell probe that passes through cell membranes and is converted into cellular reaction products, would allow us to label the yeast vacuole. Its excitation at a different wavelength to GFP meant that we could visualise both dyes in one cell and analyse the co-localisation of both the CMAC dye and the synthetic a1-5FAM pheromone. We selected groups of cells (Figure 3.6. A) that had begun to switch to filamentous growth and compared the pheromone signal (Figure 3.6. B), with the CellTracker™ Blue CMAC signal (Figure 3.6. C) pictures from the HBO lamp for co-localisation before aligning them using MetaMorph® (Figure 3.6. D). It was found that the signals co-localised suggesting the synthetic a1-5FAM pheromone did in fact localise with the CMAC in the cell vacuoles.

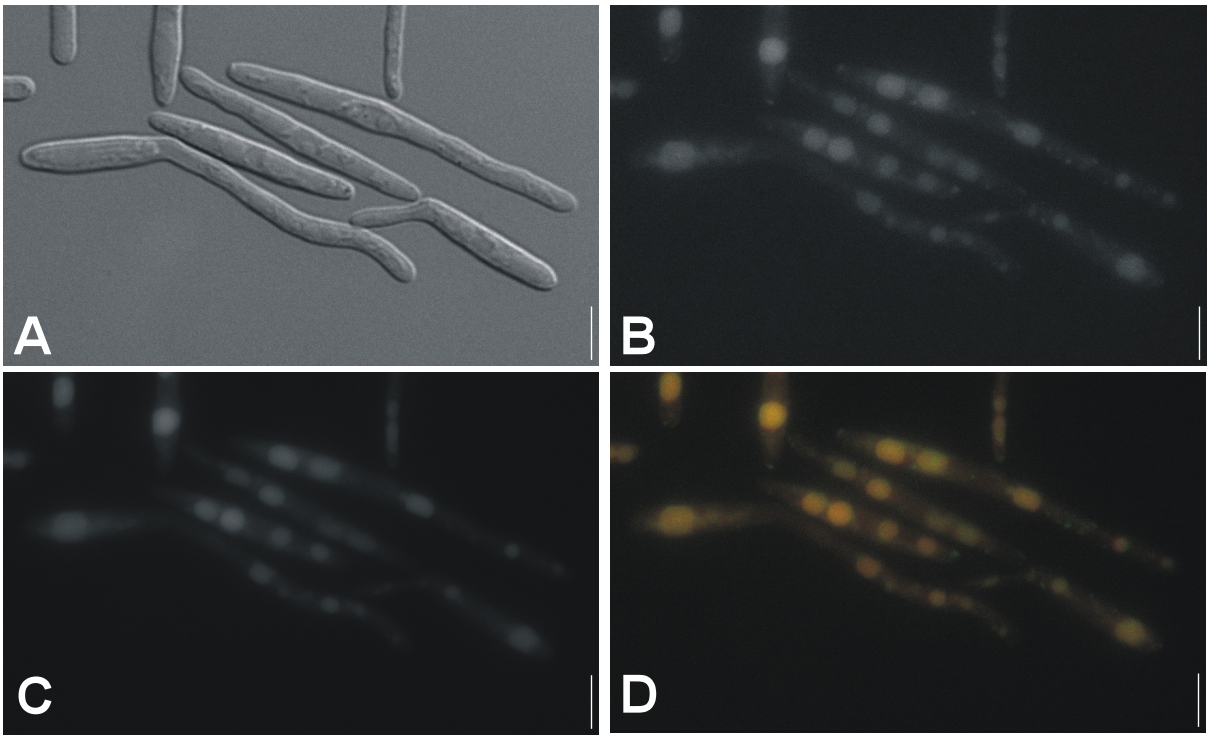

Figure 3.6. The end point of a1-5FAM endocytosis is the cell vacuole.

A. DIC picture of FB2 cells induced for 4 hours with a1-5FAM pheromone.
B. Fluorescently FAM labelled FB2 cells induced for 4 hours with a1-5FAM pheromone.
C. FB2 cells stained with vacuolar cell dye, cell tracker blue.
D. Alignment of B and C to observe alignment. Pheromone signal aligns completely with the cell tracker blue signal

3.2.7. Endocytosis of a1-5FAM synthetic pheromone is receptor-mediated.

In animal cells, receptor-mediated endocytosis occurs when receptors are exposed to specific ligands, inducing a clustering of receptor–ligand complexes into the plasma membrane (Anderson et al., 1978, Goldstein et al., 1979). *S. cerevisiae* has also been shown to carry out receptor-mediated endocytosis of its mating factors (Jenness and Spatrick, 1986, Davis et al., 1993). Immunofluorescence microscopy has shown that Ste2 (the receptor for the yeast mating pheromone α-factor) internalizes bound α factor pheromone

in a time-, energy-, and temperature-dependent manner (Jenness and Spatrick, 1986, Dulic and Riezman, 1990). Mutants such as Ren1, have been found to be defective in receptor endocytosis and shown to accumulate the internalised a-factor receptor in a pre-vacuolar compartments (Davis et al., 1993). To provide evidence as to whether endocytosis of the a1-5FAM pheromone is indeed receptor-mediated, we incubated the a1-5FAM pheromone with both FB1 and FB2. FB1 cells contain the Pra1 receptor whereas FB2 cells contain the compatible Pra2 receptor for the a1 pheromone. Upon microscopic observation after 3 hours, we could observe that FB1 cells did not internalize or transport the a1-5FAM pheromone into the cell vacuoles (Figure 3.7. A). This varied significantly with the FB2 cells that internalised and accumulated large quantities of the pheromone in their cell vacuoles (Figure 3.7. B). In order to quantify this further, we incubated the a1-5FAM synthetic pheromone with both cell lines for 8 hours and measured every hour, the average fluorescence intensity of cell vacuoles. It was found that the average intensity for FB1 cells remained throughout at no more than 100 AU, whereas the FB2 cells showed an significant increase over the first three hours, peaking at 3 hours with an intensity reading of 725 AU, before reaching a plateau and entering a decline in the remaining hours of the experiment (Figure 3.7 C). This steep incline and then gradual decline suggests that an optimum level of pheromone is required to induce the filamentous response and that once the signal cascade is initiated the pheromone is no longer required and is therefore degraded.

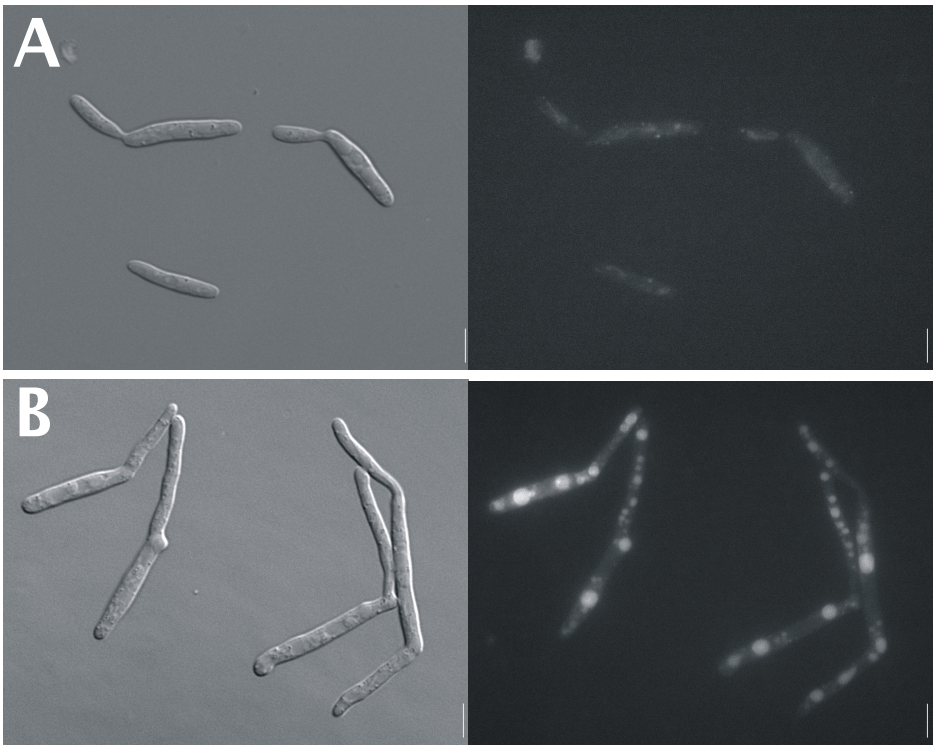

Scale bar represents 5 µm.

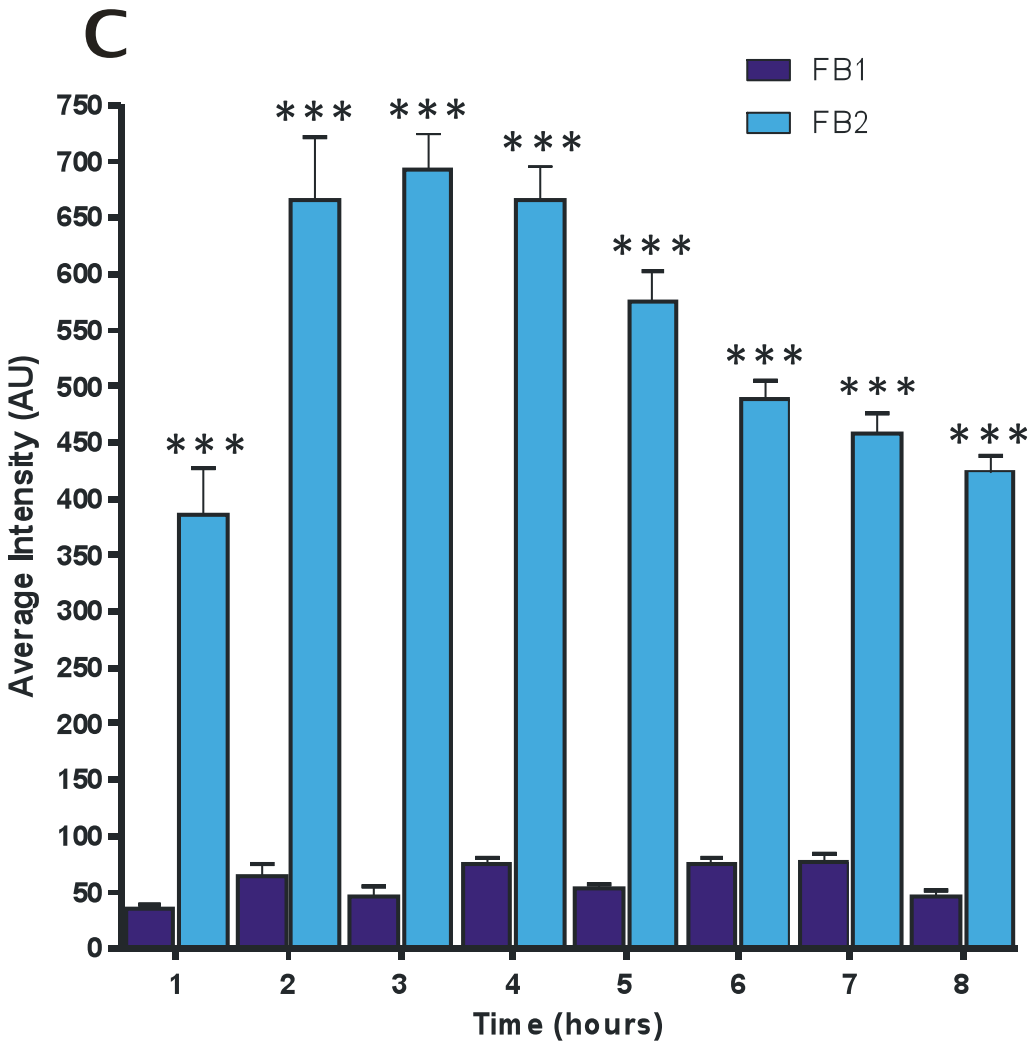

Figure 3.7. Endocytosis of a1-5FAM is receptor-mediated

A. DIC (left panel) and fluorescently FAM labelled (right panel) pictures showing FB1 cells after 3 hours incubation with a1-5FAM pheromone. No uptake is visible.
B. DIC (left panel) and fluorescently FAM labelled (right panel) pictures showing FB2 cells after 3 hours incubation with a1-5FAM pheromone. The pheromone is delivered to the vacuoles.
C. Quantification of the average intensity of cell vacuoles following incubation of both cell lines, FB1 and FB2 with the a1-5FAM pheromone over 8 hours. Bars are given as ± standard error of the mean; the sample size ranges from 130-150 cells per bar. Triple asterisk indicates significant difference between FB1 and FB2 at each time point, with $P < 0.001$ using a t-test assuming for unequal variances.

3.2.8. The actin and microtubule cytoskeleton is important for endocytosis of the a1-5FAM pheromone

3.2.8.1. Cytoskeletal inhibitors benomyl and latrunculin A act as cytoskeleton disruptors in U. maydis

Inhibitors such as benomyl and latrunculin A have long been used in cellular biology experiments to disrupt the microtubule and actin cytoskeletons respectively (Straube et al., 2003, Berepiki et al., 2010). Benomyl is a member of the benzimidazole class of compounds that, at appropriate concentration, cause the de-polymerisation of MTs within 15 minutes of incubation, both in yeast (Stearns et al., 1990) and filamentous fungi such as *U. maydis* (Straube et al., 2003). Latrunculin A, a toxin purified from the red sea sponge *Latrunculia magnifica*, causes complete disruption of the yeast actin cytoskeleton within 2–5 min (Ayscough et al., 1997) and in *U. maydis,* it has been shown to disrupt the localisation of myosin-5 (Weber et al., 2003), Pra1 (Fuchs et al., 2006) and actin patch component Fim1 (Castillo-Lluva et al., 2007).

In order to confirm that these inhibitors show the expected effects in *U. maydis,* we tested known working concentrations of each inhibitor, using information from previous studies (Castillo-Lluva et al., 2007, Weber et al.,

2003) against tagged control strains to check for the inhibitor efficiency. A GFP-tagged tubulin strain was used to test benomyl (Figure 3.8. A). In order to show the effects of the drugs were indeed reversible, we washed the cells with fresh media and allowed the cells to recover for two hours, after which time, cells displayed long MTs again (Figure 3.8. A, right panel). An eGFP tagged lifeact peptide strain was used to test latrunculin (Figure 3.8. B). The use of the 17 aa lifeact peptide was first developed to visualise F-actin in budding yeast (Riedl et al., 2008) but then extended to filamentous fungi (Berepiki et al., 2010) and *U. maydis* (Schuster et al., 2011c). Prior to treatment, dynamic actin patches were clearly visible throughout the cell (Figure 3.8. B, first panel), however these patches had disappeared and the fluorescence background in the cell was significantly increased following a 15 minute incubation in Lat A (Figure 3.8. B, centre panel). When we washed the cells with fresh media and allowed the cells to recover for two hours, we found that the effect of latrunculin A was indeed reversible, and the cells displayed actin patches throughout the cell and a decrease in fluorescent cellular background (Figure 3.8. B, right panel). These results suggest that both benomyl and latrunculin are functional in *U. maydis* and that the destablising effects they induce are reversible.

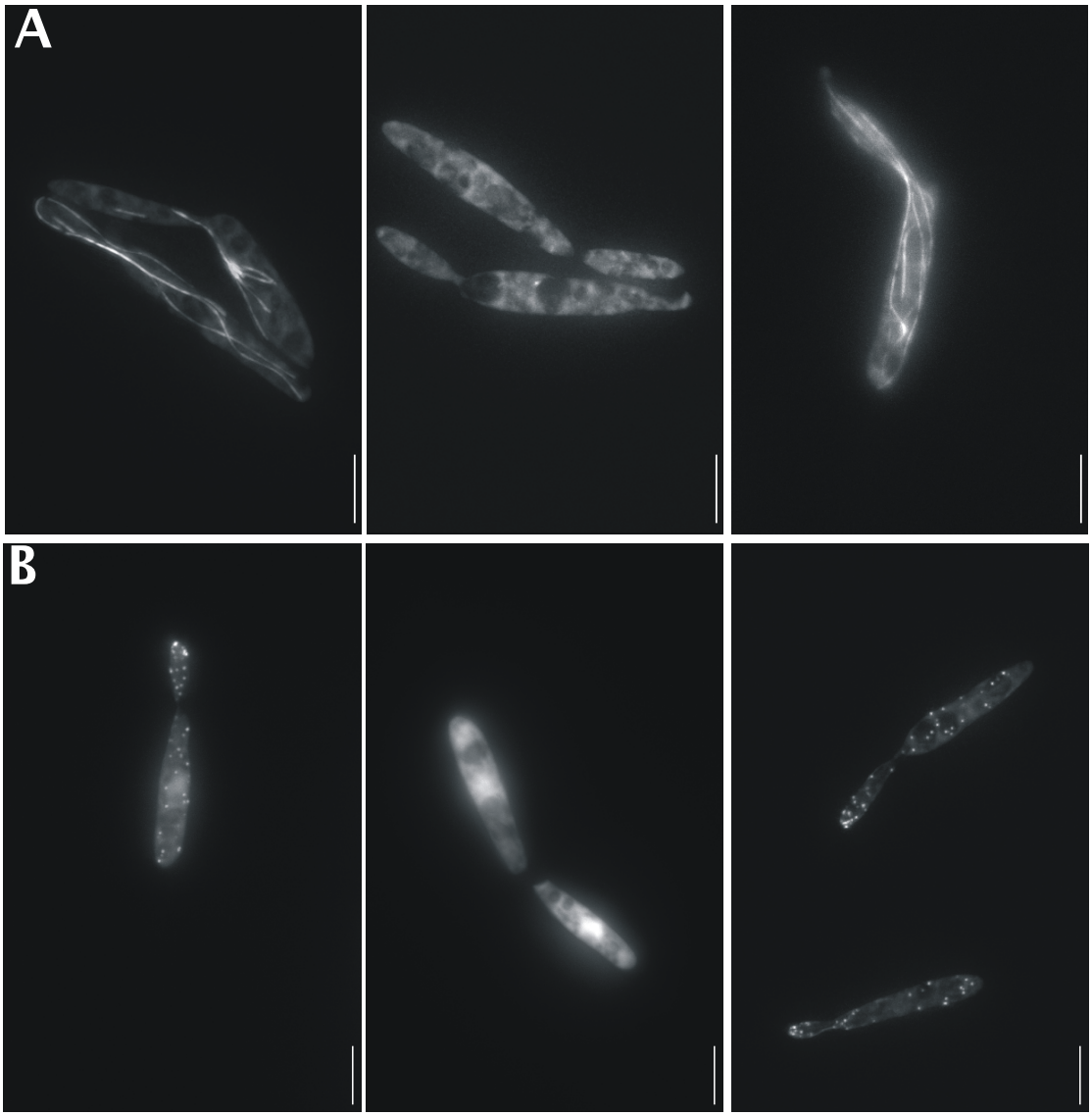

Figure 3.8. Cellular inhibitors benomyl and latrunculin A work in *U. maydis*

A. Control strain GFP-labelled tubulin before (left panel), during treatment with 20 µM benomyl (middle panel) and after washing and recovery of 2 hours (right panel).
B. Control strain of GFP-labelled lifeact before (left panel), during treatment with 10 µM latrunculin A (middle panel), after washing and recovery of 2 hours (right panel).

3.2.8.2. The actin and microtubule cytoskeleton is important for endocytosis of the a1-5FAM pheromone

The cytoskeleton has been shown to be essential in many cellular processes in both fission and budding yeast (Hagan, 1998, Moseley and Goode, 2006). Temperature-sensitive actin mutants of *S. cerevisiae* were found to be defective in the internalisation of a-factor (Kübler and Riezman, 1993) which was found to be consistent with de-polymerization of actin filaments blocking endocytosis at the apical surface of polarised epithelial cells (Gottlieb et al., 1993). In *U. maydis,* polar growth of cells is dependent on an intact actin cytoskeleton (Fuchs et al., 2005) and the microtubule cytoskeleton is required for long distance hyphal growth. To show whether the endocytosis or more specifically, the uptake of the synthetic pheromone, is dependent on the cell cytoskeleton, we incubated FB2 cells with either benomyl or latrunculin A and then added 2.5 µg/µl of a1-5FAM. To account for any potential issues with the use of DMSO as a solvent for both inhibitory drugs, we also incubated cells with DMSO alone and then added the a1-5FAM synthetic pheromone (Figure 3.9. A, B). We observed that the cells were still able to internalize and transport the pheromone to the cell vacuole in the presence of DMSO, suggesting it has no effect on endocytosis or cellular functions. In comparison, cells treated with benomyl (Figure 3.9. C, D) and latrunculin A (Figure 3.9. E, F) appeared to be able to internalize the pheromone, as it accumulated in fluorescent aggregates throughout the cell, but, it was not transported to its end point, the cell vacuole, as we have shown in previous experiments. This suggests that there is a problem with the transport process between the plasma membrane and the cell vacuole. We statistically quantified the average fluorescence intensity of cell vacuoles under each set of conditions and found that over a time course of three hours, the vacuoles for both the benomyl and latrunculin A conditions did not show any fluorescence (Figure 3.9. G). This varied significantly to that of the FB2 and FB2 DMSO conditions, in which we observed peaks in fluorescence of 693 AU and 600 AU, respectively. From this experiment, it was also noted that none of the cells visualised, showed signs of switching to filamentous growth, suggesting they were defective in the perception of the pheromone.

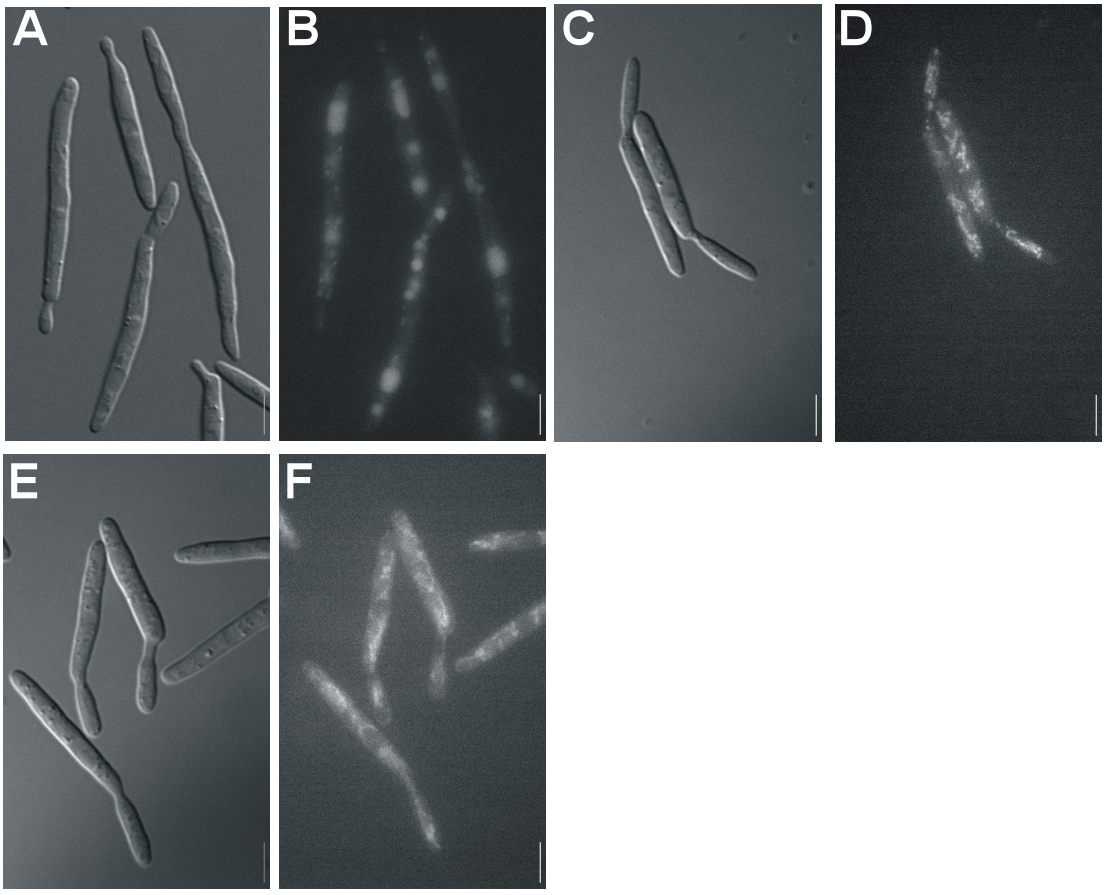

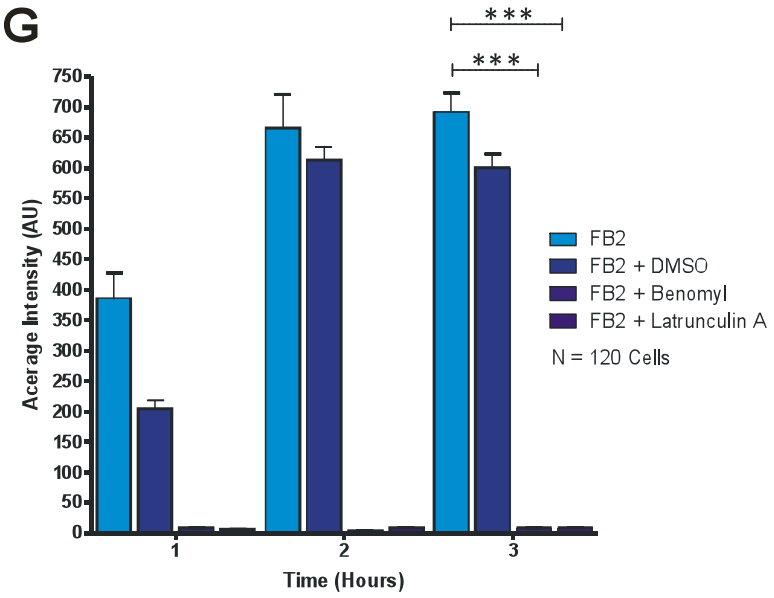

Figure 3.9. The cytoskeleton is important in endocytosis of a1-5FAM.

A. DIC picture of FB2 cells incubated with DMSO and a1-5FAM for 3 hours.
B. Fluorescently 5FAM labelled picture of FB2 cells incubated with DMSO and a1-5FAM for 3 hours.
C. DIC picture of FB2 cells incubated with benomyl and a1-5FAM for 3 hours.

D. Fluorescently 5FAM labelled picture of FB2 cells incubated with benomyl and a1-5FAM for 3 hours.
E. DIC picture of FB2 cells incubated with latrunculin A and a1-5FAM for 3 hours.
F. Fluorescently 5FAM labelled picture of FB2 cells incubated with latrunculin A and a1-5FAM for 3 hours.
G. Quantification of the average intensity of cell vacuoles following incubation of FB2 cells with the a1-5FAM pheromone and either DMSO as a control, or inhibitors benomyl and latrunculin A over 3 hours. Bars are given as ± standard error of the mean; the sample size is 120 cells per bar. Triple asterisk indicates significant difference between FB2 cells and FB2 cells treated with benomyl and latrunculin A, with $P < 0.001$ using a t test assuming for unequal variances.

3.3. Discussion

3.3.1. The synthetic a1-5FAM pheromone is a suitable candidate for in vivo molecular biology experiments

In this chapter we have shown evidence for a synthetically modified a1 pheromone, which can be used in *in vivo* studies and does not appear to interfere with the pheromone-receptor interaction in living cells. When wild-type *U. maydis* cells were incubated with the a1 pheromone, this triggered a signalling cascade which enhances pheromone and receptor production, as well as initiating a morphogenic switch to filamentous growth (Muller et al., 2003). We tested various derivatives of both the a1 and a2 pheromone to determine which were viable. The switch from a methyl ester to a primary amide in the C-terminal of the a1 pheromone did not inhibit function or the ability of the cell to produce conjugation hyphae. However, changing the aa in the position 5 of the a1 pheromone, from a glycine to a lysine gave a peptide, which did not induce a filamentous growth response when incubated with wild-type cells. This was in agreement with a previous study that showed the switch of a glycine residue at this position to a *D*-ala gave a peptide that was

less active than the natural version (Szabo et al., 2002). This suggests that the glycine at position 5 of the a1 pheromone is important for biological function of the a1 pheromone and may be one of the amino acids that is inserted into the binding pocket of the receptor in order to establish cellular recognition (Szabo et al., 2002). The addition of fluorophores ROX and TEXAS RED to the a1 pheromone gave peptides, which, resulted in no filamentous growth, but they could be internalised and visualised within the cell. This suggests that they do not inhibit the initial binding with the receptor but prevent the peptide from being transported to the vacuole, which proved to be possible with our other synthetic derivatives. The synthetic ROX pheromone is not transported to the vacuole which could be caused by a missing linker, such as in the case of TEXAS RED, which means it could interfere with an amino side chain along the length of the pheromone. The fact that both peptides were internalized, suggests that they perhaps bind irreversibly to the receptors, inhibiting the recycling and therefore, only a limited amount of the pheromone can be internalised but not to a level over the threshold required to induce the signalling cascade which induces the morphogenic switch to filamentous growth. This was indeed similar to EE mutants such as Yup1TS where the pheromone receptor Pra1 accumulated in small vesicular structures and lead to a defect in pheromone perception (Fuchs et al., 2006). However the addition of the a1-5FAM pheromone was still internalised in the cell and transported to the cell vacuole for degradation, suggesting that it behaves in a similar way to the natural pheromone. The degradation of the pheromone in the vacuole suggests that it follows a similar endocytosis pathway as seen in *S. cerevisiae* (alpha factor) where the pheromone is recycled to the vacuole so that its receptor Ste3 can return to the plasma membrane for continued rounds of pheromone binding and internalisation (Chen and Davis, 2000). Our results suggest that the a1 pheromone tagged with the 5-FAM fluorophore, may produce a signalling cascade at approximately the same concentration as the natural pheromone and does not produce any inhibitory cell morphologies, making it a viable marker for pheromone-receptor interactions and as a specific *U. maydis* cellular marker for endocytosis.

3.3.2. The a1-5FAM pheromone can be used as a marker for receptor-mediated endocytosis

Various studies have shown a role for endocytosis in filamentous fungi (Vida and Emr, 1995, Hoffmann and Mendgen, 1998). However, until this point endocytosis had only been visualised in *U. maydis* using the FM4-64 dye, which labels fluid-phase endocytosis events as well as organelles such as mitochondria and the endoplasmic reticulum. This non-specific labeling makes it difficult to conclude that a FM4-64 positively labelled organelle is an endocytic compartment (Read, 2000). Therefore, a cargo such as the a1 pheromone, shown to be naturally endocytosed by the cell, would be a more suitable alternative. In this study we provide evidence that the pheromone is endocytosed constitutively for the first 2 hours 30 minutes of incubation with wild-type cells, as we observed a continuous rise in cell vacuole fluorescent intensity. This suggests that the pheromone is constitutively endocytosed, and gives an indication that the receptor participates in multiple rounds of ligand binding and internalization, as is the case in mammalian cells (Ciechanover et al., 1983, Goldstein et al., 1985). We found after 2 hours and 30 minutes of constitutive endocytosis, that the cell intensity entered a plateau, closely followed by a decline over the 8 hours of the experiment, suggesting that there is a threshold of pheromone internalisation. This is not the case of the α-factor pheromone in *S. cerevisiae* which shows that the internalisation of the α-factor pheromone is synchronized with the down-regulation of its receptor, Ste2 (Schandel and Jenness, 1994). However, neither Ste2 nor its ligand is recycled, instead they are degraded within the vacuole (Schandel and Jenness, 1994, Singer and Riezman, 1990). We found evidence in this study that endocytosis in *U. maydis* is receptor-mediated, as only cells possessing the correct receptor Pra2 were able to internalize and transport the pheromone. Receptor-mediated endocytosis has been reported in yeasts, such as *S. cerevisiae* (Geli and Riezman, 1998) and in mammalian cells.

3.3.3. The endocytosis of the a1-5FAM pheromone is dependent on the actin and microtubule cytoskeletons

In this study we found evidence that both the actin and microtubule cytoskeleton is essential for endocytosis of the fluorescently labelled a1 pheromone. It has been shown previously in *U. maydis* that disruption of actin dramatically increased the signal of the Pra1 receptor in the plasma membrane at the cell surface (Fuchs and Steinberg, 2005). Disruption of actin is well known to inhibit endocytic removal of receptors from the cell surface in yeast (Kaksonen et al., 2003) and mutants of fimbrin in *A. nidulans* have shown disruption in FM4-64 uptake (Upadhyay and Shaw, 2008). Furthermore, it has been shown that actin patches and actin cables can be visualised in *U. maydis* (Steinberg and Schuster, 2011). Also research in *S. cerevisiae* has also shown that actin patches are sites of endocytosis (Ayscough, 2005, Kaksonen et al., 2005, Gachet and Hyams, 2005) and filamentous fungi (Upadhyay and Shaw, 2008, Steinberg and Schuster, 2011) as well as being involved in cell wall morphogenesis, endocytosis and plasma membrane invagination (Evangelista et al., 2002, Evangelista et al., 2003, Ayscough, 2005). In yeast has been it is suggested that actin patches interact with proteins of the clathrin-mediated endocytosis pathway (Newpher et al., 2005). Therefore, the effects of latrunculin A on pheromone accumulation in the vacuole could suggest an involvement of the actin cytoskeleton, specifically the actin patches, in the internalisation step of endocytosis. We have provided evidence that the microtubule cytoskeleton is important for the endocytosis of the a1 pheromone and it could be suggested that this is more a transport issue and not one of internalisation. The background fluorescence of the cell is dramatically increased, suggesting the a1 pheromone is internalised but due to the breakdown of the microtubules, it cannot be transported to the vacuole and therefore, the receptor cannot be recycled for continuous rounds of internalisation. As a result, the ability of the cell to switch to filamentous growth and form conjugation hyphae would be inhibited, which is not in agreement with previous work done in *U. maydis,* where treatment of pheromone-induced cells with benomyl did not affect formation of conjugated hyphae (Fuchs et al., 2005). However, in Fuchs et al, they added the benomyl 1 hour 30 minutes after the pheromone induction, which would suggest that

the cells would have already had time to form conjugated hyphae. We have shown that they take up the pheromone within 15 minutes and can, therefore, make the switch to filamentous growth before the inhibitor is added.

4. CHAPTER 4 – THE ROLE OF THE ACTIN CYTOSKELETON DURING ENDOCYOTOSIS OF THE *USTILAGO MAYDIS* a1 PHEROMONE

4.1. Introduction

Actin is a monomeric subunit of actin filaments, which form one of the cytoskeletal networks of eukaryotic cells (Cardelli et al., 2009). In yeast and other organisms, it has been shown to consist of three components; patches, cables and rings (Ayscough, 2005, Berepiki et al., 2010, Kovar et al., 2011). Actin patches are thought to be the sites of endocytosis (Lee and Dominguez, 2010) whereas actin cables are bundles of actin filaments that align along the long axis of the cell and are crucial for establishing cell polarity (Yang and Pon, 2002). Acto-myosin rings in *S. cerevisiae* aid in the physical separation of daughter cells during cytokinesis (Bi et al., 1998). Furthermore, The position of actin patches at the cell periphery, as well as their dynamic movement away from the plasma membrane, are thought to aid their role as markers of endocytosis (Kaksonen et al., 2003). The role of actin cables has been described in various organisms and is thought to include transportation of secretory vesicles and other cargoes such as actin patches, peroxisomes, mRNA and mitochondrion (Suelmann and Fischer, 2000, Motegi et al., 2001, Rossanese et al., 2001, Fehrenbacher et al., 2004, Upadhyay and Shaw, 2008, Pantazopoulou and Peñalva, 2009, Berepiki et al., 2010). It is thought that motor proteins such as the myosins use these fibres of the cytoskeleton to transport cargo through the cell (Xiang and Plamann, 2003, Vale, 2003). Indeed, myosin-5 motors are thought to deliver secretory vesicles to the growth region in *S. cerevisiae* (Johnston et al., 1991, Govindan et al., 1995, Schott et al., 2002) and *S. pombe* (Motegi et al., 2001, Win et al., 2001, Mulvihill et al., 2006). Myosin-2 has also been found to have links to the actin cytoskeleton; particularly in reference to the acto-myosin contractile ring and cytokinesis (Tolliday et al., 2002). In animal cells myosin-2 is most abundant in muscle cells with a function to generate mechanical force, however it has

also been linked to motility and adhesion events in eukaryotic cells (Vicente-Manzanares et al., 2009). Additionally, a deletion of myosin-1 in *S. cerevisiae*, impaired endocytosis and almost abolished growth (Geli and Riezman, 1996). In filamentous fungi, analysis of the actin cytoskeleton has proven difficult until recently as a live cell imaging probe did not exist.

Lifeact, a 17 amino acid peptide derived from the N-terminus of the budding yeast actin-binding protein Abp140 (Asakura et al., 1998, Yang and Pon, 2002) has been shown to be a universal live-cell imaging probe in both mouse embryonic fibroblasts (Riedl et al., 2008), and filamentous fungi (Berepiki et al., 2010, Steinberg and Schuster, 2011). In *N. crassa*, lifeact was used to visualise all components of the actin cytoskeleton and inform on their function (Berepiki et al., 2010). Both actin patches and cables were found at the tip of germ tubes and actin cables were present in a dense array, suggesting a role for actin cable-mediated transport of secretory vesicles as it is found in budding yeast. Furthermore, in a later paper, it was suggested that actin patches cover endocytic vesicles that are internalised into the cell and loaded onto actin cables (Berepiki et al., 2011). Considering the organisation and importance of F-actin in hyphae, it is likely that myosin-based transport of secretory vesicles along microfilaments supports fungal growth. Moreover, deletion mutants of class-V myosin in *C. albicans* were unable to grow as filamentous cells suggesting that myosins are good candidates for actin based transport machinery (Woo et al., 2003). The sequenced genomes of filamentous fungi encode four classes of myosins, including myosin-1, myosin-2 (conventional myosin), myosin-5, and the fungus-specific myosin-17, which contains a myosin motor domain fused to a chitin synthase domain (Schuster et al., 2011c). In *A. nidulans* (McGoldrick et al., 1995, Osherov et al., 1998) and in *C. albicans* (Oberholzer et al., 2002, Oberholzer et al., 2004), myosin-1 is essential for hyphal growth. Additionally, in both species, myosin-1 activity is required to mediate the endocytic uptake of the endocytic marker dye FM4-64 into the vacuole (Oberholzer et al., 2002, Yamashita et al., 2000). Furthermore, myosin-2 localises to the contractile rings at forming septa in *A. nidulans*. It was found to be critical for septation and normal distribution of chitin, but not for hyphal extension (Taheri-Talesh et al., 2012).

In *U. maydis*, myosin-5 is not essential but required for normal cell separation, hyphal growth during mating and pathogenicity (Weber et al., 2003). Furthermore, it has been shown to deliver chitin synthases to the growth region (Schuster et al., 2011c). In *U. maydis,* the actin cytoskeleton has been shown to be essential for hyphal growth (Fuchs and Steinberg, 2005) and peripheral actin patches and cables that connect the bud with the mother cell have been visualised in cells (Steinberg and Schuster, 2011). The function of cortical actin patches and their role in endocytosis has been studied in *S. cerevisiae* however nothing is known about their relationship in *U. maydis*. In the previous chapter, we have shown that the a1 pheromone uptake is inhibited in function by the absence of actin, however we do not know with which components it interacts and how it is transported once it is internalised to the cell. Therefore, using the synthetic pheromone as a marker, the aims of the work described in this chapter are

- To observe in more detail, the dynamics of actin patches and ascertain if these dynamics are affected by the induction with the a1 pheromone.
- To provide evidence on whether actin cables, with the aid of molecular motors, are the means to transport the a1 pheromone to the vacuole.
- To investigate the role of myosin-1, myosin-2 and myosin-5 during transport of the pheromone as well as their involvement with actin patches.

4.2. Results

4.2.1. Localisation of actin patches and cables in U. maydis

In order to visualise actin in *U. maydis* cells, we used a strain incorporating the imaging probe lifeact. We visualise actin patches in the tip of budded cells and they can be observed throughout the tip through a z-stack image of the cell (Figure 4.1 A). We also observed filamentous actin cables in the tip of budded cells where they span from the tip of the budded cell and extend down

into the mother cell (Figure 4.1 B) (Steinberg and Schuster, 2011). In additon, we analysed the location of patches throughout the cell, to determine where the majority of patches are located; the growing bud or mother cell. If actin patches were involved in endocytosis, we would find the majority in the tip of budded cells. However, in order to account for the surface area of each part of the cell (i.e. mother or daughter cell) and therefore get an accurate indication of the number of patches per square μm of both bud and mother cells, we used an ellipsoid surface area equation (Figure 4.1. C) then measured the number of patches in 20 budded cells, using Z stacks (Figure 4.1. D). We found that the bud contained significantly more patches per square μm (Figure 4.1. D, t-test $P < 0.001$) than the mother cells, suggesting that actin patches are required for growth at the tip of the cell and positioned accurately at sites of endocytosis for uptake of material such as the a1-5FAM pheromone.

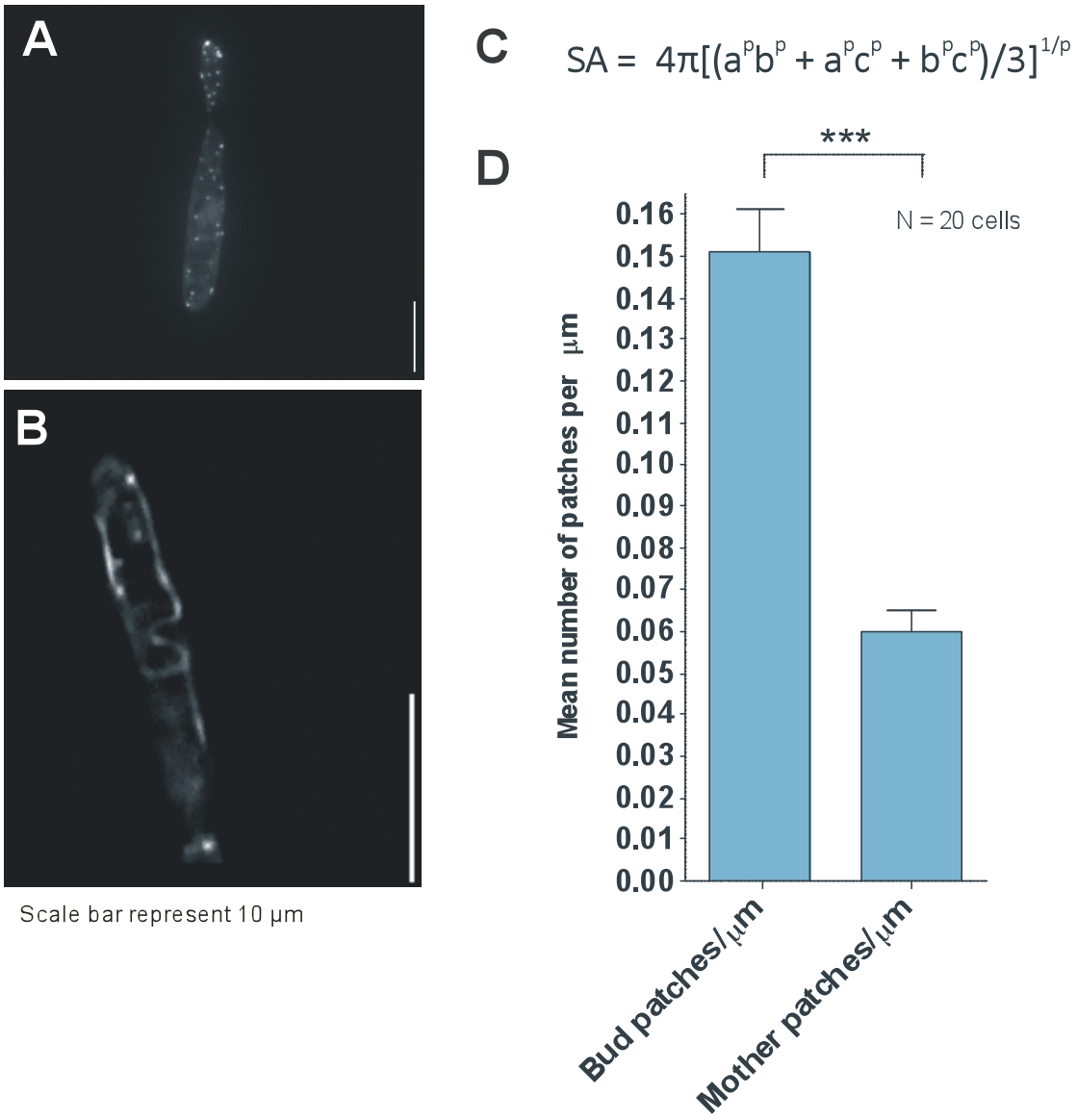

Figure 4.1. The actin cytoskeleton in *U. maydis*

A. Single image depicting GFP labelled lifeact strain, which shows the location of actin patches throughout the cell.

B. Single image depicting GFP labelled lifeact strain, which shows the location of actin cables through the budded part of a *U. maydis* cell.

C. Ellipsoid equation for surface area (SA = 4 π [$a^p b^p + a^p c^p + b^p c^p$ / 3] $^{1/p}$, where P = 1.6075, a = cell length, b = cell height , c = cell depth) was used to determine the location of actin patches. Bar graph depicting the mean number of patches per square µm in both the bud and mother of *U. maydis* cells. Each bar is given as mean ± standard error of the mean. The sample size n is 20 cells per bar; triple asterisk indicates significant difference from each other at P<0.0001, using a standard t-test assuming Welsch's correction.

4.2.2. The dynamics of actin patches

In order to understand actin patches further, we decided to study their dynamics. We visualise actin patches throughout *U. maydis* cells (Figure 4.2. A) and when we looked more closely at the actin patches we observe that they move away from the plasma membrane. In a kymograph taken from a line scan of a budded cell (Figure 4.2. B) we view the complete maturation of an actin patch. Initially we observe a stationary line, which increases in intensity, and we suggest this identifies the formation (Figure 4.2 B. red boxes). This is succeeded by a zig-zag line, denoting movement of the actin patch and then disappearance from the focal plane of the kymograph, which we suggest indicates a scission movement into the cytoplasm (Figure 4.2 B, green boxes).

4.2.2.1. Patch dynamics in the presence of the a1 pheromone

As we have shown previously, the a1-5FAM pheromone is involved in receptor-mediated endocytosis (Figure 3.7). We assume that actin patches are involved in the internalisation of the receptors from the plasma membrane. Therefore, to further understand these events and to determine whether the dynamics of actin patches are regulated by ligand-bound receptors, which they are internalising, we measured the timing of both the formation and scission events when the a1-5FAM pheromone was incorporated into the culture. In Figure 4.1 A, the bud contains the majority of actin patches and would therefore, be the most appropriate site to look more closely at actin patch dynamics. In these experiments we measured the actin patch dynamics in the presence of synthetically produced a1-5FAM pheromone and in the presence of DMSO, a solvent used to dissolve the a1-5FAM pheromone. Here, DMSO was used as a control to ensure that merely adding to the cells media caused changes in the actin patch dynamics. In comparison to the control, the mean number of patches is significantly increased in the presence of the a1 pheromone (Figure 4.2. C $p=0.0158$) suggesting a function in endocytosis. Additionally, we analysed the patch formation and scission times under both conditions, to establish whether the presence of the a1 pheromone would affect these processes. It was found that both the formation time

(Figure 4.2. D, p=<0.0001) and the scission time (Figure 4.2. E, p=<0.001) of actin patches was significantly decreased in the presence of the a1 pheromone. This suggests that pheromone treatment affects actin patch dynamics, in particular, the number and turnover from formation to scission events.

4.2.2.2. Patch average intensity from formation to maturation

Furthermore, as we observed that the patches appear, increase in intensity and then disappear from the plasma membrane we therefore measured the average intensity measurements of individual patches as they arrived at the plasma membrane, matured and disappeared again. It was found that patches had a steep incline in the average intensity of the patch once it appeared, it then reached a peak (Figure 4.2. F). The intensity remained high for an average of 6.1 s before dropping again, which was consistent with the patch disappearing from the plane of view. As all the measurements for patch intensity were taken using GFP lasers, an equation was used after acquiring the images to account for bleaching of the cell during the course of the movie acquisition. These results suggest that the formation of actin patches requires a pre-defined amount of actin and that they have a pre-defined lifespan. Taken together, these results propose that actin patches are regulated components with pre-determined function, which is significantly increased in the presence of the a1 pheromone.

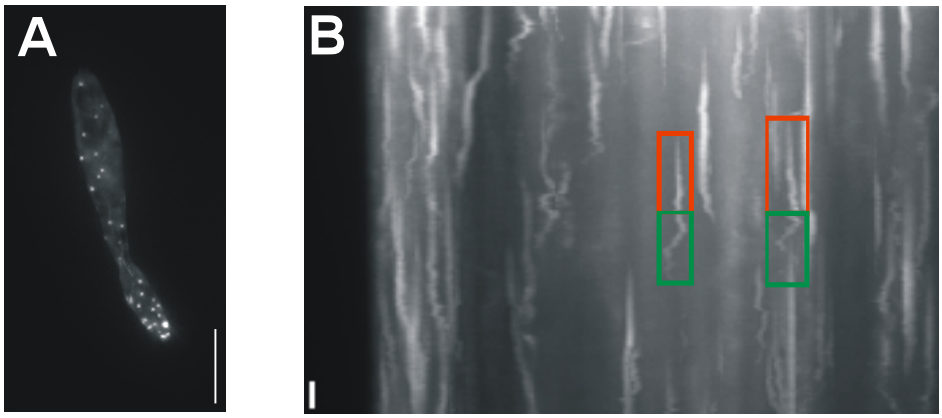
A
B
Scale bar represent 10 µm

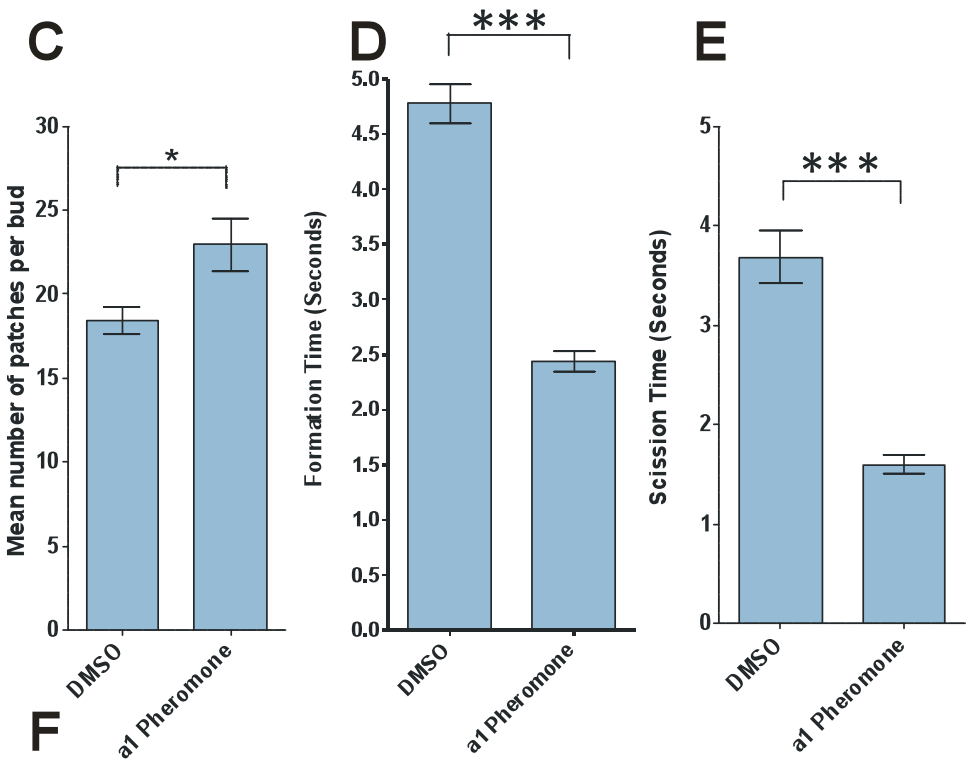
C
Mean number of patches per bud
30
25
20
15
10
5
0
*
DMSO
a1 Pheromone
D
***
Formation Time (Seconds)
5.0
4.5
4.0
3.5
3.0
2.5
2.0
1.5
1.0
0.5
0.0
DMSO
a1 Pheromone
E
***
Scission Time (Seconds)
5
4
3
2
1
0
DMSO
a1 Pheromone

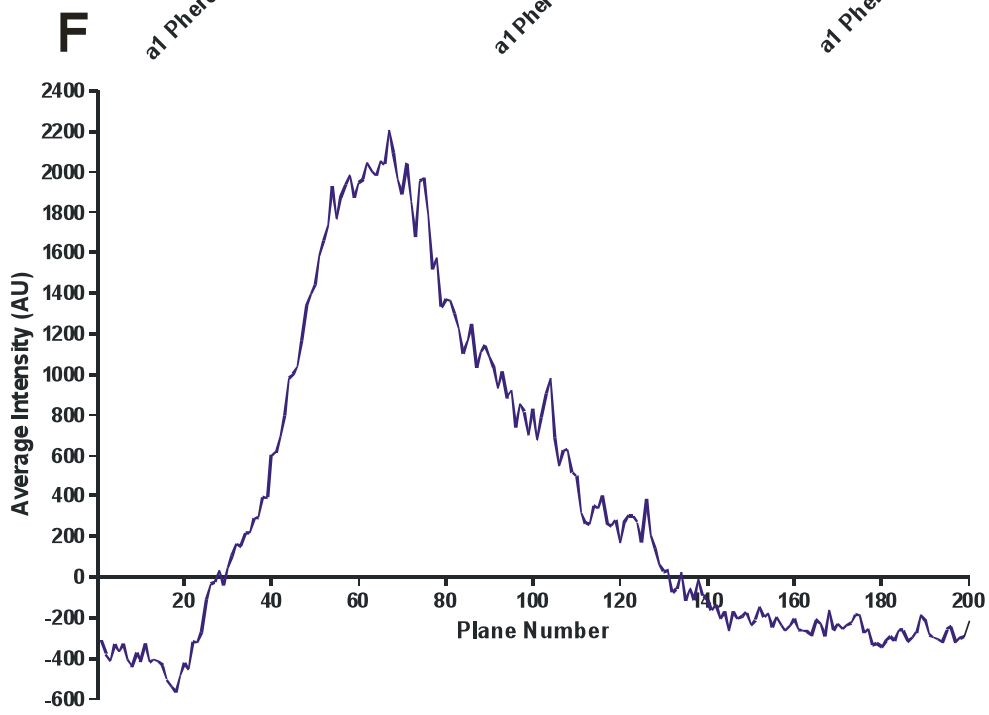
F
Average Intensity (AU)
2400
2200
2000
1800
1600
1400
1200
1000
800
600
400
200
0
-200
-400
-600
20
40
60
80
100
120
140
160
180
200
Plane Number

Figure 4.2. The dynamics of actin patches.

A. Image depicting a still from a movie of actin patches showing the position of actin patches throughout the cell.
B. Kymograph showing actin patch dynamics throughout a cell. X axis denotes distance (μm) whereas y axis denotes time (seconds) Red boxes depict formation events and green boxes depict scission events. Time shown by white bar on the kymograph is given in seconds.
C. A graph depicting the mean number of actin patches per bud when induced with DMSO and a1 pheromone. Bars are given as mean ± standard error of the mean; the sample size n is 20 cells per bar; triple asterisk indicates significant difference between DMSO and a1 pheromone at P = 0.0158, using a t-test assuming for unequal variances.
D. A graph depicting the formation time of actin patches in seconds when induced with DMSO and a1 pheromone. Bars are given as mean ± standard error of the mean; the sample size n is 50 cells per bar; triple asterisk indicate significant difference between DMSO and a1 pheromone at P < 0.001, using a t-test assuming for unequal variances.
E. A graph depicting the scission time of actin patches in seconds when induced with DMSO and a1 pheromone. Bars are given as mean ± standard error of the mean; the sample size n is 50 cells per bar; triple asterisk indicate significant difference between DMSO and a1 pheromone at P < 0.001, using a t-test assuming for unequal variances.
F. A line graph detailing an example of the progression in intensity of an actin patch. The patch intensity was taken at each frame of the movie along with a control for background substitution.

4.2.3. Transport of cellular material from actin patches to cell vacuoles

Actin patches have been shown to be the local sites of endocytosis and as we have shown previously the vacuole is the end point of endocytosis (Figure 3.5.). In order to establish whether there is a direct connection between actin patches and vacuoles, we analysed the average distribution of each component throughout the cell in a large sample size of budded cells. We

visualised the vacuoles by staining with Cell Tracker Blue, a yeast vacuole marker (Figure 4.3. A) and the actin patches with an incorporated lifeact GFP tag (Figure 4.3. B). We found that a pattern is formed, whereby patches were found in the daughter cell and cell vacuoles were found in the mother cell (Figure 4.3. C). Predominantly the highest average intensity and therefore the likely position of the cellular vacuoles was found in the mother cell just after the point of septation and between 6 – 10 µm from the tip of the daughter cell. The actin patches have a peak intensity between 0 - 2 µm from the tip of the daughter cell. These results suggest actin patches are not directly linked to the vacuole and therefore require another mechanism such as molecular motors to cover the distance and delivery cargo from the actin patches to the cell vacuole.

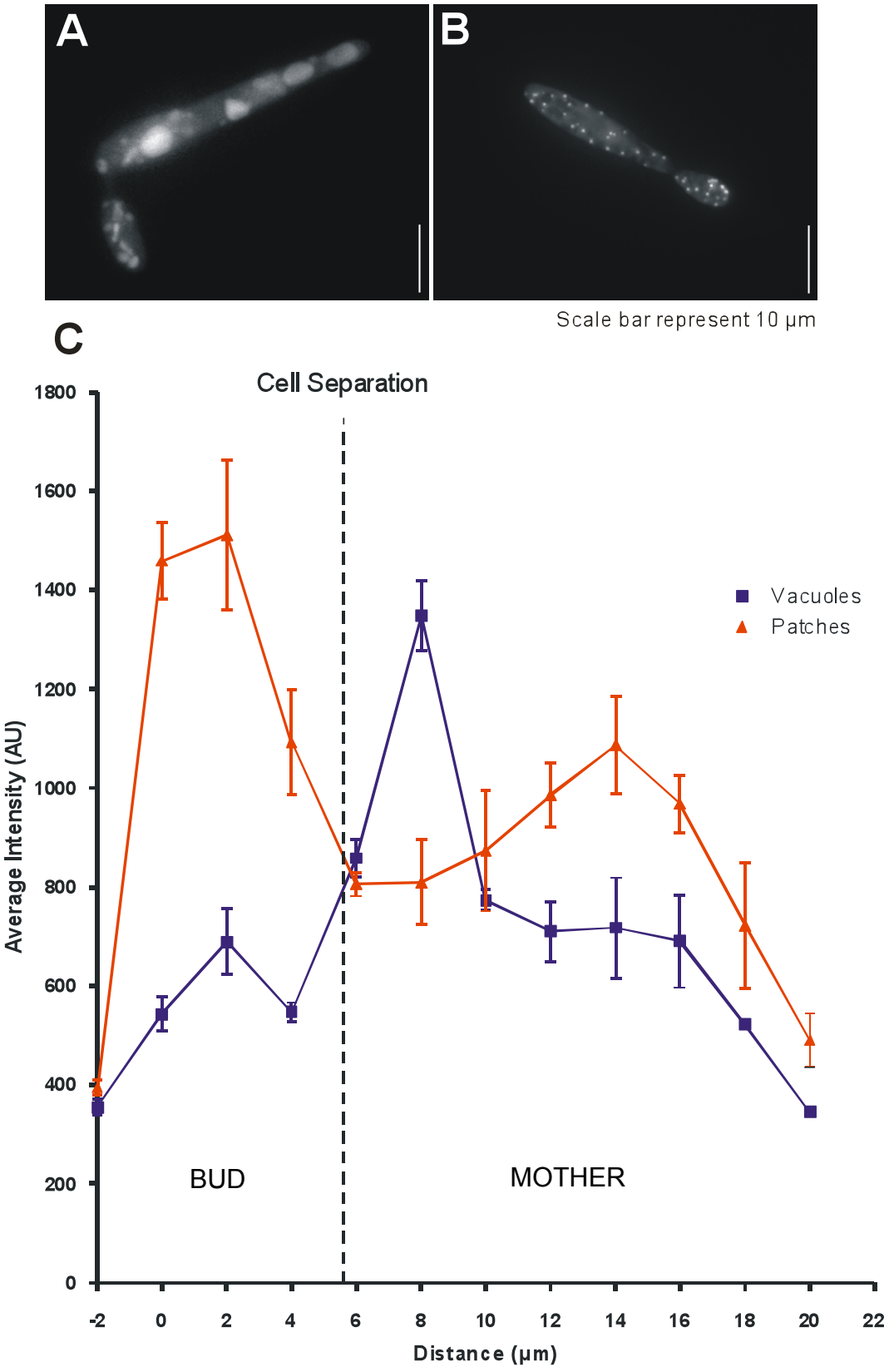

Figure 4.3. The requirement of motors to transport a1-5FAM pheromone from the patches to the cell vacuole.

A. Image depicting a lifeact labelled strain stained with Cell Tracker Blue to identify the positioning of cellular vacuoles. Scale bar represents 5 µm.

B. Image shows a wild-type cell labelled with GFP lifeact strain depicting the positioning of actin patches throughout the cell. Scale bar represents 5 μm.
C. Graph shows the average intensity of 20 line scans of 20 cells. The blue line represents the actin patches and the red line represents the vacuoles throughout the cell. Each point represents the mean ± standard error of the mean of 20 cells at a pre-defined and measured distance from the tip of the bud through the cell into the mother cell. The black dotted line depicts the location of the cell separation between the mother and the daughter cell.

4.2.4. Over-expression of myosin tails causes phenotypes in yeast-like and hyphae cells

The presence of actin cables in the cell suggests they provide the bridge between the actin patches at the site of endocytosis and the vacuole, which has been deemed to be the end point of endocytosis. In order to test whether the actin cables do indeed support this, we looked at myosin motors. Specifically, we constructed over-expression tail mutants of myosin-1, myosin-2 and myosin-5 under a regulatable *CRG* promoter. All myosins are thought to contain a head (motor) domain, a neck with a IQ motifs for light chain binding, and a tail domain with coiled-coil regions and membrane/cargo-binding domains (Figure 4.4. A). However, with the over-expression of just the tail regions, we attempted to outcompete the wild-type myosins for the availability of anchorage sites on the cargo, therefore inhibiting the cell from secreting cell wall components and potentially completing the internalisation of endocytic vesicles. In order to confirm the presence of over-expression, we carried out a western blot analysis under 'OFF' condition (CM-GLU) and 'ON' condition (CM-ARA) (Figure 4.4. B, top panel). As each tail construct was tagged with HA, therefore the presence of a band suggests an over-expression of myosin tails. As a loading control α tubulin was used (Figure 4.4. B bottom panel).

4.2.4.1. Over-expression of myosin tails induces morphological phenotype in yeast-like cells

Microscopic analysis showed various cell morphology defects for each myosin transformed strain. In contrast to characteristic elongated, cigar-shaped wild-type cells (Figure 4.4. C, D, E left panel), cells that contained the myosin-1 tail over-expression were distinctly thicker (Figure 4.4. C right panel). This is in contrast to myosin-2 tail over-expression, where cells appear to elongate and become thinner without the ability to separate (Figure 4.4. D, right panel). With the over-expression of the myosin-5 tails, we observed thicker and more rounded cells suggesting, an inability for polarised growth (Figure 4.4. D, right panel). These thicker cells were consistent with data previously published by our laboratory with a myosin-5 deletion (Weber et al., 2003). Taken together these results propose that over-expression of myosin tails inhibits the cells ability to establish its shape. We suggest that the cell separation defect observed with myosin-2 is due to a cytokinesis defect and therefore, is most likely not linked to endocytosis events.

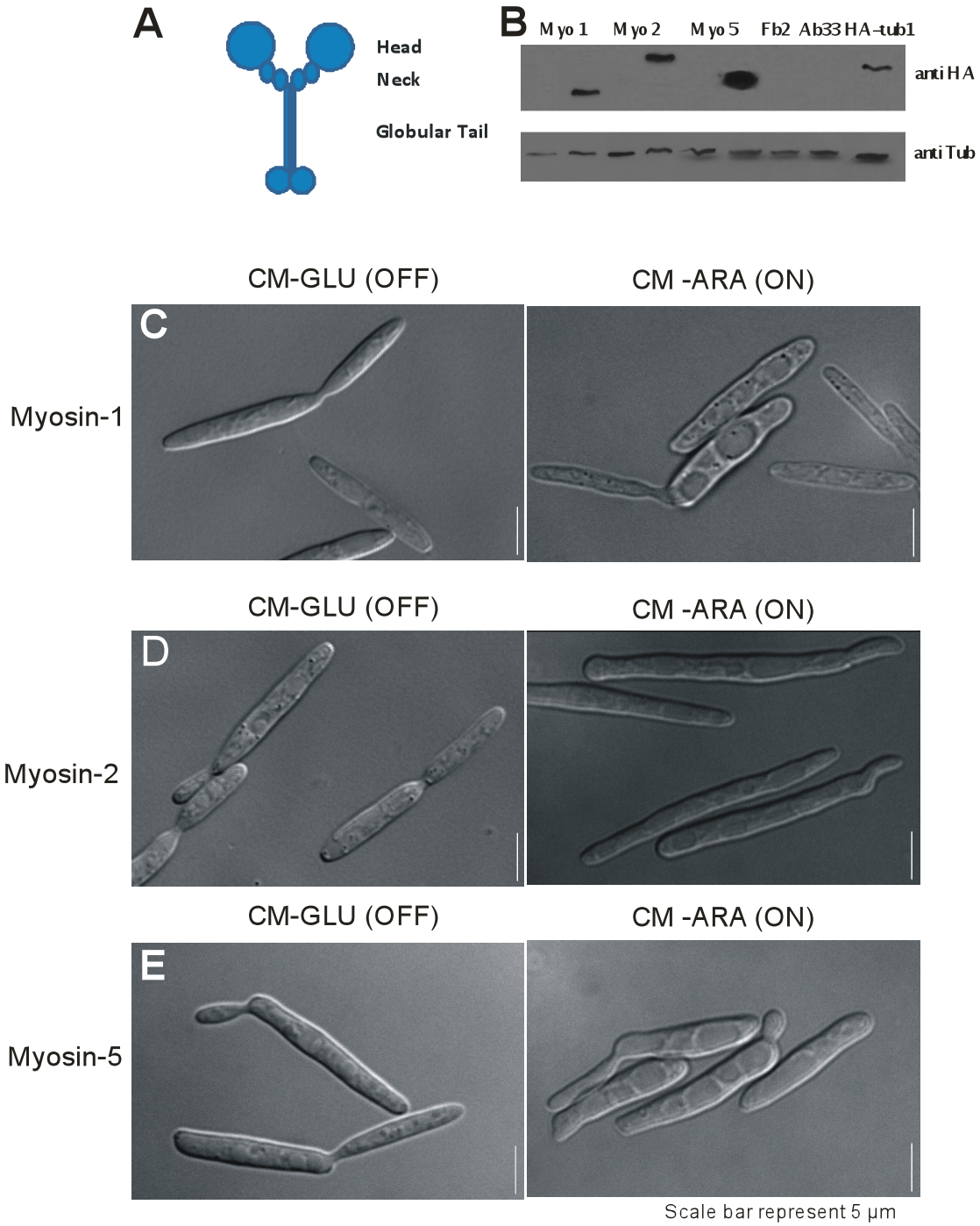

Figure 4.4. The morphology of myosin tail over-expression mutants in yeast-like cells.

A. Schematic drawing of the myosin motor complex from *U. maydis* and *S. cerevisiae*. It consists at the N terminus (N) of two heavy chains (HC; ~180 kDa) that interact and bind F-actin (ABS) and at their neck region. The coiled-coil region in the tail is interrupted by loose areas and runs into a globular carboxyl-terminus (modified from Cheney et al., 1993).

B. A western blot showing all tail domain proteins expressed under the control of the *crg* promoter (Bottin et al, 1996;) in a FB2 pheromone inducible background. After shifting cells to glucose-containing medium the promoter is repressed (OFF), which results in protein depletion. Images show expression of the myosin-1, myosin-2 and myosin-5 tail over-expression in both glucose-containing medium (OFF) and after switching of media to arabinose-containing medium (ON). Time of growth in repressive conditions was 12 hours, over-expressed 6 hours.
C. Images depicting the myosin-1 tail over-expression strains in both the glucose-containing medium (OFF, Left panel) overnight and after switching of media to arabinose-containing medium (ON, Right panel) for 6 hours.
D. Images depicting the myosin-2 tail over-expression strains in both the glucose-containing medium (OFF, Left panel) overnight and after switching of media to arabinose-containing medium (ON, Right panel) for 6 hours.
E. Images depicting the myosin-5 tail over-expression strains in both the glucose-containing medium (OFF, Left panel) overnight and after switching of media to arabinose-containing medium (ON, Right panel) for 6 hours.

4.2.4.2. Over-expression of myosin-1 or myosin-5 tails affects the cells ability to form hyphae

As the strain used for hyphae experiments was different from that used in the yeast-like cell studies, another western blot was performed with the anti-HA (Figure 4.5. A, top panel) antibody and α-tubulin as a loading control (Figure 4.5. A, bottom panel), to confirm the over-expression of the tail constructs for the new strains. Upon completion of this control, filamentous growth of the myosin tail mutants was then established via crossing colonies of the FB2 myosin mutant with FB1 wild-type cells. In the wild-type (FB1 x FB2) the colony appears white and fuzzy (Figure 4.5. B, left panel), which is similar to what has been reported previously for *U. maydis* wild-type (Spellig et al., 1994, Hartmann et al., 1996). A closer look shows mycelium with fuzzy appearance suggesting the presence of aerial hyphae (Figure 4.5. B, right panel). In comparison with the colony shown for myosin-1 tail *CRG* (Figure 4.5. C, left panel). The over-expression causes colonies with a less fuzzy appearance and of a more greyish colour, suggesting an effect in hypha formation, which accompanies slower growth and enlarged colony, which

looked more disorganized and less uniform (Figure 4.5. C, right panel). A myosin-2 tail over-expression strain does not appear to have an effect hyphal formation (Figure 4.5. D, left panel). The colony was white and fuzzy (Figure 4.5. D, left and right panel). There was a disparity in hyphal growth in myosin-5 tail over-expression mutants (Figure 4.5. E, left panel). The colony seems less fuzzy and of a greyish colour similar to that seen in myosin-1 tail over-expression. A closer look shows a less fuzzy and more disorganized colony compared to the wild-type (Figure 4.5. E, right panel). A myosin-5 deletion mutant was used to show the complete inability of forming hypha (Figure 4.5. F, left panel). Indeed, at the higher magnification the cells are unable to form filamentous hyphae, which form a greyish and non-fuzzy colony (Figure 4.5. F, right panel). The cells ability to form functional hyphae at a wild-type speed appears to be inhibited in the presence of myosin-1 and myosin-5 tails over-expression, suggesting a role for the myosins in hyphal growth.

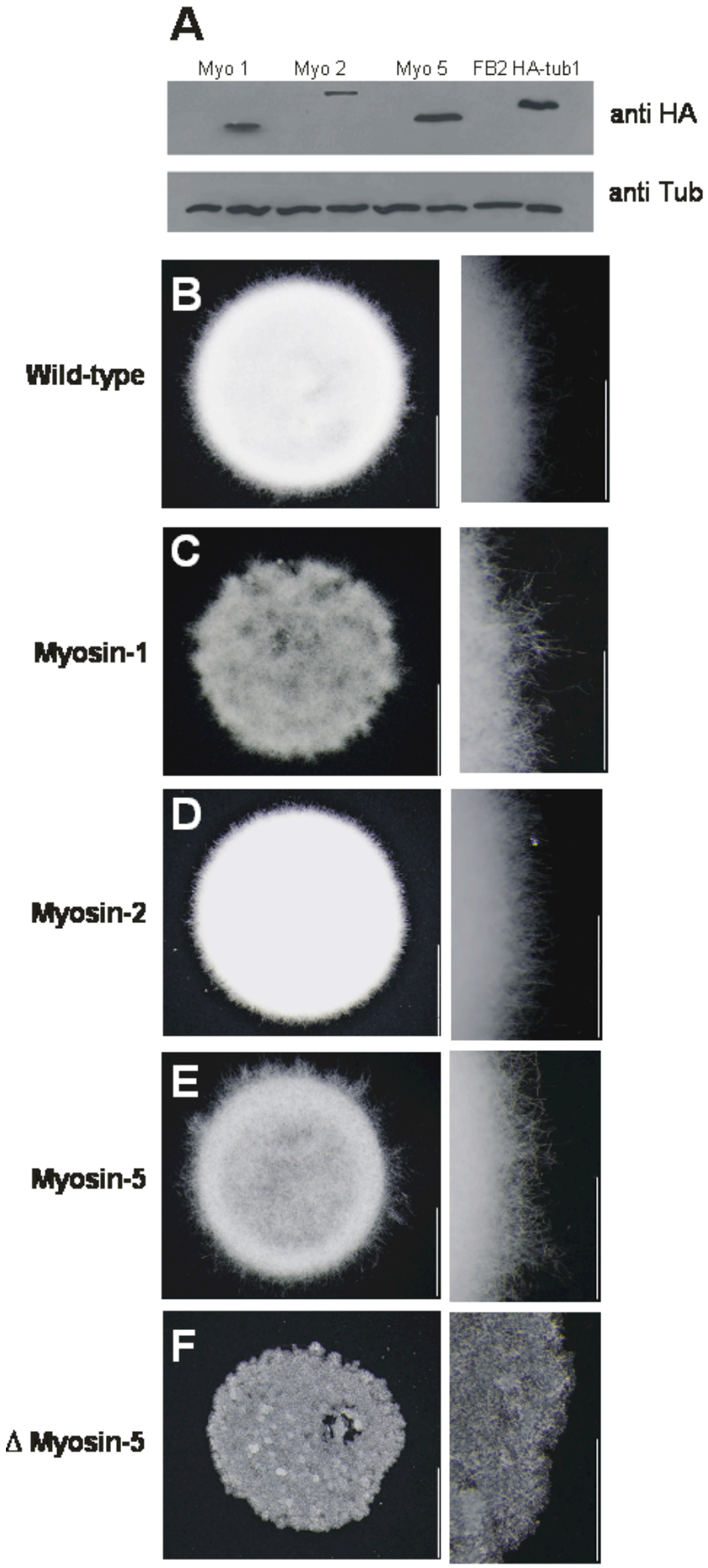

Scale bar represents 5 mm Scale bar represents 1mm.

Figure 4.5. Phenotypic analysis of myosin tail over-expression strains ability to form filamentous hyphae.

A. A western blot showing all proteins expressed under the control of the *crg* promoter (Bottin et al, 1996;) in a GFP lifeact background strain. After shifting cells to glucose-containing medium the promoter is repressed (CM-GLU, OFF), which results in protein depletion. Images shows expression of the myosin-1, myosin-2 and myosin-5 tail over-expression strains in both glucose-containing medium (CM-GLU, OFF) and after switching of media to arabinose-containing medium (CM-ARA, ON). Time of growth in repressive conditions was 18 hours, over-expressed 18 hours.
B. Images depicting colony of wild-type strain lifeact induced via overnight shift to CM-ARA media and then spotted on CM charcoal plates, containing arabinose as the sole carbon source. The right panel shows an enlarged view of the hyphae at the edge of the colony.
C. Images depicting colony of myosin-1 tail over-expression strain induced via overnight culture and shift to CM-ARA media. The culture was then spotted on CM charcoal plates, containing arabinose as the sole carbon source. The right panel shows an enlarged view of the hyphae at the edge of the colony.
D. Images depicting colony of a myosin-2 tail over-expression strain induced via overnight culture and shift to CM-ARA media. The culture was then spotted on CM charcoal plates, containing arabinose as the sole carbon source. The right panel shows an enlarged view of the hyphae at the edge of the colony.
E. Images depicting colony of a myosin-5 tail over-expression strain induced via overnight culture and shift to CM-ARA media. The culture was then spotted on CM charcoal plates, containing arabinose as the sole carbon source. The right panel shows an enlarged view of the hyphae at the edge of the colony.
F. Images depicting colony of a myosin-5 deletion strain induced via overnight culture and shift to CM-ARA media. The culture was then spotted on CM charcoal plates, containing arabinose as the sole carbon source. The right panel shows an enlarged view of the hyphae at the edge of the colony.

4.2.5. Over-expression of myosin-1 or -5 tails lead to a defect in a1 pheromone delivery to the cell vacuole

As we know from previous research, a deletion of myosin-5 leads to problems with mating (Weber et al., 2003). In order to establish whether over-expression of myosin tails would have an effect on endocytosis, we therefore

examined the delivery of a1 pheromone marker to the vacuole. We transformed the *CRG* tail plasmids for myosin-1, -2 and -5 into a pheromone-compatible strain (FB2) and switched to arabinose containing media in order to induce the *CRG* promoter and over-express the myosin tail domains. In order to confirm whether the vacuoles were intact after up to three hours of induction, FM4-64 was added and visualised along with the a1 pheromone. The control strain, FB2 showed an accumulation of pheromone in the vacuole (Figure 4.6. A, middle panel) and intact vacuoles (Figure 4.6. A, right panel). In comparison, the myosin-1 tail over-expression shows no pheromone accumulation in the vacuole, instead there appears to be a significant increase in the cellular background (Figure 4.6. B, middle panel). However, the vacuoles appear to be intact (Figure 4.6. B right panel). Taken together, there is a defect in a1 pheromone delivery to the vacuole. Over-expression of the myosin-2 tail (Figure 4.6. C) showed no defect in endocytosis and transport of pheromone to the cell vacuole (Figure 4.6. C middle panel). The vacuoles under these conditions are intact (Figure 4.6. C, right panel), suggesting that an over-expression of myosin-2 tail does not affect the translocation of the pheromone to the vacuole. In case of over-expression of the myosin-5 tail (Figure 4.6. D), the vacuoles show no accumulation of pheromone in the vacuoles (Figure 4.6. D, middle panel), which is not caused by broken vacuoles, as they appear intact (Figure 4.6. D right panel) and it is observed from the images that the pheromone is also not accumulated in the cytoplasm. This suggests that myosin-5 could be involved in receptor localisation to the plasma membrane. In order to quantify these findings, the average intensity of vacuoles were measured and compared to the wild-type (Figure 4.7. A). A significant difference in the cell vacuole intensity between the over-expression of the myosin-1 tail (Figure 4.7. A $p = 0.0021$) and the myosin-5 tail (Figure 4.7. A $p= 0.001$) was found when compared with the wild-type. Collectively, these data suggest that the transport of the pheromone to the vacuole is inhibited in the presence of tail over-expression of both myosin-1 and myosin-5.

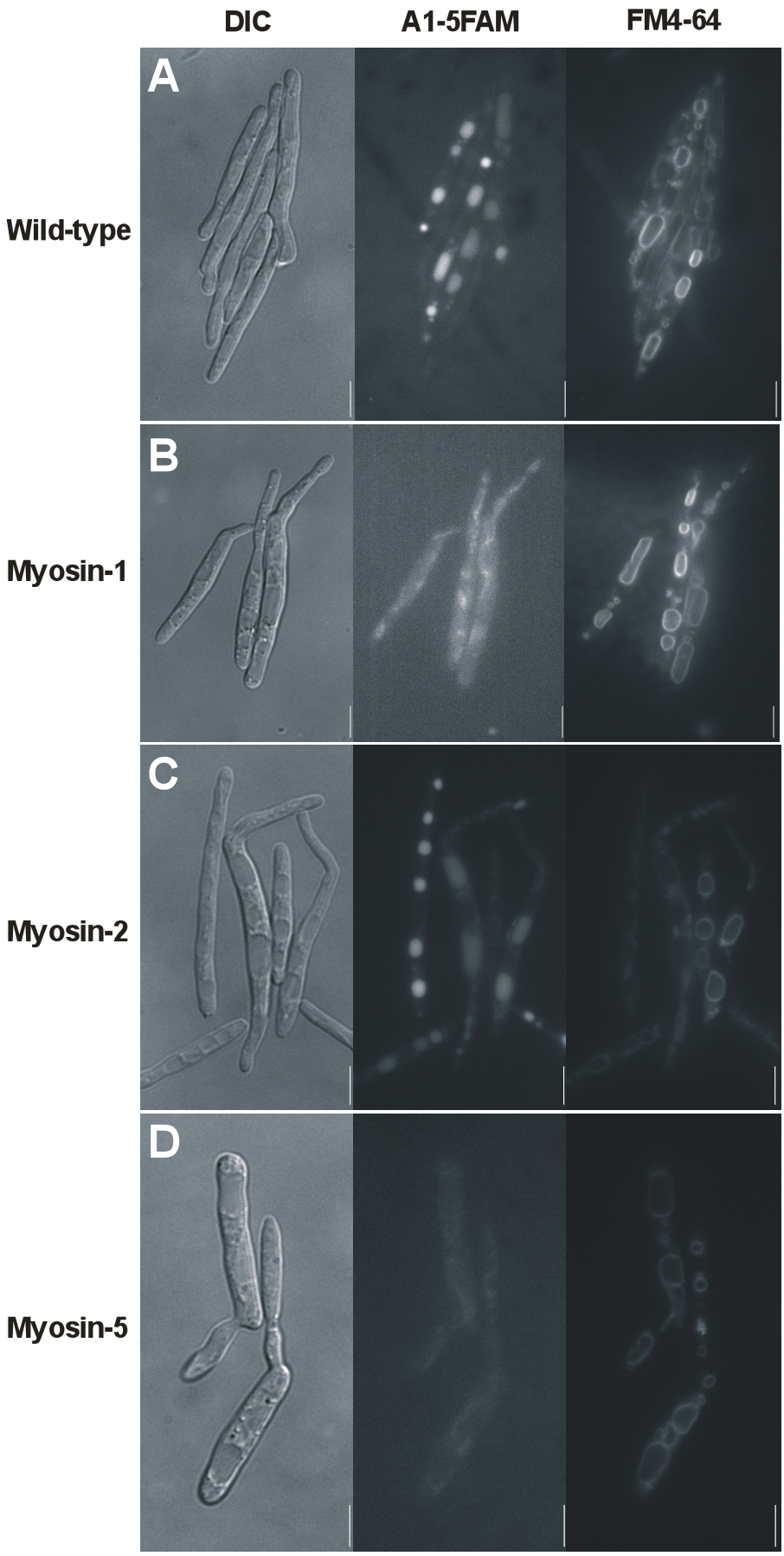

Scale bar represent 5 µm

Figure 4.6. The over-expression of myosin 1and 5 perturbs the expression of the a1-5FAM pheromones in the cell vacuoles even though they remain intact.

A. Images depicting the wild-type cells FB2 in DIC (left panel), cells induced for 3 hours with a1-5FAM pheromone, captured using the GFP laser (middle panel), and, induced with cellular dye FM4-64 captured using the DAPI-HBO lamp.
B. Images depicting the myosin-1 over-expression strain in DIC (left panel), cells induced for 3 hours with a1-5FAM, captured using the GFP laser (middle panel), and, induced with cellular dye FM4-64 captured using the DAPI-HBO lamp.
C. Images depicting the myosin-2 over-expression strain in DIC (left panel), cells induced for 3 hours with a1-5FAM, captured using the GFP laser (middle panel), and, induced with cellular dye FM4-64 captured using the DAPI-HBO lamp.
D. Images depicting the myosin-5 over-expression strain in DIC (left panel), cells induced for 3 hours with a1-5FAM, captured using the GFP laser (middle panel), and, induced with cellular dye FM4-64 captured using the DAPI-HBO lamp.

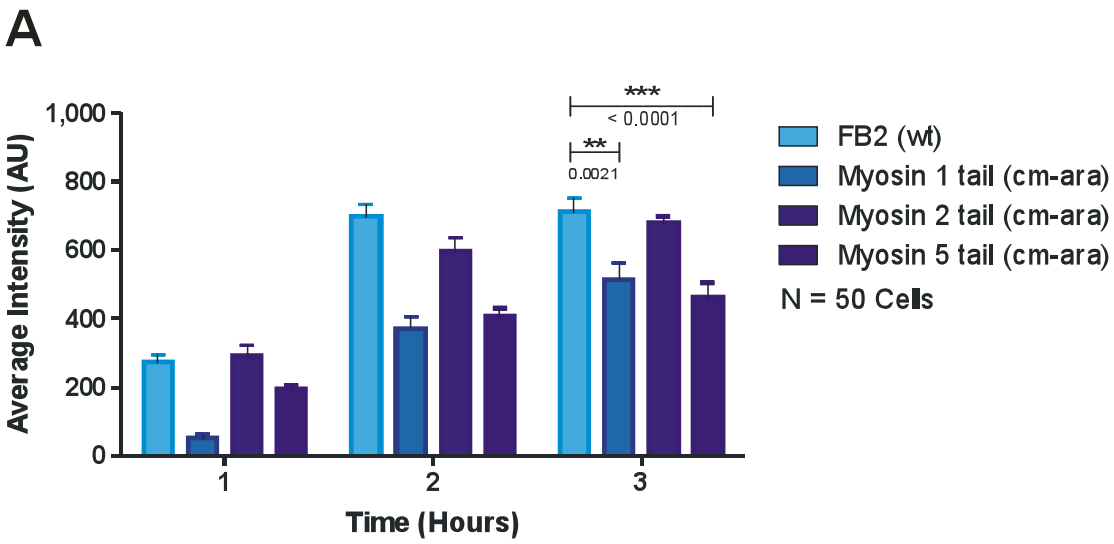

Figure 4.7. Quantitative analysis of the average intensity of cell vacuoles in the myosin tail over-expression mutants.

A. A bar chart depicting the average intensity of cell vacuoles in both the wild-type and myosin-1, -2 and -5 tail over-expression mutants when induced with a1-5FAM pheromone, over a time course of three hours. Bars are given as mean ± standard error of the mean; the sample size n is 50 cells per bar.

Double asterisk indicates significant difference between wild-type FB2 cells and myosin-1 at P <0.005 whereas triple asterisk indicates significant difference between wild-type FB2 and myosin-5 at P < 0.001, using a t test assuming for unequal variances.

4.2.6. Over-expression of myosin-1 affects patch number, whereas over-expression of myosin-5 affects actin patch number, dynamics and patch intensity

Peripheral actin patches mark sites of endocytosis and their continuous turnover supports endocytosis (Kaksonen et al., 2003, Rodal et al., 2005). We have shown that myosin-1 and myosin-5 are involved in endocytosis. To test which myosin motor has an effect on actin patch dynamics, we measured the mean number of patches, and their formation/scission times in the presence of an over-expression of myosin-1, myosin-2 and myosin-5 tails. We found that the mean number of patches was significantly increased in the presence of over-expression of both myosin-1 and myosin-5 tails (Figure 4.8. A, p = < 0.001). However, only myosin-5 showed a significant increase in formation (Figure 4.8. B, p = < 0.001) and scission times (Figure 4.8. C, p = < 0.001). Additionally, we tested whether the over-expression of myosin tails affect the average patch intensity. 25 patches under “OFF” and “ON” condition were measured for each myosin tail mutant and only the over-expression of myosin-5 tail caused a significant decrease in average patch intensity (Figure 4.9.B p = < 0.001). Taken together, these results suggest that over-expression of both myosin-1 and myosin-5 tails affects the number of patches available to the cell but only myosin-5 plays a role in regulation of actin patch dynamics. Furthermore, myosin-5 could play a role in regulation of actin patch maturation at the plasma membrane either directly or via delivery of patch components.

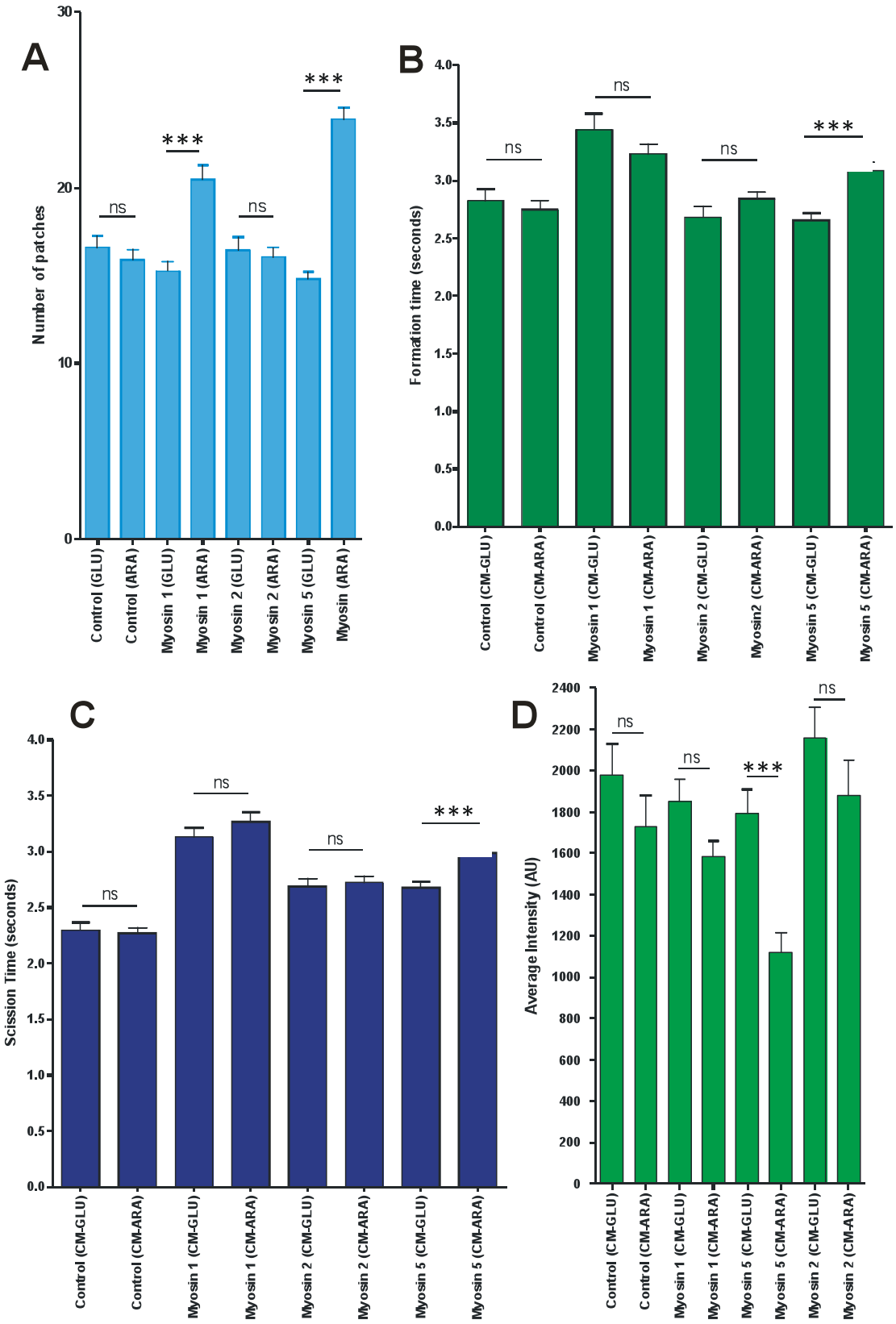

Figure 2.8. Over-expression of myosin tails affects the number of actin patches, their formation and scission time and the average patch intensity.

A. A chart depicting the average number of actin patches in both the wild-type and myosin-1, -2 and -5 tail over-expression strains in both in both glucose-containing medium (CM-GLU, OFF) and after switching of media to arabinose-containing medium (CM-ARA, ON). Time of growth under repressive conditions was 18 hours, over-expressed 18 hours. Bars are given as mean ± standard error of the mean; the sample size n is 20 cells per bar; ns signifies no significant difference between wild-type and myosin over-expression strains, triple asterisk indicates significant difference between wild-type FB2 and myosin over-expression strains at $P < 0.001$, using a t-test assuming for unequal variances.
B. A chart depicting the average timing of actin patch formation events in both the wild-type and myosin-1, -2 and -5 tail over-expression strains in both in both glucose-containing medium (CM-GLU, OFF) and after switching of media to arabinose-containing medium (CM-ARA, ON). Time of growth under repressive conditions was 18 hours, over-expressed 18 hours. Bars are given as mean ± standard error of the mean; the sample size n is 75 patches per bar; ns signifies no significant difference between wild-type and myosin strains, triple asterisk indicates significant difference between wild-type and myosin over-expression strains at $P < 0.001$, using a t-test assuming for unequal variances.
C. A chart depicting the average timing of actin patch scissioning events in both the wild-type and myosin -1, -2 and -5 tail over-expression strains in both in both glucose-containing medium (CM-GLU, OFF) and after switching of media to arabinose-containing medium (CM-ARA, ON). Time of growth under repressive conditions was 18 hours, over-expressed 18 hours. Bars are given as mean ± standard error of the mean; the sample size n is 75 patches per bar; ns signifies no significant difference between wild-type and myosin over-expression strains, triple asterisk indicates significant difference between wild-type and myosin over-expression strains at $P < 0.001$, using a t-test assuming for unequal variances.
D. A chart depicting the average intensity of actin patches in both the wild-type FB2 strain and myosin-1, -2 and -5 tail over-expression mutants and in the presence of both the glucose-containing medium (CM-GLU, OFF) and after switching of media to arabinose-containing medium (CM-ARA, ON). Bars are given as mean ± standard error of the mean; the sample size n is 25 patches per bar; triple asterisk indicates significant difference between wild-type FB2

and myosin over-expression strains at $P < 0.001$, using a t-test assuming for unequal variances.

4.3. Discussion

4.3.1. Actin patches as possible sites of cellular endocytosis

In *S. cerevisiae*, it has been shown that actin cables form tracks for myosin-5-dependent transport of secretory vesicles, whereas actin patches are involved in endocytosis and membrane invagination (Kübler and Riezman, 1993, Pelham and Chang, 2001, Moseley and Goode, 2006). Both patches and cables localise to buds in *S. cerevisiae* but only actin cables were shown to be required for polarised secretion (Pruyne et al., 1998, Yang and Pon, 2002, Huckaba et al., 2004). This study showed an accumulation of actin patches at sites of active growth in *U. maydis* supporting the idea that the actin patches are involved in hyphal growth. In *N. crassa* it has been shown that actin patches have a predictable behaviour pattern; they appear, mature and subsequently disappear into the cytoplasm (Pelham and Chang, 2001, Huckaba et al., 2004, Berepiki et al., 2010). It is thought that these patches are endocytic vesicles, covered with F-actin, which are internalised into the cell, where they are loaded onto actin cables for further transport into the cell (Berepiki et al., 2011). Indeed, we found that the actin patches display a distinctive behaviour, where they appear to grow in intensity and then disappear from the focal plane. In addition, the induction with the a1 pheromone causes a significant increase in patch number, as well as a decrease in time for turnover events, specifically the time a patch needs to form and then scission away from the plasma membrane. This suggests that the a1 pheromone causes an up regulation of patch dynamics in order to endocytose the a1 pheromone/ Pra2 receptor complex as quickly as possible and pass communication signals to the expanding tip of the cell. The cell is therefore able to grow in the direction of the pheromone source to fuse with the opposite mating-type (Bölker et al., 1992, Bortfeld et al., 2004). This up-regulation of actin corroborates with work carried out in mammalian cells, which suggests that receptor-mediated endocytosis is reliant on intact actin filaments (Lamaze et al., 1997).

4.3.2. Cytoskeleton requires the action of molecular motors to bridge the gap between plasma membrane and vacuoles

Many studies have shown that actin has a crucial role in hyphal growth (Heath and Steinberg, 1999, Fuchs and Steinberg, 2005). However, the rapid delivery of signalling components into specific cellular locations over long distances is not possible, with only passive diffusion (Miaczynska et al., 2004) and therefore, we suggest the same is true of the distance between actin patches at the growing tip and vacuoles in the cell. In this study, we suggest that molecular motors such as myosins are involved in transport of endocytosed material. As the position of both the patches and the cell vacuole in the cell is far apart, it is our suggestion that myosins bridge the distance between actin patches and vacuoles via actin cables. This is also supported by evidence in other organisms such humans, where myosin-1 links the actin cytoskeleton to the plasma membrane (Geli and Riezman, 1996) and myosin-5 is a transporter for vesicles and organelles in filamentous fungi (Weber et al., 2003, Woo et al., 2003) whilst it also contributes to the organisation of the actin tracks in yeast (Woolner and Bement, 2009, Reymann et al., 2012).

4.3.3. Over-expression of myosin-1 and -5 tails does affect yeast-like or filamentous cell growth

In yeasts such as *S. cerevisiae* and *S. pombe*, recruitment of Myo1 to endocytic patches and targetting of Myo2 to the division site are accomplished by the tails of these proteins (Naqvi et al., 1999, Bezanilla and Pollard, 2000). In this study, we have over-expressed the tail domain of the three *U. maydis* myosin motors; myosin-1, myosin-2 and myosin-5, which we suggest leads to competition of cargo binding with the fully functional myosin and therefore a disorder of function. In order to fully understand the effect of this mechanism, we analysed both the yeast-like and filamentous growth in these mutants. Over-expression strains of myosin-1 and myosin-5 showed thicker yeast-like cells than those shown in the wild-type. This corroborates previous findings with deletion strains of myosin-5 (Weber et al., 2003). In contrast, an over-

expression of the myosin-2 tail domain lead to longer cells with an apparent inability to separate, suggesting a cell separation defect. This is corroborated by research carried out in *S. pombe,* which found irregular actin rings and septa that were impaired in cell separation (Kitayama et al., 1997). In the assays for filamentous growth, it was found that all myosin tail mutants were viable and could form hyphae but the myosin-1 and myosin-5 mutants grew slower than the control and myosin-2 cells. This again agrees with previous research (Weber et al., 2003) and suggests that the myosins are non-essential but are required for correct cell morphology and cell separation.

4.3.4. Over-expression of myosin-1 and myosin-5 tails leads to defects in pheromone transport

The lack of accumulation of a1 pheromone in the vacuole of cells that we observe in the presence of an over-expression of myosin-1 and myosin-5, suggests that both motor proteins are involved in the transport of the pheromone. This links with the cellular function of myosins that is generally assumed to be movement of cellular components (Wu et al., 2000). Furthermore in plants, it has been suggested that myosin-11, which is closely related to the fungal class-V myosin, may have an additional role in delivering organelles and vesicles to their destinations and in increasing cytosolic circulation and metabolite redistribution (Brangwynne et al., 2008). Additionally, we suggest that there is no uptake of the pheromone at all in the presence of an over-expression of myosin-5, as there is not an increase in cellular background. This is supported by previous work (Weber et al., 2003), where deletion mutants of myosin-5 were unable to form conjugated hyphae. Over-expression of myosin-1 led to an increase in cellular background and therefore, we suggest the pheromone is internalised and able to be transported, hence the accumulation of cargo such as the internalised a1 pheromone. Currently we know that myosin-5 has a role in secretion (Schuster et al., 2011c), therefore we suggest that myosin-5 has an indirect effect on the endocytosis pathway towards the cellular vacuole, as it

transports components of the actin patch complex such as Sla1, RVS167 bar protein or the Pra2 receptor itself.

4.3.5. Over-expression of myosin-5 affects patch dynamics and intensity

The labelling of F-actin and MTs in *U. maydis* has revealed that both cytoskeletal systems could serve as tracks for delivery of vesicles to the expanding growth region (Schuster et al., 2011c). This also indicates a role of actin in addressing the balance of material being exo- or endocytosed (Zeng et al., 2001, Weinberg and Drubin, 2012). We have shown that actin patches accumulate in the growing tip and that over-expression of myosin tail had a significant effect on actin organisation in particular, patch dynamics. The presence of actin cables in fungi and plants implies the use of myosin-5 in secretion (Woolner and Bement, 2009). Indeed, it has been shown that myosin-5 is required for polarised growth in *U. maydis* (Weber et al., 2003, Schuchardt et al., 2005), as well as continuous flow towards the growth region (Schuster et al., 2011c). It is known that actin patches consist of over 60 proteins such as Sla1, Sla2 and RVS167 bar protein (Stefan et al., 2005), which need to be delivered to the growth region most probably by active transport of myosin-5. Without these components, patches are unable to complete their formation step, and in yeast, it is shown that the order of protein recruitment at the site of endocytosis is crucial (Michelot et al., 2010). The absence of patch components has been proven to alter patch dynamics in organisms such as *S. cerevisiae* with Sla2 mutants (Wesp et al., 1997, Sun et al., 2005) and RVS167 bar protein (Youn et al., 2010, Boettner et al., 2011). Additionally, the use of actin inhibiting drugs such as latrunculin, that destroy actin patches, lead to the Pra1 receptor being trapped at the plasma membrane in *U. maydis* (Fuchs and Steinberg, 2005). This strengthens the evidence that myosin-5 may have a role in secretion. Finally, we found that the intensity of actin patches at the plasma membrane is significantly decreased in the presence of the over-expression of myosin-5 tail. This together with the significant decrease in patch formation and scission times, suggests that the recruitment of actin is somehow regulated by the action of

myosin-5. However this is something that requires further investigation such as by the tandem affinity purification of myosin motor cargoes by the incorporation of a TAP tag and analysis using mass spectrometry. In addition, in order to provide further evidence on the role of myosin-1 and myosin-5 in the endocytosis pathway and prove confidently that *U. maydis* does indeed use clathrin coated pits, it would be useful to link the action of actin patches with clathrin, as well as other coating proteins such as Sla1, Sla2 and RVS167 which are present in the *U. maydis*. Multiple components could be localized and as the patch forms, a timeline of acquisition to the plasma membrane, which could be, identified with the use of RFP and GFP tags to show that indeed *U. maydis* endocytosis followed the same routine as has been shown previously in yeast cells.

5. CHAPTER 5 - ROLE OF THE MICROTUBULE CYTOSKELETON DURING ENDOCYTOSIS OF THE a1 PHEROMONE

5.1. Introduction

In order for eukaryotic cells to adapt to their ever-changing environments and external stimuli, they rearrange their cytoskeletons and subsequent membrane traffic towards polarised cellular domains (Shaw et al., 2001). F-actin and MTs, in combination with associated proteins, like molecular motors, support this process by directed delivery of the cargoes required for polar growth in plant cells (Bibikova et al., 1999) and mammalian cells (Nabi, 1999). In fisson yeast, the MT cytoskeleton is essential for morphogenesis (Mata and Nurse, 1998) and as with all eukaryotes, fission yeast microtubules are polymers of α-and β-tubulin (Hagan, 1998). In filamentous fungi, the role of the MT cytoskeleton has been well established, beginning with its role in nuclear migration in *A. nidulans* (Oakley 1980) and expanding to a role in apical growth and enzyme secretion (Torralba et al., 1998b). In *U. maydis*, the MT cytoskeleton is essential, along with F-actin in polarised growth (Steinberg et al., 2001). Indeed it has been found that a disruption of MTs in hyphae significantly decreased the rate of hyphal elongation but did not stop filamentous growth completely (Fuchs et al., 2005). It is well known that molecular motors such as kinesin and dynein, use MT tracks in membrane trafficking. Indeed, both *A. nidulans* and *U. maydis* have regions of microtubules arranged uniformly or anti-parallel, to facilitate molecular motors and the bi-directional transport of their cargoes. Kinesin motors carry out plus-end-directed (anterograde) transport, while minus-end-directed (retrograde) transport is mediated by dynein. In the genomes of filamentous fungi, 10 – 12 kinesins are typically found with members of the kinesin-1 and kinesin-3 family being suggested to participate in transport (Steinberg, 2011). While multiple kinesin motors are used for anterograde motility, nearly all retrograde cytoplasmic movement in both metazoans and filamentous fungi is driven by a

single cytoplasmic dynein motor. Dynein activity is regulated by an array of associated proteins and protein complexes, including dynactin, Lis1, Nudel, and dynein-associated subunits (Kardon and Vale, 2009). It has been shown to have a role in nuclear migration in filamentous fungi such as *N. crassa*, *A. nidulans* and *Ashbya gossypii* (Plamann et al., 1994, Xiang et al., 1994, Alberti-Segui et al., 2001) and arrest of hyphal growth in *U. maydis* (Fuchs et al., 2005). In *U. maydis*, it has additionally been shown that a mutation in the motor protein dynein results in reduced MT growth and shrinkage events, as well as the frequency of catastrophe events (Carminati and Stearns, 1997) and that an accumulation of dynein at the MT plus end close to the growing tip (which is called the loading zone), serves as a reservoir for the retrograde endosome transport (Lenz et al., 2006, Schuster et al., 2011b).

It has been established that dynein and kinesin-3 support the motility of EEs in *U. maydis* (Wedlich-Söldner et al., 2002b) which, in turn, is thought to facilitate long-range communication between the nucleus and the growing hyphal tip (Lenz et al., 2006). The presence of YUP1, a t-SNARE that is known for its localisation to EE's in yeast and mammalian cells also localises on organelles in *U. maydis* that have been described as early endosomes, as they can be labelled with the endocytic marker dye FM4-64 (Wedlich-Söldner et al., 2000). Mutations in the yup1 gene lead to mutants that were impaired in the endocytosis of FM4-64 (Wedlich-Söldner et al., 2000) and failed to recycle the pheromone receptor Pra1 back to the surface (Fuchs et al., 2006). In the previous chapter, we found that the transport of the a1 pheromone to the cell vacuoles was inhibited in the presence of benomyl (Figure 3.9). In order to provide further evidence as to whether a1 pheromone transport to the vacuole is indeed MT based and specifically which parts of the microtubule cytoskeleton are involved, the aims of this chapter are therefore;

- To investigate the anterograde transport of the pheromone receptor to the plasma membrane using deletion strains of kinesin-1 and kinesin-3 treated with the synthetic a1 pheromone
- To examine whether dynein is the retrograde motor protein responsible for the transport of the a1 pheromone to the cell vacuole

- To establish whether the a1 pheromone is transported via early endosomes.

5.2. Results

5.2.1. Transport of the a1 pheromone is more dependent on kinesin-3 than kinesin-1

Kinesin-1 and kinesin-3 contain a head (motor) domain, a neck domain and a tail domain to bind cargoes (Figure 5.1. A). Microscopic analysis of control wild-type (FB2) cells showed normal cigar-shaped cells (Figure 5.1. B, left panel), with no pheromone transport defect and an accumulation of the a1 pheromone in the vacuole after three hours (Figure 5.2. B, right panel). With the deletion of kinesin-1, we noticed that some cells are rounded at their septa (Figure 5.1. C, left panel), and that accumulation of the a1 pheromone was still observed suggesting no defect in pheromone transport towards the cell vacuole after three hours (Figure 5.1. C, right panel). This contrasts with the deletion of kinesin-3 where we observed cells, which are unable to separate and form tree-like structures (Figure 5.1. D, left panel). Additionally, we observed that there is no accumulation of the a1 pheromone in the vacuole throughout the three-hour time course (Figure 5.1. D, right panel), suggesting a transport defect of the a1 pheromone. In order to quantify these findings, the average intensity of vacuoles were measured for each deletion strain and compared to wild-type cells (Figure 5.1. E). We found a significant difference in the vacuole intensity between the wild-type and both kinesin-1 ($P = 0.025$) and kinesin-3 ($P < 0.001$). This led us to the assumption that both kinesin's are involved in the transport of the pheromone towards the cell vacuole.

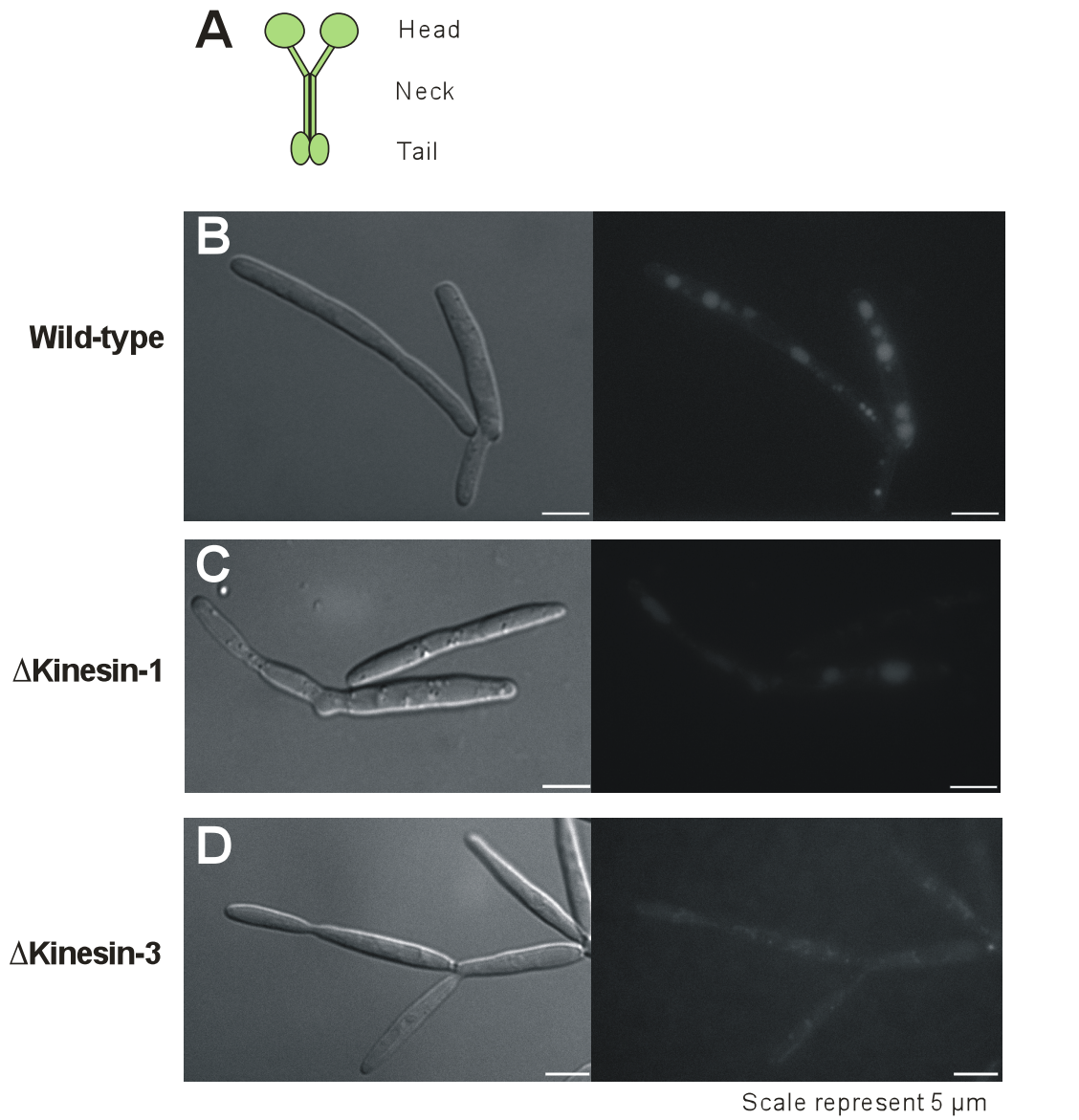
A
Head
Neck
Tail
B
Wild-type
C
ΔKinesin-1
D
ΔKinesin-3
Scale represent 5 µm
E
800
700
600
500
400
300
200
100
0
Average Intensity (AU)
1
2
3
Time (Hours)
***
**
FB2
Δkin1
Δkin3

Figure 3.1 Deletion of kinesin-1 and kinesin-3 leads to a defect in transport of the a1 pheromone to the cell vacuole.

A) Schematic drawing of fungal kinesins showing two heavy chains (~105kDa) with two microtubule binding domains in the head, as well as a cargo binding domain in the tail region.
B) Images depicting wild-type cells when induced with a1 pheromone for 3 hours. Left panel shows cells in DIC and right panel shows fluorescence of the a1-5FAM pheromone.
C) Images depicting a Δ kinesin-1 mutant when induced with a1-5FAM pheromone for 3 hours. Left panel shows cells in DIC and right panel displays fluorescence of the a1-5FAM pheromone.
D) Images depicting a Δ kinesin-3 mutant when induced with a1-5FAM pheromone for 3 hours. Left panel shows cells in DIC and right panel displays fluorescence of the a1-5FAM pheromone.
E) Graph depicting the average intensity of cell vacuoles in both wild-type and Δ kinesin-1 and Δ kinesin-3 mutants when induced with the a1-5FAM pheromone, over a time course of 3 hours. Bars given in mean ± standard error of the mean; the sample size is n = 50 cells per bar. Double asterisk indicates a significant difference between wild-type and Δkinesin-1($P = 0.025$) whereas, triple asterisk indicates significant difference between wild-type and Δkinesin-3 ($P < 0.001$) using a t-test assuming for unequal variances.

5.2.2. Transport of the a1 pheromone is dependent on the dynein motor complex

The accumulation of dynein in the hyphal tip, suggests a reservoir of the motor protein that captures arriving EE's for retrograde motility (Lenz et al., 2006). Dynein is a large protein complex, which consists of heavy chain, intermediate chain, light intermediate chain and three families of light chains (Figure 5.2, A). As dynein cannot be deleted (Straube et al., 2001), we induced a dynein temperature-sensitive (TS) strain (Wedlich-Söldner et al., 2002a) with the a1-5FAM pheromone. Microscopic analysis showed accumulation of the a1-5FAM pheromone in the cell vacuole under control conditions at its permissive temperature (22 °C) (Figure 5.2. B, left panel). There was no a1-5FAM pheromone accumulation defect observed at its

restrictive temperature of 32 °C (Figure 5.2. B, right panel). In contrast to its temperature-sensitive dynein mutant, we observed that under a permissive temperature of 22 °C, the cells appeared similar to the wild-type and there was still an accumulation of the a1-5FAM pheromone in cell vacuoles (Figure 5.2. C. left panel). This contrasts significantly with the restrictive temperature of 32 °C, where we observed a defect in the accumulation of the a1-5FAM pheromone in the vacuole (Figure 5.2. C. right panel). In order to quantify these findings, the average intensity of vacuoles were compared at both permissive and restrictive temperature for wild-type and dyneinTS cells (Figure 5.1. D). We found a significant difference in vacuole intensity between wild-type and dynein at the restrictive temperature of 32 °C ($P < 0.001$). This lead us to the conclusion that dynein is involved in the transport of the pheromone to the vacuole.

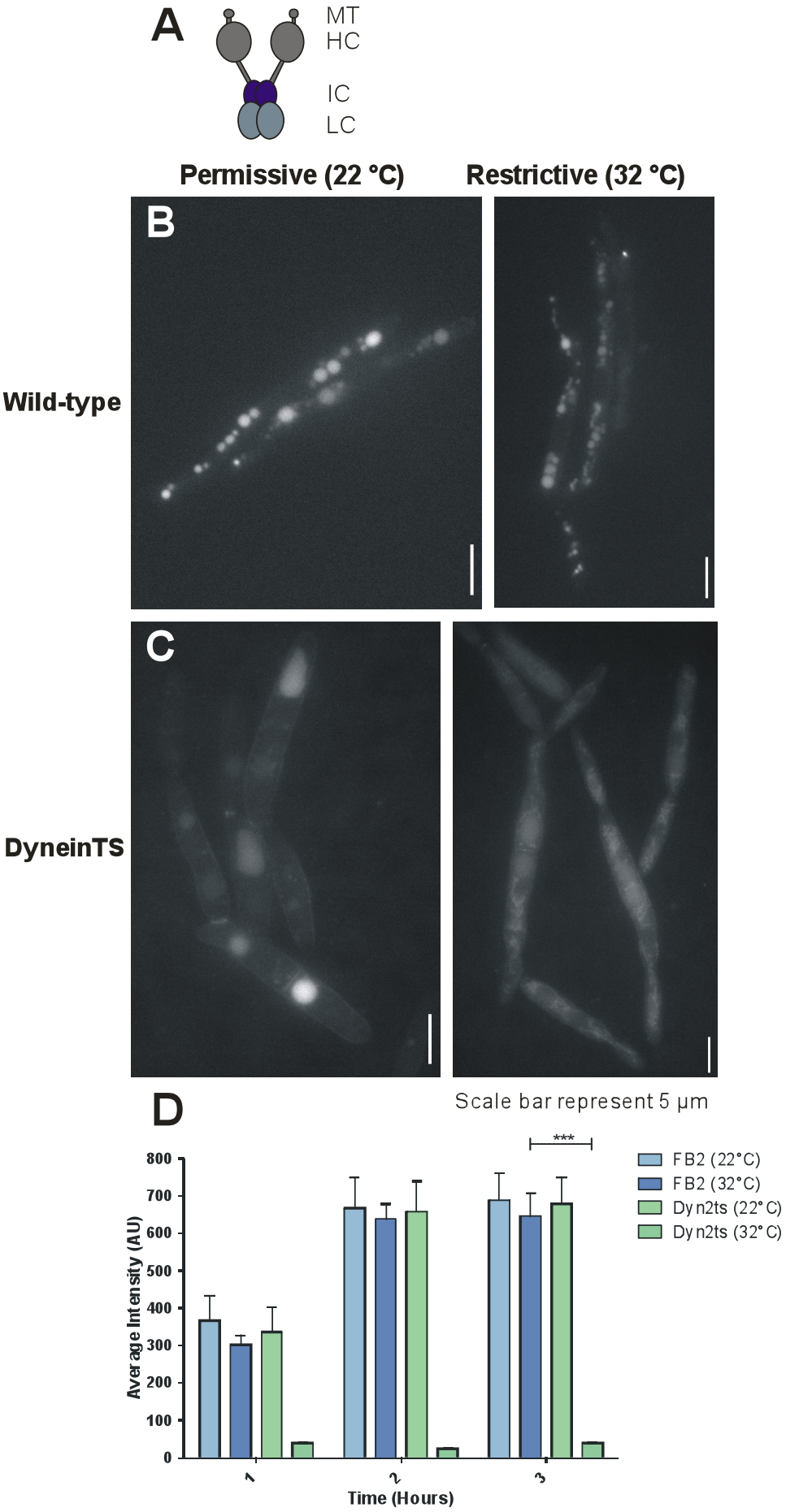
A
MT
HC
IC
LC
Permissive (22 °C)
Restrictive (32 °C)
B
Wild-type
C
DyneinTS
Scale bar represent 5 µm
D
***
FB2 (22°C)
FB2 (32°C)
Dyn2ts (22°C)
Dyn2ts (32°C)
Average Intensity (AU)
800
700
600
500
400
300
200
100
0
1
2
3
Time (Hours)

Figure 3.2. Transport defect of the a1 pheromone is observed in the recessive condition of DynTS mutant.

A) Schematic drawing of fungal dynein showing a stalk with two MT binding domains (MT) two heavy chains (HC), (~400 kDa), two intermediate chains (IC) and two light chains (LC). C denotes carboxyl terminus and N, amino terminus.

B) Images depicting wild-type cells when induced with the GFP labelled a1-5FAM pheromone for 3 hours. Left panel displays cells at restrictive 22 °C temperature, right panel shows cells at 32 °C temperature.

C) Images depicting Dynein TS mutants when induced with GFP labelled a1-5FAM pheromone for 3 hours. Left panel displays cells at recessive 22 °C temperature, right panel shows cells at 32 °C temperature.

D) Graph depicting the average intensity of cell vacuoles in both wild-type and Dynein TS mutants when induced with the a1-5FAM pheromone over a time course of 3 hours. Bars given as mean ± standard error of the mean; the sample size is n = 50 cells per bar. Triple asterisk indicates significant difference between wild-type and Dynein TS mutant ($P < 0.001$) using a t-test assuming for unequal variances.

5.2.3. Transport of the a1 pheromone is dependent on functional Yup1 protein

Yup1 is a t-SNARE protein, which controls the membrane fusion with EEs. When a TS mutation to this protein was introduced, it causes a lack of this fusion and it has been shown previously to impair endocytosis (Wedlich-Söldner et al., 2000). In order to establish whether the transport of the a1-5FAM pheromone is dependent on fusion to the early endosomes, we induced a Yup1TS strain and treated it with the a1-5FAM pheromone. Microscopic analysis in wild-type (FB2) cells showed accumulation of the a1 pheromone in vacuoles at the permissive temperature (22 °C) (Figure 3.3. B, left panel) and a1 pheromone accumulation was observed in the vacuole at the restrictive temperature of 34 °C (Figure 3.3. B, right panel), suggesting the increase in temperature did not affect the EE dynamics. Yup1TS cells appeared similar to wild-type cells with an accumulation of the a1-5FAM pheromone in vacuoles (Figure 3.3. C, left panel). However, at the restrictive

temperature, no a1-5FAM pheromone accumulation was observed in the vacuole (Figure 3.3. C, right panel), suggesting a defect in the transport of a1-5FAM pheromone to the vacuole. In order to quantify these findings, the average intensities of vacuoles were compared at both permissive and restrictive temperature for wild-type and Yup1TS cells (Figure 3.1. D). We found a significant difference in intensity between wild-type and Yup1TS at restrictive temperature ($P < 0.001$). Therefore, we summarize that EE's are responsible for travel of either the pheromone receptor to the plasma membrane or the delivery of the a1-5FAM pheromone to the cell vacuole.

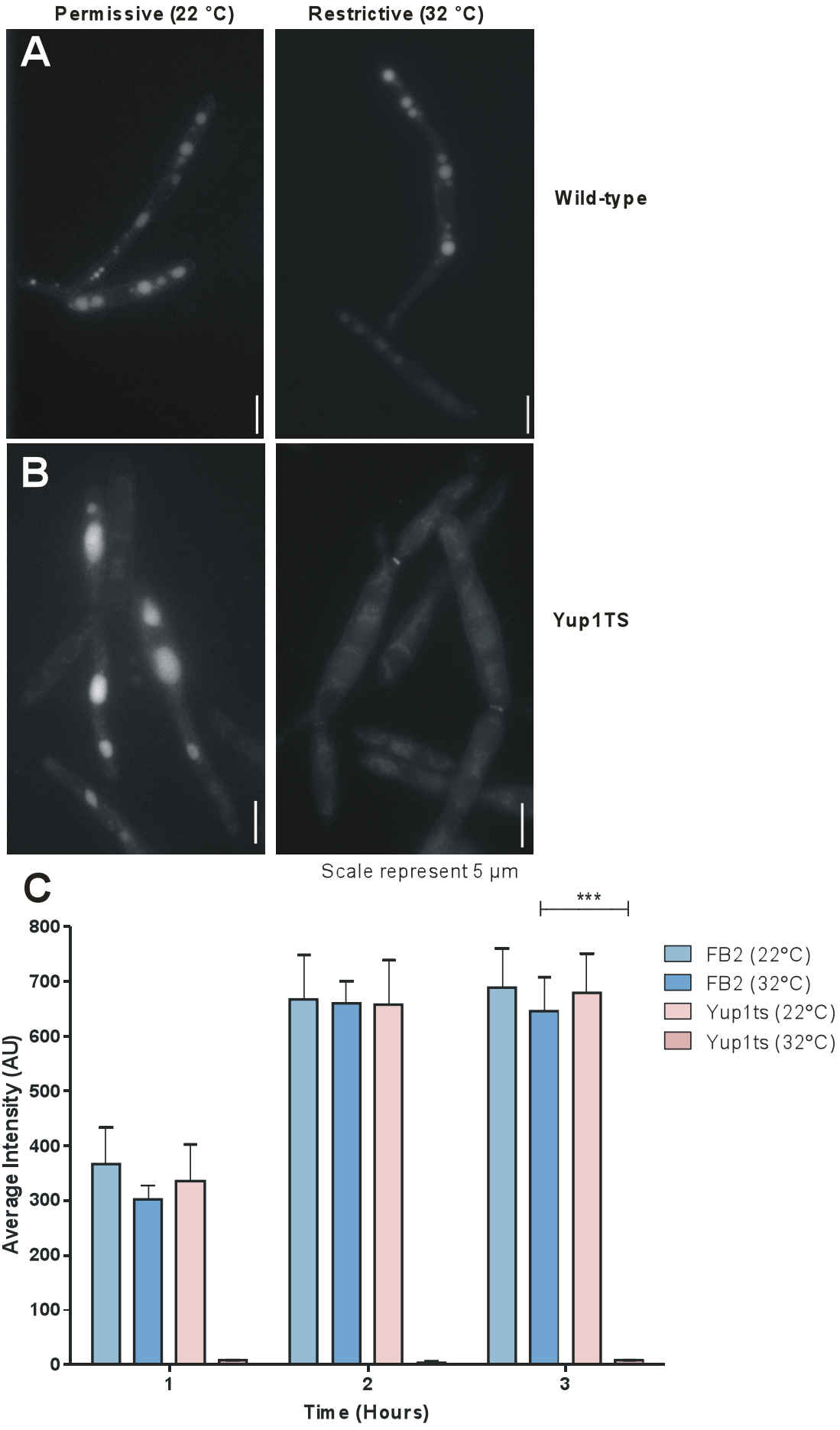
Permissive (22 °C)
Restrictive (32 °C)
A
Wild-type
B
Yup1TS
Scale represent 5 µm
C
***
800
700
600
500
400
300
200
100
0
Average Intensity (AU)
1
2
3
Time (Hours)
FB2 (22°C)
FB2 (32°C)
Yup1ts (22°C)
Yup1ts (32°C)

Figure 3.3. Transport defect of the a1-5FAM pheromone is observed under recessive condition of Yup1TS mutant.

A) Images depicting wild-type when induced with the a1-5FAM pheromone for three hours. Left panel displays cells taken at recessive 22 °C temperature and right panel shows cells at 32 °C temperature.
B) Images depicting a Yup1TS mutant when induced with the GFP labelled a1-5FAM pheromone for 3 hours. Left panel shows cells at recessive 22 °C temperature and right panel displays cells at 32 °C temperature.
C) Graph depicting the average intensity of cell vacuoles in both wild-type and Yup1TS mutants when induced with the a1-5FAM pheromone over a time course of 3 hours. Bars given as mean ± standard error of the mean; the sample size is n = 50 cells per bar. Triple asterisk indicates significant difference between wild-type and Yup1TS mutant ($P < 0.001$) using a t-test assuming unequal variances.

5.3. Discussion

5.3.1. Transport of the a1-5FAM pheromone to the cell vacuole relies on the kinesin-3 and dynein motor complexes

Bidirectional motility of organelles is a very complex process, which is important for various organelles, including endosomes, secretory vesicles, lysosomes and mitochondria (Gross et al., 2002, Welte, 2004). In *U. maydis,* bi-directional long-range transport is mediated by the opposing motor proteins dynein and kinesin-3 (Wedlich-Söldner et al., 2002b). We showed here that deletion of kinesin-3 causes a significant decrease in accumulation of the a1-5FAM synthetic pheromone in the vacuole. We propose that that a deletion of kinesin-3 leads to an absence of the Pra2 receptor at the plasma membrane, as it is unable to be recycled back to the growth region. This leads to a defect in the endocytosis of the a1 pheromone and its delivery to the vacuole. Similarly, in the absence of kinesin-1, we again observe a significant decrease in accumulation of the a1-5FAM pheromone in the vacuoles. However, the difference was not as significant as what is found for kinesin-3 suggesting that

kinesin-1 may have a more indirect effect on the transport of the a1 pheromone because of the delivery of dynein via kinesin-1.

Therefore, a deletion of kinesin-1 causes clustering of dynein at the plus-ends of MTs (Zhang et al., 2003, Lenz et al., 2006). Dynein is delivered to the plus end of microtubules and serves as a reservoir to prevent that EEs from falling off the track (Schuster et al., 2011a). Indeed, we found that the cell cannot cope with a full deletion of dynein and therefore only a temperature sensitive mutant was used. Additionally, we found that at a restrictive temperature, no transport of the pheromone towards the cell vacuole occurred providing further evidence that dynein was indeed essential in the membrane trafficking process. Furthermore, we speculate that it has a role in delivery of the a1 pheromone/ receptor complex to the cell interior. We however do not suggest that dynein has a direct role in endocytosis, more that in its role as a bi-directional motor it regulates the movement of EEs, which internalize the pheromone.

5.3.2. a1 pheromone travels with Yup1 on early endosomes

Bi-directional motility has also been described for EEs in yeast-like cells of *U. maydis* (Wedlich-Söldner et al., 2002b, Lenz et al., 2006, Schuster et al., 2011b). EEs reach the plus-ends in the hyphal tip by the activity of kinesin-3, where they were apparently loaded onto the dynein/dynactin complex, which transports EEs retrograde towards the minus end (Lenz et al., 2006). The Yup1 t-SNARE was identified on EEs and shown to be essential in pathogenic development, as well as being a marker for EE transport (Fuchs et al., 2006). We found that Yup1 also has a role in the transport of the a1 pheromone to the cell vacuole. This confirms what was already found for the opposing mating-type receptor Pra1, whereby the use of a Yup1TS mutant led to endocytic transport vesicles that were unable to fuse with the EEs (Fuchs et al., 2006). The inability of the cell to transport the a1 pheromone to the vacuole leads to a blockage of the degradation and recycling pathways. Although this may not affect the initial step of endocytosis as some of the Pra2 receptor is already present at the plasma membrane, an accumulation of

transport vesicles unable to bind to EEs, will lead to a depletion of Pra2 receptor at the cell surface and consequently pathogenic development was not initiated.

CHAPTER 6 – FINAL DISCUSSION

6.1. Summary and Outlook

These studies present new understanding for the function of the actin and microtubule cytoskeleton in the endocytosis pathway of the fungus *U. maydis*. We have developed a suitable marker to visualise endocytosis in *U. maydis* cells, with a fluorescently tagged synthetically produced a1 pheromone labelled with a 5-FAM fluorophore. We have shown that the synthetic alternative peptide is internalised in the same manner as the natural a1 pheromone and it is thought to bind directly at the fungal cell surface to its corresponding Pra2 receptor, which contains the correct binding sequence and is subsequently internalised into the cell. Alongside studies on the Pra1 receptor and its function in *U. maydis* where they have shown that Pra1 is constitutively endocytosed and accumulates in small vesicular structures in yup1^{ts} mutants. (Fuchs et al., 2006). A similar phenotype was reported in *rcy1Δ* cells of *S. cerevisiae*, in which an accumulation of the pheromone receptor Ste2 was found in an uncharacterized endocytic compartment (Wiederkehr et al., 2000). We have provided further lines of evidence that *U. maydis* participates in receptor-mediated endocytosis and that cells rely on endocytosis for growth and achieving correct cell morphology. This is in agreement with previous research carried out in yeast (Geli and Riezman, 1998) and other filamentous fungi (Upadhyay and Shaw, 2008). We have delivered evidence that a synthetically produced, fluorescently labelled marker such as the 5 FAM-labelled a1 pheromone can be successfully used in *in vivo* experiments and is a suitable alternative to that isolated from wild-type cells. An interesting addition in this area would be the synthesis of the a2 pheromone with a fluorescent tag to examine whether it too could be a viable marker for endocytosis. Additionally, if we were to tag each one with a different fluorophore emitting at different wavelengths and observe the accumulation of pheromone, as well as, their transport during mating of FB1 and FB2 cells, we could ascertain whether they both follow the same endocytosis pathway.

Furthermore, we have provided evidence that the pheromone is internalised into the cell and over time, accumulated in the vacuole. In order to bridge the gap between plasma membrane and the vacuole, we looked in more detail at the actin and MT cytoskeleton and their associated molecular motors. Furthermore, we observed that the long distance transport of the pheromone was shown to be reliant on microtubule-associated motors, such as dynein and kinesin-3. In addition, the pheromone interacts with the t-SNARE protein Yup1, which is present on EEs. This suggests strongly that the 5-FAM-labelled a1 pheromone and its Pra2 receptor are cargos of EEs. An extension of these studies would be to further investigate the role of Ras-associated binding (Rab) GTPases in the transport of the a1 pheromone and its receptor during endocytosis. Rab GTPases are a conserved group, found throughout all species and they are involved in a variety of functions (reviewed in (Seabra and Coudrier, 2004, Barr, 2013)). Rab proteins, in particular Rab5 proteins, have been found in *U. maydis* (Fuchs and Steinberg, 2005) and confirmed to be a marker of EEs *in vivo* (Fuchs *et al.*, 2006). Recently our laboratory has shown that it is also essential for plant infection (Higuchi, Bielska et al., unpublished). This could suggest a role in recruitment of proteins to EEs and a 'hitchhike' mechanism of Rab5 on EEs towards the growth region at the tip, in order to facilitate plant infection. More research on the role of Rab5 is necessary, as well as localising and assigning a role for other Rab GTPases, known to exist in the *U. maydis* genome, such as Rab4, Rab5b and Rab7. Research on these proteins would allow us to establish whether they have the same roles in endocytosis as research in yeast and mammalian cells suggest (Bielli et al., 2001, Gorvel et al., 1991, Horgan and McCaffrey, 2011, Banks et al., 2011). Additionally, it would be beneficial to add Rab11 as we were not able to delete the Rab11 gene, which could suggest that it is essential and would also be a likely candidate for defects in pathogenicity.

Furthermore this study shows that actin patches accumulate at sites of active growth in *U. maydis*, which supports the idea of their involvement in hyphal growth. In addition we have shown that actin patches display a distinct behaviour with growth in intensity and subsequently disappearance from the focal plane, which was shown already in *N. crassa* (Pelham and Chang, 2001,

Huckaba et al., 2004, Berepiki et al., 2010). As assumed, the induction of the a1 pheromone response causes a significant increase in patch number and a decrease in the time of turnover events, which suggests an up regulation of patch dynamics in order to endocytose the a1/Pra2 complex as quickly as possible, delivering information/signals from and to the expanding tip of the cell. This enables the cell to grow towards the pheromone source and fuse with the opposite mating type (Bölker et al., 1992, Bortfeld et al., 2004) which is in agreement with work carried out in mammalian cells where receptor-mediated endocytosis is dependent on actin (Lamaze et al., 1997). Furthermore it would be useful to prove that *U. maydis* does indeed use clathrin coated pits in order to link the action of actin patches with clathrin and other coating proteins such as Sla1, Sla2 and RVS167. Multiple components of these named proteins could be tagged with RFP and/or GFP and localized and as the patch forms, a timeline of acquisition to the plasma membrane made. This could give us inside into the involvement of clathrin and other coating proteins in the initiation of endocytosis.

In addition to widening the knowledge and understanding of involvement of the MT motors, this thesis has provided evidence on a potential new role for the actin-dependent molecular motors myosin-1 and myosin-5. In order to interfere with the function of each motor, it was found that an over-expression of the tail domain of both myosin motors led to absence of a1 pheromone accumulation in the vacuole and specifically, in comparison to myosin-1, myosin-5 does not even show an uptake of the a1 pheromone as there is no increase in the cellular background. Therefore both myosin-1 and myosin-5 show defects in pheromone transport, and subsequently in cell morphology, which suggests a role in the endocytosis pathway. This was further established by the finding that the over-expression of myosin-5 tail domain affects actin patch dynamics, specifically their formation and scission times, as well as the overall actin patch intensity. At present we know that myosin-5 is involved in secretion (Schuster et al., 2011c) which suggests that myosin-5 shows an indirect effect on the endocytosis pathway to the vacuole. Numerous reports have suggested a role for actin patches in the delivery mechanism for endocytosed material from the plasma membrane into the cell

(reviewed in (Moseley and Goode, 2006)), however, two major questions still need to be addressed. First, what is the role of myosin-5 in patch dynamics and intensity? Does the motor interact directly with actin patches and therefore, play a similar role to that observed in yeast, where myosin-1 is used to propel the clathrin-coated pits into the cell. Alternatively, is it purely used as the motor to transport the internalised material short distances before it is loaded onto EE's where the microtubule cytoskeleton, with its molecular motors, takes over? The generation of deletion mutants, as well as fluorescently tagged constructs of proteins involved in the endocytosis pathway such as Sla1, Sla2 and RVS161/RVS167, could extend this project and help to identify at which stage myosin-5 is involved in endocytosis. Secondly, what is the role of myosin-1? We have highlighted that it is not directly involved in actin patch dynamics or intensity but it still affects the transport of the a1 pheromone to the cellular vacuole. Therefore, through the generation of a fluorescently tagged myosin-1, we would like to identify using co-localisation, which proteins of the endocytosis pathway it interacts with and gather more evidence on how it affects the transport of the pheromone.

Furthermore the deletion of the microtubule motor kinesin-3 causes a significant decrease of the synthetic pheromone accumulation in the vacuole. The same applies to kinesin-1, but here the effect is not as significant as for kinesin-3 which suggests a more indirect role for kinesin-1 in the a1 pheromone transport as it is responsible for the delivery of dynein towards the plus-end (Zhang et al., 2003, Lenz et al., 2006). Likewise dynein shows no transport of pheromone towards the cellular vacuole which provides further evidence that it is essential in membrane trafficking. However these findings do not suggest a direct role of these motor proteins in endocytosis, more that in their role of a motor they regulate the EEs movement which internalise the pheromone with its receptor. In addition the EE marker Yup1 which is a t-SNARE was shown to be essential in pathogenic development (Fuchs et al., 2006). Here we found that it has a role in a1 pheromone transport towards the cellular vacuole which was already confirmed for the opposing mating type receptor Pra1 where they have shown that the endocytic vesicles are unable to fuse with EEs (Fuchs et al., 2006). But the initial internalisation may not be

affected as some Pra receptors are already present at the plasma membrane, which will be accumulated in transport vesicles unable to fuse with EEs over time, and led to a depletion of Pra2 receptor at the plasma membrane. Therefore it would be interesting to visualise the receptor and colocalise with components of the transport vesicles in order to confirm this assumption.

To summarize the work of this thesis we would like to propose a modified model for the endocytosis of a1 pheromone into the *Ustilago maydis* (Figure 6.1.) which consolidates work carried out in *U. maydis* as well as new information presented in this thesis. The first step of this endocytosis is the internalization of the a1 pheromone through its binding with the Pra2 receptor. Subsequently it is coated in actin to incorporate it as part of an actin patch complex (Figure 6.1, A). This is followed by the internalization of the actin patch through the action of myosin-5 and the translocation from the expanding growth region to the tips of the microtubules, through the action of myosin-1 motor proteins (Figure 6.1 B). The a1 pheromone and Pra2 receptor complex is then fused with the early endosomes, therefore losing its actin coat before being loaded onto the dynein motor complex and transported to the cell vacuole (Figure 6.1. C). The final stage of this process involves the release of the a1/Pra2 complex into the vacuole, whereby we believe the change in pH from the early endosome to vacuolar compartment causes the receptor to dissociate from the a1 pheromone so that it can be re-used, while the a1 pheromone is degraded (Figure 6.1. D). We believe the action of kinesin-3 and the early endosomes takes the receptor back towards the cell periphery so that it can bind with more of the a1 pheromone.

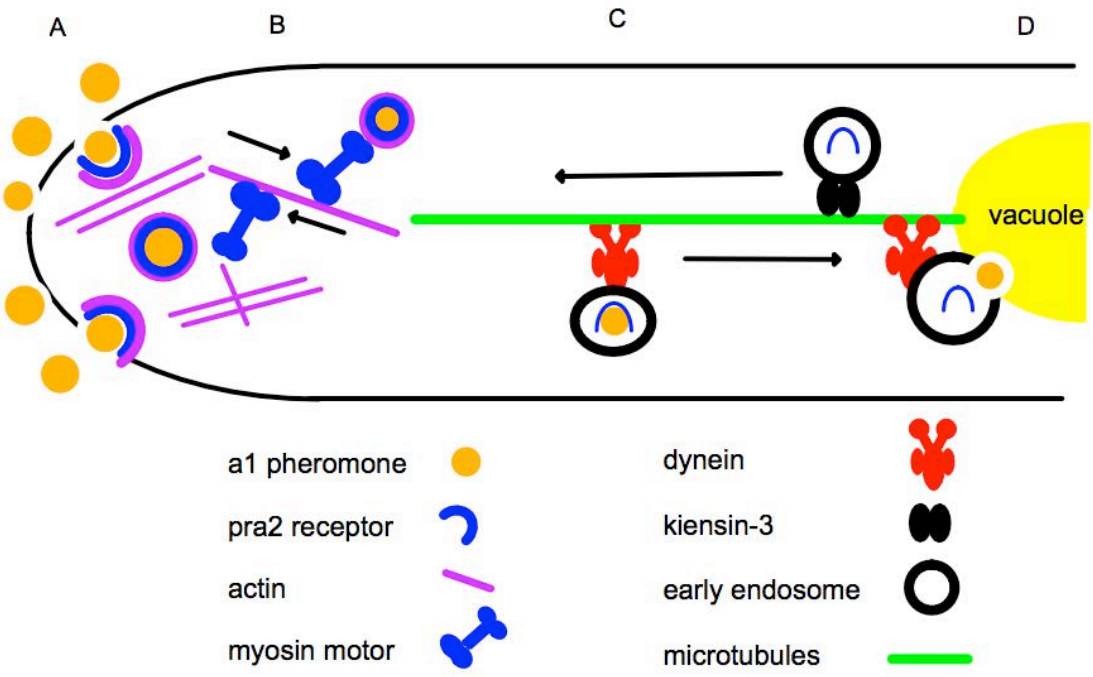

Figure 6.1. Model depicting the endocytosis pathway of a1 pheromone in *U. maydis.*

A) a1 pheromone is internalised at the leading edge of the expanding cell via its interaction with the Pra2 receptor, whereby the a1/Pra2 complex is integrated into actin patches

B) The actin patch is internalised into the cell by the work of myosin-5 and translocated along actin filaments to the tips of microtubules.

C) At the tips of microtubules the a1/Pra2 complex loses its actin coat and is fused with the EE's via the action of Yup1. The EE's are bound to the dynein motor complex and travel along the microtubules towards the cell vacuole.

D) At the cell vacuole the a1/Pra2 complex is released from the EE and enters the vacuole. The Pra2 receptor dissociates from the a1 pheromone to be reintegrated into the EE and return to the cell edge to continue binding more of the a1 pheromone, whereas the a1 pheromone remains in the vacuole and is degraded.

CHAPTER 7 – REFERENCES

ADAMS, A. E., BOTSTEIN, D. & DRUBIN, D. G. 1991. Requirement of yeast fimbrin for actin organization and morphogenesis *in vivo*. *Nature,* 354**,** 404-408.

ADAMS, A. E. & PRINGLE, J. R. 1984. Relationship of actin and tubulin distribution to bud growth in wild-type and morphogenetic-mutant *Saccharomyces cerevisiae*. *The Journal of Cell Biology,* 98**,** 934-945.

AGHAMOHAMMADZADH, S. & AYSCOUGH, K. R. 2009. Differential requirements for actin during yeast and mammalian endocytosis. *Nature Cell Biology,* 11**,** 1039-1042.

AIZAWA, H., SEKINE, Y., TAKEMURA, R., ZHANG, Z., NANGAKU, M. & HIROKAWA, N. 1992. Kinesin family in murine central nervous system. *The Journal of Cell Biology,* 119**,** 1287-1296.

AKADA, R., MINOMI, K., KAI, J., YAMASHITA, I., MIYAKAWA, T. & FUKUI, S. 1989. Multiple genes coding for precursors of rhodotorucine A, a farnesyl peptide mating pheromone of the basidiomycetous yeast *Rhodosporidium toruloides*. *Molecular and Cellular Biology,* 9**,** 3491-3498.

ALBERTI-SEGUI, C., DIETRICH, F., ALTMANN-JOHL, R., HOEPFNER, D. & PHILIPPSEN, P. 2001. Cytoplasmic dynein is required to oppose the force that moves nuclei towards the hyphal tip in the filamentous ascomycete *Ashbya gossypii*. *Journal of Cell Science,* 114**,** 975-986.

ALLAN, V. 1995. Protein phosphatase 1 regulates the cytoplasmic dynein-driven formation of endoplasmic reticulum networks *in vitro*. *The Journal of Cell Biology,* 128**,** 879-891.

ALLAN, V. J. 2011. Cytoplasmic dynein. *Biochemical Society Transactions,* 39**,** 1169-1178.

ALLY, S., LARSON, A. G., BARLAN, K., RICE, S. E. & GELFAND, V. I. 2009. Opposite-polarity motors activate one another to trigger cargo transport in live cells. *The Journal of Cell Biology,* 187**,** 1071-1082.

ANDEREGG, R. J., BETZ, R., CARR, S. A., CRABB, J. W. & DUNTZE, W. 1988. Structure of *Saccharomyces cerevisiae* mating hormone a-factor.

Identification of *S*-farnesyl cysteine as a structural component. *Journal of Biological Chemistry,* 263**,** 18236-18240.

ANDERSON, C. M., WILLITS, D. A., KOSTED, P. J., FORD, E. J., MARTINEZ-ESPINOZA, A. D. & SHERWOOD, J. E. 1999. Molecular analysis of the pheromone and pheromone receptor genes of *Ustilago hordei*. *Gene,* 240**,** 89-97.

ANDERSON, R. G., BROWN, M. S., BEISIEGEL, U. & GOLDSTEIN, J. L. 1982. Surface distribution and recycling of the low density lipoprotein receptor as visualized with antireceptor antibodies. *The Journal of Cell Biology,* 93**,** 523-531.

ANDERSON, R. G. W., VASILE, E., MELLO, R. J., BROWN, M. S. & GOLDSTEIN, J. L. 1978. Immunocytochemical visualization of coated pits and vesicles in human fibroblasts: Relation to low density lipoprotein receptor distribution. *Cell,* 15**,** 919-933.

ASAKURA, T., SASAKI, T., NAGANO, F., SATOH, A., OBAISHI, H., NISHIOKA, H., IMAMURA, H., HOTTA, K., TANAKA, K., NAKANISHI, H. & TAKAI, Y. 1998. Isolation and characterization of a novel actin filament-binding protein from *Saccharomyces cerevisiae*. *Oncogene,* 16**,** 121-130.

ATKINSON, H. A., DANIELS, A. & READ, N. D. 2002. Live-cell imaging of endocytosis during conidial germination in the rice blast fungus, *Magnaporthe grisea*. *Fungal Genetics and Biology,* 37**,** 233-244.

AYSCOUGH, K. R. 2000. Endocytosis and the development of cell polarity in yeast require a dynamic F-actin cytoskeleton. *Current Biology,* 10**,** 1587-1590.

AYSCOUGH, K. R. 2005. Coupling actin dynamics to the endocytic process in *Saccharomyces cerevisiae*. *Protoplasma,* 226**,** 81-88.

AYSCOUGH, K. R., STRYKER, J., POKALA, N., SANDERS, M., CREWS, P. & DRUBIN, D. G. 1997. High rates of actin filament turnover in budding yeast and roles for actin in establishment and maintenance of cell polarity revealed using the actin inhibitor Latrunculin-A. *The Journal of Cell Biology,* 137**,** 399-416.

BALAKIN, K. V., TKACHENKO, S. E., LANG, S. A., OKUN, I., IVASHCHENKO, A. A. & SAVCHUK, N. P. 2002. Property-based

design of GPCR-targeted library. *Journal of Chemical Information and Computer Sciences,* 42**,** 1332-1342.

BANKS, S. M., CHO, B., EUN, S. H., LEE, J. H., WINDLER, S. L., XIE, X., BILDER, D. & FISCHER, J. A. 2011. The functions of auxilin and Rab11 in Drosophila suggest that the fundamental role of ligand endocytosis in notch signaling cells is not recycling. *PLoS One,* 6.

BANUETT, F. 1995. Genetics of *Ustilago maydis*, a fungal pathogen that induces tumors in maize. *Annual Review Genetics,* 29**,** 179-208.

BANUETT, F. & HERSKOWITZ, I. 1989. Different a alleles of *Ustilago maydis* are necessary for maintenance of filamentous growth but not for meiosis. *Proceedings of the National Academy of Sciences of the United States of America,* 86**,** 5878-5882.

BANUETT, F. & HERSKOWITZ, I. 1994a. Identification of fuz7, a *Ustilago maydis* MEK/MAPKK homolog required for a-locus-dependent and-independent steps in the fungal life cycle. *Genes & Development,* 8**,** 1367-1378.

BANUETT, F. & HERSKOWITZ, I. 1994b. Morphological transitions in the life cycle of *Ustilago maydis* and their genetic control by the a and b Loci. *Experimental Mycology,* 18**,** 247-266.

BANUETT, F. & HERSKOWITZ, I. 1996. Discrete developmental stages during teliospore formation in the corn smut fungus, *Ustilago maydis*. *Development,* 122**,** 2965-2976.

BARJA, F., THI, B. N. & TURIAN, G. 1991. Localization of actin and characterization of its isoforms in the hyphae of *Neurospora crassa*. *FEMS Microbiology Letters,* 61**,** 19-24.

BARR, F. A. 2013. Rab GTPases and membrane identity: Causal or inconsequential? *The Journal of Cell Biology,* 202**,** 191-199.

BARRAL, D. C. & SEABRA, M. C. 2004. The melanosome as a model to study organelle motility in mammals. *Pigment Cell Research,* 17**,** 111-118.

BARTNICKI-GARCIA, S., BARTNICKI, D. D., GIERZ, G., LOPEZ-FRANCO, R. & BRACKER, C. E. 1995. Evidence that spitzenkorper behavior determines the shape of a fungal hypha: a test of the hyphoid model. *Experimental Mycology,* 19**,** 153-9.

BASSE, C. W. & STEINBERG, G. 2004. *Ustilago maydis*, model system for analysis of the molecular basis of fungal pathogenicity. *Molecular Plant Pathology,* 5**,** 83-92.

BEHNIA, R. & MUNRO, S. 2005. Organelle identity and the signposts for membrane traffic. *Nature,* 438**,** 597-604.

BEREPIKI, A., LICHIUS, A. & READ, N. D. 2011. Actin organization and dynamics in filamentous fungi. *Nature Reviews Microbiology,* 9**,** 876-887.

BEREPIKI, A., LICHIUS, A., SHOJI, J.-Y., TILSNER, J. & READ, N. D. 2010. F-Actin dynamics in *Neurospora crassa*. *Eukaryotic Cell,* 9**,** 547-557.

BERG, J. S., POWELL, B. C. & CHENEY, R. E. 2001. A millennial myosin census. *Molecular Biology of the Cell,* 12**,** 780-794.

BEZANILLA, M. & POLLARD, T. D. 2000. Myosin-II tails confer Unique functions in *Schizosaccharomyces pombe*: characterization of a novel myosin-II tail. *Molecular Biology of the Cell,* 11**,** 79-91.

BI, E., MADDOX, P., LEW, D. J., SALMON, E. D., MCMILLAN, J. N., YEH, E. & PRINGLE, J. R. 1998. Involvement of an actomyosin contractile ring in *Saccharomyces cerevisiae* cytokinesis. *The Journal of Cell Biology,* 142**,** 1301-12.

BIBIKOVA, T. N., BLANCAFLOR, E. B. & GILROY, S. 1999. Microtubules regulate tip growth and orientation in root hairs of *Arabidopsis thaliana*. *Plant Journal,* 17**,** 657-665.

BIELLI, A., THORNQVIST, P. O., HENDRICK, A. G., FINN, R., FITZGERALD, K. & MCCAFFREY, M. W. 2001. The small GTPase Rab4A interacts with the central region of cytoplasmic dynein light intermediate chain-1. *Biochemical and Biophysical Research Communications,* 281**,** 1141-1153.

BLOOM, K. 2001. Nuclear migration: cortical anchors for cytoplasmic dynein. *Current Biology,* 11**,** 326-329.

BOETTNER, D. R., CHI, R. J. & LEMMON, S. K. 2012. Lessons from yeast for clathrin-mediated endocytosis. *Nature Cell Biology,* 14**,** 2-10.

BOETTNER, D. R., FRIESEN, H., ANDREWS, B. & LEMMON, S. K. 2011. Clathrin light chain directs endocytosis by influencing the binding of the

yeast Hip1R homologue, Sla2, to F-actin. *Molecular Biology of the Cell,* 22**,** 3699-3714.

BÖLKER, M., GENIN, S., LEHMLER, C. & KAHMANN, R. 1995. Genetic regulation of mating and dimorphism in *Ustilago maydis*. *Canadian Journal of Botany,* 73**,** 320-325.

BÖLKER, M. & KAHMANN, R. 1993. Sexual pheromones and mating responses in fungi. *Plant Cell,* 5**,** 1461-1469.

BÖLKER, M., URBAN, M. & KAHMANN, R. 1992. The a mating type locus of *Ustilago maydis* specifies cell signaling components. *Cell,* 68**,** 441-450.

BONIFACINO, J. S. & LIPPINCOTT-SCHWARTZ, J. 2003. Coat proteins: shaping membrane transport. *Nature Reviews Molecular Cell Biology,* 4**,** 409-414.

BORTFELD, M., AUFFARTH, K., KAHMANN, R. & BASSE, C. W. 2004. The *Ustilago maydis* a2 mating-type locus genes *lga2* and *rga2* compromise pathogenicity in the absence of the mitochondrial p32 family protein Mrb1. *The Plant Cell Online,* 16**,** 2233-2248.

BOTTIN, A., KAMPER, J. & KAHMANN, R. 1996. Isolation of a carbon source-regulated gene from Ustilago maydis. *Mol Gen Genet,* 253**,** 342-52.

BRACHMANN, A., WEINZIERL, G., KAMPER, J. & KAHMANN, R. 2001. Identification of genes in the bW/bE regulatory cascade in *Ustilago maydis*. *Molecular Microbiology,* 42**,** 1047-1063.

BRADY, S. T. 1985. A novel brain ATPase with properties expected for the fast axonal transport motor. *Nature,* 317**,** 73-75.

BRANGWYNNE, C. P., KOENDERINK, G. H., MACKINTOSH, F. C. & WEITZ, D. A. 2008. Cytoplasmic diffusion: molecular motors mix it up. *The Journal of Cell Biology,* 183**,** 583-587.

BRENDZA, R. P., SERBUS, L. R., DUFFY, J. B. & SAXTON, W. M. 2000. A function for kinesin-I in the posterior transport of oskar mRNA and Staufen protein. *Science,* 289**,** 2120-2122.

BRETON, A. M., SCHAEFFER, J. & AIGLE, M. 2001. The yeast Rvs161 and Rvs167 proteins are involved in secretory vesicles targeting the plasma membrane and in cell integrity. *Yeast,* 18**,** 1053-1068.

BUCCI, C., PARTON, R. G., MATHER, I. H., STUNNENBERG, H., SIMONS, K., HOFLACK, B. & ZERIAL, M. 1992. The small GTPase rab5 functions as a regulatory factor in the early endocytic pathway. *Cell,* 70**,** 715-728.

CAI, D., HOPPE, A. D., SWANSON, J. A. & VERHEY, K. J. 2007. Kinesin-1 structural organization and conformational changes revealed by FRET stoichiometry in live cells. *The Journal of Cell Biology,* 176**,** 51-63.

CALVERT, M. E., WRIGHT, G. D., LEONG, F. Y., CHIAM, K. H., CHEN, Y., JEDD, G. & BALASUBRAMANIAN, M. K. 2011. Myosin concentration underlies cell size-dependent scalability of actomyosin ring constriction. *The Journal of Cell Biology,* 195**,** 799-813.

CARDELLI, L., CARON, E., GARDNER, P., KAHRAMANO, O. & PHILLIPS, A. 2009. A process model of actin polymerisation. *Electronic Notes in Theoretical Computer Science,* 229**,** 127-144.

CARMINATI, J. L. & STEARNS, T. 1997. Microtubules orient the mitotic spindle in yeast through dynein-dependent interactions with the cell cortex. *The Journal of Cell Biology,* 138**,** 629-641.

CARPENTER, G. & COHEN, S. 1979. Epidermal growth factor. *Annual Review of Biochemistry* 48**,** 193-216.

CASTILLO-LLUVA, S., ALVAREZ-TABARÉS, I., WEBER, I., STEINBERG, G. & PÉREZ-MARTÍN, J. 2007. Sustained cell polarity and virulence in the phytopathogenic fungus *Ustilago maydis* depends on an essential cyclin-dependent kinase from the Cdk5/Pho85 family. *Journal of Cell Science,* 120**,** 1584-1595.

CHEN, L. & DAVIS, N. G. 2000. Recycling of the yeast a-factor receptor. *The Journal of Cell Biology,* 151**,** 731-738.

CHESARONE, M. A., DUPAGE, A. G. & GOODE, B. L. 2010. Unleashing formins to remodel the actin and microtubule cytoskeletons. *Nature Reviews Molecular Cell Biology,* 11**,** 62-74.

CHRISTENSEN, J. J. 1963. *Corn smut caused by Ustilago maydis*, American Phytopathological Society St Paul, Minn.

CHRISTOFORIDIS, S., MCBRIDE, H. M., BURGOYNE, R. D. & ZERIAL, M. 1999. The Rab5 effector EEA1 is a core component of endosome docking. *Nature,* 397**,** 621-625.

CHUANG, J. S. & SCHEKMAN, R. W. 1996. Differential trafficking and timed localization of two chitin synthase proteins, Chs2p and Chs3p. *The Journal of Cell Biology,* 135**,** 597-610.

CIECHANOVER, A., SCHWARTZ, A. L. & LODISH, H. F. 1983. Sorting and recycling of cell surface receptors and endocytosed ligands: the asialoglycoprotein and transferrin receptors. *Journal of Biological Chemistry,* 23**,** 107-130.

CONDE, C. & CACERES, A. 2009. Microtubule assembly, organization and dynamics in axons and dendrites. *Nature,* 10**,** 319 - 332.

CORTHESY-THEULAZ, I., PAULOIN, A. & PFEFFER, S. R. 1992. Cytoplasmic dynein participates in the centrosomal localization of the Golgi complex. *The Journal of Cell Biology,* 118**,** 1333-1345.

D'HONDT, K., HEESE-PECK, A. & RIEZMAN, H. 2000. Protein and lipid requirements for endocytosis. *Annual Review Genetics,* 34**,** 255-295.

DAVEY, J. 1992. Mating pheromones of the fission yeast *Schizosaccharomyces pombe*: purification and structural characterization of M-factor and isolation and analysis of two genes encoding the pheromone. *The EMBO Journal,* 11**,** 951-960.

DAVIS, N. G., HORECKA, J. L. & SPRAGUE, G. F. 1993. Cis- and trans-acting functions required for endocytosis of the yeast pheromone receptors. *The Journal of Cell Biology,* 122**,** 53-65.

DELGADO-ÁLVAREZ, D. L., CALLEJAS-NEGRETE, O. A., GÓMEZ, N., FREITAG, M., ROBERSON, R. W., SMITH, L. G. & MOURIÑO-PÉREZ, R. R. 2010. Visualization of F-actin localization and dynamics with live cell markers in *Neurospora crassa*. *Fungal Genetics and Biology,* 47**,** 573-586.

DESNOS, C., HUET, S. & DARCHEN, F. 2007. 'Should I stay or should I go?': myosin V function in organelle trafficking. *Biology of the Cell,* 99**,** 411-423.

DIETRICH, K. A., SINDELAR, C. V., BREWER, P. D., DOWNING, K. H., CREMO, C. R. & RICE, S. E. 2008. The kinesin-1 motor protein is regulated by a direct interaction of its head and tail. *Proceedings of the National Academy of Sciences of the United States of America,* 105**,** 8938-8943.

DOHERTY, G. J. & MCMAHON, H. T. 2009. Mechanisms of endocytosis. *Annual Review Biochemistry,* 78**,** 857-902.

DOHLMAN, H. G., THORNER, J., CARON, M. G. & LEFKOWITZ, R. J. 1991. Model systems for the study of seven-transmembrane-segment receptors. *Annual Review of Biochemistry,* 60**,** 653-688.

DOMINGUEZ, R. & HOLMES, K. C. 2011. Actin structure and function. *Annual Review of Biophysics,* 40**,** 169-186.

DOWELL, S. J. & BROWN, A. J. 2009. yeast assays for G protein-coupled receptors. *T G Protein-Coupled Receptors in Drug Discovery.*

DRUMMOND, D. R. & CROSS, R. A. 2000. Dynamics of interphase microtubules in *Schizosaccharomyces pombe*. *Current Biology,* 10**,** 766-775.

DULIC, V. & RIEZMAN, H. 1990. *Saccharomyces cerevisiae* mutants lacking a functional vacuole are defective for aspects of the pheromone response. *Journal of Cell Science,* 97**,** 517-525.

EATON, D. F. 1980. Reference materials for fluorescence measurement. 1107-1114.

ELION, E. A. 2000. Pheromone response, mating and cell biology. *Current Opinion in Microbiology,* 3**,** 573-581.

EVANGELISTA, M., PRUYNE, D., AMBERG, D. C., BOONE, C. & BRETSCHER, A. 2002. Formins direct Arp2/3-independent actin filament assembly to polarize cell growth in yeast. *Nature Cell Biology,* 4**,** 32-41.

EVANGELISTA, M., ZIGMOND, S. & BOONE, C. 2003. Formins: signaling effectors for assembly and polarization of actin filaments. *Journal of Cell Science,* 116**,** 2603-2611.

FEHRENBACHER, K. L., YANG, H.-C., GAY, A. C., HUCKABA, T. M. & PON, L. A. 2004. Live Cell Imaging of Mitochondrial Movement along Actin Cables in Budding Yeast. *Current Biology,* 14**,** 1996-2004.

FELDBRÜGGE, M., KÄMPER, J., STEINBERG, G. & KAHMANN, R. 2004. Regulation of mating and pathogenic development in *Ustilago maydis*. *Current Opinion in Microbiology,* 7**,** 666-672.

FINLEY, K. R. & BERMAN, J. 2005. Microtubules in *Candida albicans* hyphae drive nuclear dynamics and connect cell cycle progression to morphogenesis. *Eukaryotic Cell,* 4**,** 1697-1711.

FINLEY, K. R., BOUCHONVILLE, K. J., QUICK, A. & BERMAN, J. 2008. Dynein-dependent nuclear dynamics affect morphogenesis in *Candida albicans* by means of the Bub2p spindle checkpoint. *Journal of Cell Science,* 121**,** 466-476.

FISCHER-PARTON, S., PARTON, R. M., HICKEY, P. C., DIJKSTERHUIS, J., ATKINSON, H. A. & READ, N. D. 2000. Confocal microscopy of FM4-64 as a tool for analysing endocytosis and vesicle trafficking in living fungal hyphae. *Journal of Microscopy,* 198**,** 246-259.

FISHKIND, D. J. & WANG, Y. L. 1995. New horizons for cytokinesis. *Current Opinion in Cell Biology,* 7**,** 23-31.

FORD, M. G., MILLS, I. G., PETER, B. J., VALLIS, Y., PRAEFCKE, G. J., EVANS, P. R. & MCMAHON, H. T. 2002. Curvature of clathrin-coated pits driven by epsin. *Nature,* 419**,** 361-366.

FRANK, R. & GAUSEPOHL, H. 1988. Continuous flow peptide synthesis. *Modern Methods in Protein Chemistry,* 3**,** 41-60.

FREITAG, M., HICKEY, P. C., RAJU, N. B., SELKER, E. U. & READ, N. D. 2004. GFP as a tool to analyze the organization, dynamics and function of nuclei and microtubules in *Neurospora crassa*. *Fungal Genetics and Biology,* 41**,** 897-910.

FUCHS, F., PROKISCH, H., NEUPERT, W. & WESTERMANN, B. 2002. Interaction of mitochondria with microtubules in the filamentous fungus *Neurospora crassa*. *Journal of Cell Science,* 115**,** 1931-1937.

FUCHS, F. & WESTERMANN, B. 2005. Role of Unc104/KIF1-related motor proteins in mitochondrial transport in *Neurospora crassa*. *Molecular Biology of the Cell,* 16**,** 153-161.

FUCHS, U., HAUSE, G., SCHUCHARDT, I. & STEINBERG, G. 2006. Endocytosis is essential for pathogenic development in the corn smut fungus *Ustilago maydis*. *The Plant Cell Online,* 18**,** 2066-2081.

FUCHS, U., MANNS, I. & STEINBERG, G. 2005. Microtubules are dispensable for the initial pathogenic development but required for

long-distance hyphal growth in the corn smut fungus *Ustilago maydis*. *Molecular Biology of the Cell,* 16**,** 2746-2758.

FUCHS, U. & STEINBERG, G. 2005. Endocytosis in the plant-pathogenic fungus *Ustilago maydis*. *Protoplasma,* 226**,** 75-80.

FUJIMURA, H., YANAGISHIMA, N., SAKURAI, A., KITADA, C., FUJINO, M. & BANNO, I. 1982. Sex pheromone of α mating type in the yeast *Saccharomyces kluyveri* and its synthetic analogues in relation to sex pheromones in *Saccharomyces cerevisiae* and *Hansenula wingei*. *Archives of Microbiology,* 132**,** 225-229.

GACHET, Y. & HYAMS, J. S. 2005. Endocytosis in fission yeast is spatially associated with the actin cytoskeleton during polarised cell growth and cytokinesis. *Journal of Cell Science,* 118**,** 4231-4242.

GALLETTA, B. J. & COOPER, J. A. 2009. Actin and endocytosis: mechanisms and phylogeny. *Current Opinion in Cell Biology,* 21**,** 20-27.

GARCÍA-MUSE, T., STEINBERG, G. & PÉREZ-MARTÍN, J. 2003. Pheromone-induced G2 Arrest in the phytopathogenic fungus *Ustilago maydis*. *Eukaryotic Cell,* 2**,** 494-500.

GEITMANN, A. & EMONS, A. M. 2000. The cytoskeleton in plant and fungal cell tip growth. *Journal of Microscopy,* 198**,** 218-245.

GEKLE, M., MILDENBERGER, S., FREUDINGER, R., SCHWERDT, G. & SILBERNAGL, S. 1997. Albumin endocytosis in OK cells: dependence on actin and microtubules and regulation by protein kinases. *American Journal of Physiology,* 272**,** 668-677.

GELI, M. I. & RIEZMAN, H. 1996. Role of type I myosins in receptor-mediated endocytosis in yeast. *Science,* 272**,** 533-535.

GELI, M. I. & RIEZMAN, H. 1998. Endocytic internalization in yeast and animal cells: similar and different. *Journal of Cell Science,* 111**,** 1031-1037.

GEUZE, H. J., SLOT, J. W. & SCHWARTZ, A. L. 1987. Membranes of sorting organelles display lateral heterogeneity in receptor distribution. *The Journal of Cell Biology,* 104**,** 1715-1723.

GEUZE, H. J., SLOT, J. W., STROUS, G. J., HASILIK, A. & VON FIGURA, K. 1985. Possible pathways for lysosomal enzyme delivery. *The Journal of Cell Biology,* 101**,** 2253-2262.

GEUZE, H. J., STOORVOGEL, W., STROUS, G. J., SLOT, J. W., BLEEKEMOLEN, J. E. & MELLMAN, I. 1988. Sorting of mannose 6-phosphate receptors and lysosomal membrane proteins in endocytic vesicles. *The Journal of Cell Biology,* 107**,** 2491-2501.

GIBBONS, B. H., ASAI, D. J., TANG, W. J., HAYS, T. S. & GIBBONS, I. R. 1994. Phylogeny and expression of axonemal and cytoplasmic dynein genes in sea urchins. *Molecular Biology of the Cell,* 5**,** 57-70.

GIBBONS, I. R. & ROWE, A. J. 1965. Dynein: a protein with adenosine triphosphatase activity from cilia. *Science,* 149**,** 424-426.

GIRAO, H., GELI, M. I. & IDRISSI, F. Z. 2008. Actin in the endocytic pathway: from yeast to mammals. *FEBS Letters,* 582**,** 2112-2119.

GOLDSTEIN, J. L., ANDERSON, R. G. & BROWN, M. S. 1979. Coated pits, coated vesicles, and receptor-mediated endocytosis. *Nature,* 279**,** 679-685.

GOLDSTEIN, J. L., BROWN, M. S., ANDERSON, R. G., RUSSELL, D. W. & SCHNEIDER, W. J. 1985. Receptor-mediated endocytosis: concepts emerging from the LDL receptor system. *Annual Review of Cell Biology,* 1**,** 1-39.

GORVEL, J.-P., CHAVRIER, P., ZERIAL, M. & GRUENBERG, J. 1991. Rab5 controls early endosome fusion in vitro. *Cell,* 64**,** 915-925.

GOTTLIEB, T. A., IVANOV, I. E., ADESNIK, M. & SABATINI, D. D. 1993. Actin microfilaments play a critical role in endocytosis at the apical but not the basolateral surface of polarized epithelial cells. *The Journal of Cell Biology,* 120**,** 695-710.

GOVINDAN, B., BOWSER, R. & NOVICK, P. 1995. The role of Myo2, a yeast class V myosin, in vesicular transport. *The Journal of Cell Biology,* 128**,** 1055-1068.

GOW, N. 1995. Yeast-hyphal dimorphism. *In:* GOW, N. G., G M (ed.) *The growing fungus.*

GOW, N. A. R., BROWN, A. J. P. & ODDS, F. C. 2002. Fungal morphogenesis and host invasion. *Current Opinion in Microbiology,* 5**,** 366-371.

GOW, N. A. R., GADD, G. M. & HEATH, I. B. 1995. The Cytoskeleton. *The growing fungus.* Springer Netherlands.

GRANT, B. D. & DONALDSON, J. G. 2009. Pathways and mechanisms of endocytic recycling. *Nature Reviews Molecular Cell Biology,* 10**,** 597-608.

GRIFFITHS, G., HOFLACK, B., SIMONS, K., MELLMAN, I. & KORNFELD, S. 1988. The mannose 6-phosphate receptor and the biogenesis of lysosomes. *Cell,* 52**,** 329-341.

GROSS, S. P. 2004. Hither and yon: a review of bi-directional microtubule-based transport. *Physical Biology,* 1**,** 1-11.

GROSS, S. P., TUMA, M. C., DEACON, S. W., SERPINSKAYA, A. S., REILEIN, A. R. & GELFAND, V. I. 2002. Interactions and regulation of molecular motors in *Xenopus melanophores*. *The Journal of Cell Biology,* 156**,** 855-865.

GRUENBERG, J. 2001. The endocytic pathway: a mosaic of domains. *Nature Reviews Molecular Cell Biology,* 2**,** 721-730.

HABURA, A., TIKHONENKO, I., CHISHOLM, R. L. & KOONCE, M. P. 1999. Interaction mapping of a dynein heavy chain. Identification of dimerization and intermediate-chain binding domains. *Journal of Biological Chemistry,* 274**,** 15447-15453.

HACKNEY, D. D. 1994. The rate-limiting step in microtubule-stimulated ATP hydrolysis by dimeric kinesin head domains occurs while bound to the microtubule. *Journal of Biological Chemistry,* 269**,** 16508-16511.

HACKNEY, D. D. & STOCK, M. F. 2008. Kinesin tail domains and Mg2+ directly inhibit release of ADP from head domains in the absence of microtubules. *Biochemistry,* 47**,** 7770-7778.

HAGAN, I. M. 1998. The fission yeast microtubule cytoskeleton. *Journal of Cell Science,* 111**,** 1603-1612.

HALL, D. H. & HEDGECOCK, E. M. 1991. Kinesin-related gene unc-104 is required for axonal transport of synaptic vesicles in *Candida elegans*. *Cell,* 65**,** 837-847.

HAMMER, J. A., 3RD & WAGNER, W. 2013. Functions of class V myosins in neurons. *Journal of Biological Chemistry,* 288**,** 28428-28434.

HARADA, A., TAKEI, Y., KANAI, Y., TANAKA, Y., NONAKA, S. & HIROKAWA, N. 1998. Golgi vesiculation and lysosome dispersion in cells lacking cytoplasmic dynein. *The Journal of Cell Biology,* 141**,** 51-59.

HARRIS, S. D., READ, N. D., ROBERSON, R. W., SHAW, B., SEILER, S., PLAMANN, M. & MOMANY, M. 2005. Polarisome meets spitzenkorper: microscopy, genetics, and genomics converge. *Eukaryotic Cell,* 4**,** 225-229.

HARRIS, S. L., NA, S., ZHU, X., SETO-YOUNG, D., PERLIN, D. S., TEEM, J. H. & HABER, J. E. 1994. Dominant lethal mutations in the plasma membrane H(+)-ATPase gene of *Saccharomyces cerevisiae*. *Proceedings of the National Academy of Sciences of the United States of America,* 91**,** 10531-10535.

HARTMANN, H. A., KAHMANN, R. & BÖLKER, M. 1996. The pheromone response factor coordinates filamentous growth and pathogenicity in *Ustilago maydis*. *The EMBO Journal,* 15**,** 1632-1641.

HEATH, I. B. 2000. Organization and functions of actin in hyphal tip growth. *In:* STAIGER, C. J., BALUŠKA, F., VOLKMANN, D. & BARLOW, P. W. (eds.) *Actin: A Dynamic Framework for Multiple Plant Cell Functions.* Springer Netherlands.

HEATH, I. B. & STEINBERG, G. 1999. Mechanisms of hyphal tip growth: tube dwelling amebae revisited. *Fungal Genetics and Biology,* 28**,** 79-93.

HENDRICKS, A. G., PERLSON, E., ROSS, J. L., SCHROEDER, H. W., 3RD, TOKITO, M. & HOLZBAUR, E. L. 2010. Motor coordination via a tug-of-war mechanism drives bidirectional vesicle transport. *Current Biology,* 20**,** 697-702.

HENNE, W. M., BOUCROT, E., MEINECKE, M., EVERGREN, E., VALLIS, Y., MITTAL, R. & MCMAHON, H. T. 2010. FCHO proteins are nucleators of clathrin-mediated endocytosis. *Science,* 328**,** 1281-1284.

HIGUCHI, Y., NAKAHAMA, T., SHOJI, J. Y., ARIOKA, M. & KITAMOTO, K. 2006. Visualization of the endocytic pathway in the filamentous fungus *Aspergillus oryzae* using an EGFP-fused plasma membrane protein.

Biochemical and Biophysical Research Communications, 340**,** 784-791.

HILL, K. L., CATLETT, N. L. & WEISMAN, L. S. 1996. Actin and myosin function in directed vacuole movement during cell division in *Saccharomyces cerevisiae*. *The Journal of Cell Biology,* 135**,** 1535-1549.

HINSHAW, J. E. & SCHMID, S. L. 1995. Dynamin self-assembles into rings suggesting a mechanism for coated vesicle budding. *Nature,* 374**,** 190-192.

HIROKAWA, N. 1998. Kinesin and dynein superfamily proteins and the mechanism of organelle transport. *Science,* 279**,** 519-526.

HIROKAWA, N., NODA, Y. & OKADA, Y. 1998. Kinesin and dynein superfamily proteins in organelle transport and cell division. *Current Opinion in Cell Biology,* 10**,** 60-73.

HIROKAWA, N. & TAKEMURA, R. 2004. Kinesin superfamily proteins and their various functions and dynamics. *Experimental Cell Reseach,* 301**,** 50-59.

HOFFMANN, J. & MENDGEN, K. 1998. Endocytosis and membrane turnover in the germ tube of *Uromyces fabae*. *Fungal Genetics and Biology,* 24**,** 77-85.

HOLLIDAY, R. 1975. Further evidence for an inducible recombination repair system in *Ustilago maydis*. *Mutation Research/ Fundamental and Molecular Mechanisms of Mutagenesis,* 29**,** 149-153.

HOPKINS, C. R. 1983. Intracellular routing of transferrin and transferrin receptors in epidermoid carcinoma A431 cells. *Cell,* 35**,** 321-330.

HOPKINS, C. R., MILLER, K. & BEARDMORE, J. M. 1985. Receptor-mediated endocytosis of transferrin and epidermal growth factor receptors: A comparison of constitutive and ligand-induced uptake. *Journal of Cell Science,* 1985**,** 173-186.

HORGAN, C. P. & MCCAFFREY, M. W. 2011. Rab GTPases and microtubule motors. *Biochemical Society Transactions,* 39**,** 1202-1206.

HOWARD, J., HUDSPETH, A. J. & VALE, R. D. 1989. Movement of microtubules by single kinesin molecules. *Nature,* 342**,** 154-158.

HOWARD, J. & HYMAN, A. A. 2007. Microtubule polymerases and depolymerases. *Current Opinion in Cell Biology,* 19**,** 31-35.

HUBBARD, A. L. 1989. Endocytosis. *Current Opinion in Cell Biology,* 1**,** 675-683.

HUCKABA, T. M., GAY, A. C., PANTALENA, L. F., YANG, H.-C. & PON, L. A. 2004. Live cell imaging of the assembly, disassembly, and actin cable dependent movement of endosomes and actin patches in the budding yeast, *Saccharomyces cerevisiae*. *The Journal of Cell Biology,* 167**,** 519-530.

ITOH, T., WATABE, A., TOH, E. A. & MATSUI, Y. 2002. Complex formation with Ypt11p, a rab-type small GTPase, is essential to facilitate the function of Myo2p, a class V myosin, in mitochondrial distribution in *Saccharomyces cerevisiae*. *Molecular Cell Biology,* 22**,** 7744-7757.

JAHN, R. & SUDHOF, T. C. 1999. Membrane fusion and exocytosis. *Annual Review Biochemistry,* 68**,** 863-911.

JENNESS, D. D. & SPATRICK, P. 1986. Down regulation of the α factor pheromone receptor in *Saccharomyces cerevisiae*. *Cell,* 46**,** 345-353.

JOB, D., VALIRON, O. & OAKLEY, B. 2003. Microtubule nucleation. *Current Opinion in Cell Biology,* 15**,** 111-117.

JOHNSTON, G. C., PRENDERGAST, J. A. & SINGER, R. A. 1991. The *Saccharomyces cerevisiae MYO2* gene encodes an essential myosin for vectorial transport of vesicles. *The Journal of Cell Biology,* 113**,** 539-551.

JONSDOTTIR, G. A. & LI, R. 2004. Dynamics of yeast myosin I: evidence for a possible role in scission of endocytic vesicles. *Current Biology,* 14**,** 1604-1609.

KAKSONEN, M., SUN, Y. & DRUBIN, D. G. 2003. A pathway for association of receptors, adaptors, and actin during endocytic internalization. *Cell,* 115**,** 475-487.

KAKSONEN, M., TORET, C. P. & DRUBIN, D. G. 2005. A modular design for the clathrin- and actin-mediated endocytosis machinery. *Cell,* 123**,** 305-320.

KAMIYA, Y., SAKURAI, A., TAMURA, S. & TAKAHASHI, N. 1978. Structure of rhodotorucine A, a novel lipopeptide, inducing mating tube formation

in *Rhodosporidium toruloides*. *Biochemical and Biophysical Research Communications,* 83**,** 1077-1083.

KÄMPER, J., KAHMANN, R., BOLKER, M., MA, L. J., BREFORT, T., SAVILLE, B. J., BANUETT, F., KRONSTAD, J. W., GOLD, S. E., MULLER, O., PERLIN, M. H., WOSTEN, H. A., DE VRIES, R., RUIZ-HERRERA, J., REYNAGA-PENA, C. G., SNETSELAAR, K., MCCANN, M., PEREZ-MARTIN, J., FELDBRUGGE, M., BASSE, C. W., STEINBERG, G., IBEAS, J. I., HOLLOMAN, W., GUZMAN, P., FARMAN, M., STAJICH, J. E., SENTANDREU, R., GONZALEZ-PRIETO, J. M., KENNELL, J. C., MOLINA, L., SCHIRAWSKI, J., MENDOZA-MENDOZA, A., GREILINGER, D., MUNCH, K., ROSSEL, N., SCHERER, M., VRANES, M., LADENDORF, O., VINCON, V., FUCHS, U., SANDROCK, B., MENG, S., HO, E. C., CAHILL, M. J., BOYCE, K. J., KLOSE, J., KLOSTERMAN, S. J., DEELSTRA, H. J., ORTIZ-CASTELLANOS, L., LI, W., SANCHEZ-ALONSO, P., SCHREIER, P. H., HAUSER-HAHN, I., VAUPEL, M., KOOPMANN, E., FRIEDRICH, G., VOSS, H., SCHLUTER, T., MARGOLIS, J., PLATT, D., SWIMMER, C., GNIRKE, A., CHEN, F., VYSOTSKAIA, V., MANNHAUPT, G., GULDENER, U., MUNSTERKOTTER, M., HAASE, D., OESTERHELD, M., MEWES, H. W., MAUCELI, E. W., DECAPRIO, D., WADE, C. M., BUTLER, J., YOUNG, S., JAFFE, D. B., CALVO, S., NUSBAUM, C., GALAGAN, J. & BIRREN, B. W. 2006. Insights from the genome of the biotrophic fungal plant pathogen *Ustilago maydis*. *Nature,* 444**,** 97-101.

KÄMPER, J., REICHMANN, M., ROMEIS, T., BÖLKER, M. & KAHMANN, R. 1995. Multiallelic recognition: nonself-dependent dimerization of the bE and bW homeodomain proteins in *Ustilago maydis*. *Cell,* 81**,** 73-84.

KARDON, J. R. & VALE, R. D. 2009. Regulators of the cytoplasmic dynein motor. *Nature Reviews Molecular Cell Biology,* 10**,** 854-865.

KARPOVA, T. S., MCNALLY, J. G., MOLTZ, S. L. & COOPER, J. A. 1998. Assembly and function of the actin cytoskeleton of yeast: relationships between cables and patches. *The Journal of Cell Biology,* 142**,** 1501-1517.

KATZMANN, D. J., ODORIZZI, G. & EMR, S. D. 2002. Receptor downregulation and multivesicular-body sorting. *Nature Reviews Molecular Cell Biology,* 3**,** 893-905.

KILMARTIN, J. V. & ADAMS, A. E. 1984. Structural rearrangements of tubulin and actin during the cell cycle of the yeast *Saccharomyces cerevisiae*. *The Journal of Cell Biology,* 98**,** 922-933.

KINCHEN, J. M. & RAVICHANDRAN, K. S. 2008. Phagosome maturation: going through the acid test. *Nature Reviews Molecular Cell Biology,* 9**,** 781-95.

KING, S. M. 2000. The dynein microtubule motor. *Biochimica et Biophysica Acta (BBA) - Molecular and Cell Biology of Lipids,* 1496**,** 60-75.

KITAYAMA, C., SUGIMOTO, A. & YAMAMOTO, M. 1997. Type II myosin heavy chain encoded by the *MYO2* gene composes the contractile ring during cytokinesis in *Schizosaccharomyces pombe*. *The Journal of Cell Biology,* 137**,** 1309-1319.

KLABUNDE, T. & HESSLER, G. 2002. Drug design strategies for targeting G-protein-coupled receptors. *European Journal of Chemical Biology,* 3**,** 928-944.

KLOSTERMAN, S. J., PERLIN, M. H., GARCIA-PEDRAJAS, M., COVERT, S. F. & GOLD, S. E. 2007. Genetics of morphogenesis and pathogenic development of *Ustilago maydis*. *Advances in Genetics,* 57**,** 1-47.

KONZACK, S., RISCHITOR, P. E., ENKE, C. & FISCHER, R. 2005. The role of the kinesin motor KipA in microtubule organization and polarized growth of *Aspergillus nidulans*. *Molecular Biology of the Cell,* 16**,** 497-506.

KOPPITZ, M., SPELLIG, T., KAHMANN, R. & KESSLER, H. 1996. Lipoconjugates: structure—activity studies for pheromone analogues of *Ustilago maydis* with varied lipophilicity. *International Journal of Peptide and Protein Research,* 48**,** 377-390.

KOROBOVA, F., GAUVIN, T. J. & HIGGS, H. N. 2014. A role for myosin II in mammalian mitochondrial fission. *Current Biology,* 24**,** 409-414.

KOVAR, D. R., SIROTKIN, V. & LORD, M. 2011. Three's company: the fission yeast actin cytoskeleton. *Trends in Cell Biology,* 21**,** 177-187.

KÜBLER, E. & RIEZMAN, H. 1993. Actin and fimbrin are required for the internalization step of endocytosis in yeast. *The EMBO Journal,* 12**,** 2855-2862.

KUMARI, S. & MAYOR, S. 2008. ARF1 is directly involved in dynamin-independent endocytosis. *Nature Cell Biology,* 10**,** 30-41.

KUZNETSOV, S. A., VAISBERG, E. A., MURPHY, B. D. & GELFAND, V. I. 1989. 45 kDa fragment of the kinesin molecule possesses high ATPase activity and binds to microtubules. *Molecular Cell Biology,* 23**,** 580-587.

LAAN, L., PAVIN, N., HUSSON, J., ROMET-LEMONNE, G., VAN DUIJN, M., LOPEZ, M. P., VALE, R. D., JULICHER, F., RECK-PETERSON, S. L. & DOGTEROM, M. 2012a. Cortical dynein controls microtubule dynamics to generate pulling forces that position microtubule asters. *Cell,* 148**,** 502-514.

LAAN, L., ROTH, S. & DOGTEROM, M. 2012b. End-on microtubule-dynein interactions and pulling-based positioning of microtubule organizing centers. *Cell Cycle,* 11**,** 3750-3757.

LAKADAMYALI, M., RUST, M. J. & ZHUANG, X. 2006. Ligands for clathrin-mediated endocytosis are differentially sorted into distinct populations of early endosomes. *Cell,* 124**,** 997-1009.

LAMAZE, C., FUJIMOTO, L. M., YIN, H. L. & SCHMID, S. L. 1997. The actin cytoskeleton is required for receptor-mediated endocytosis in mammalian cells. *Journal of Biological Chemistry,* 272**,** 20332-20335.

LAPIERRE, L. A., KUMAR, R., HALES, C. M., NAVARRE, J., BHARTUR, S. G., BURNETTE, J. O., PROVANCE, D. W., JR., MERCER, J. A., BAHLER, M. & GOLDENRING, J. R. 2001. Myosin vb is associated with plasma membrane recycling systems. *Molecular Biology of the Cell,* 12**,** 1843-1857.

LAWRENCE, C. J., DAWE, R. K., CHRISTIE, K. R., CLEVELAND, D. W., DAWSON, S. C., ENDOW, S. A., GOLDSTEIN, L. S., GOODSON, H. V., HIROKAWA, N., HOWARD, J., MALMBERG, R. L., MCINTOSH, J. R., MIKI, H., MITCHISON, T. J., OKADA, Y., REDDY, A. S., SAXTON, W. M., SCHLIWA, M., SCHOLEY, J. M., VALE, R. D., WALCZAK, C. E. & WORDEMAN, L. 2004. A standardized kinesin nomenclature. *The Journal of Cell Biology,* 167**,** 19-22.

LEBERER, E., THOMAS, D. Y. & WHITEWAY, M. 1997. Pheromone signalling and polarized morphogenesis in yeast. *Current Opinion in Genetics & Development,* 7**,** 59-66.

LEE, S. & DOMINGUEZ, R. 2010. Regulation of actin cytoskeleton dynamics in cells. *Molecules and Cells,* 29**,** 311-325.

LEE, W.-L., BEZANILLA, M. & POLLARD, T. D. 2000. Fission Yeast Myosin-I, Myo1p, Stimulates Actin Assembly by Arp2/3 Complex and Shares Functions with Wasp. *The Journal of Cell Biology,* 151**,** 789-800.

LEE, W. L., OBERLE, J. R. & COOPER, J. A. 2003. The role of the lissencephaly protein Pac1 during nuclear migration in budding yeast. *The Journal of Cell Biology,* 160**,** 355-364.

LEHMLER, C., STEINBERG, G., SNETSELAAR, K. M., SCHLIWA, M., KAHMANN, R. & BÖLKER, M. 1997. Identification of a motor protein required for filamentous growth in *Ustilago maydis*. *The EMBO Journal,* 16**,** 3464-3473.

LENARDON, M. D., MUNRO, C. A. & GOW, N. A. R. 2010. Chitin synthesis and fungal pathogenesis. *Current Opinion in Microbiology,* 13**,** 416-423.

LENZ, J. H., SCHUCHARDT, I., STRAUBE, A. & STEINBERG, G. 2006. A dynein loading zone for retrograde endosome motility at microtubule plus-ends. *The EMBO Journal,* 25**,** 2275-2286.

LI, G., D'SOUZA-SCHOREY, C., BARBIERI, M. A., ROBERTS, R. L., KLIPPEL, A., WILLIAMS, L. T. & STAHL, P. D. 1995. Evidence for phosphatidylinositol 3-kinase as a regulator of endocytosis via activation of Rab5. *Proceedings of the National Academy of Sciences of the United States of America,* 92**,** 10207-10211.

LI, R. 1997. Bee1, a yeast protein with homology to wiscott-aldrich syndrome protein, is critical for the assembly of cortical actin cytoskeleton. *The Journal of Cell Biology,* 136**,** 649-658.

LI, Y., ROY, B. D., WANG, W., ZHANG, L., ZHANG, L., SAMPSON, S. B., YANG, Y. & LIN, D. T. 2012. Identification of two functionally distinct endosomal recycling pathways for dopamine D(2) receptor. *Journal of Neuroscience,* 32**,** 7178-7190.

LIU, H. & BRETSCHER, A. 1989. Disruption of the single tropomyosin gene in yeast results in the disappearance of actin cables from the cytoskeleton. *Cell,* 57**,** 233-242.

LODISH, H., BERK, A., ZIPURSKY, S. L., MATSUDAIRA, P., BALTIMORE, D. & DARNELL, J. 2000. *Myosin: the actin motor protein*.

LORD, M., LAVES, E. & POLLARD, T. D. 2005. Cytokinesis depends on the motor domains of myosin-II in fission yeast but not in budding yeast. *Molecular Biology of the Cell,* 16**,** 5346-5355.

MABUCHI, I. & OKUNO, M. 1977. The effect of myosin antibody on the division of starfish blastomeres. *The Journal of Cell Biology,* 74**,** 251-263.

MADANIA, A., DUMOULIN, P., GRAVA, S., KITAMOTO, H., SCHARER-BRODBECK, C., SOULARD, A., MOREAU, V. & WINSOR, B. 1999. The *Saccharomyces cerevisiae* homologue of human Wiskott-Aldrich syndrome protein Las17p interacts with the Arp2/3 complex. *Molecular Biology of the Cell,* 10**,** 3521-3538.

MARCHESE, A., CHEN, C., KIM, Y. M. & BENOVIC, J. L. 2003. The ins and outs of G protein-coupled receptor trafficking. *Trends in Biochemical Science,* 28**,** 369-376.

MARKS, J., HAGAN, I. M. & HYAMS, J. S. 1986. Growth polarity and cytokinesis in fission yeast: the role of the cytoskeleton. *Journal of Cell Science Supplement,* 5**,** 229-241.

MARTIN, S. G., MCDONALD, W. H., YATES, J. R. & CHANG, F. 2005. Tea4p links microtubule plus ends with the formin For3p in the establishment of cell polarity. *Developmental Cell,* 8**,** 479-491.

MATA, J. & NURSE, P. 1998. Discovering the poles in yeast. *Trends in Cell Biology,* 8**,** 163-167.

MAXFIELD, F. R. & MCGRAW, T. E. 2004. Endocytic recycling. *Nature Reviews Molecular Cell Biology,* 5**,** 121-132.

MAXFIELD, F. R. & YAMASHIRO, D. J. 1987. Endosome acidification and the pathways of receptor-mediated endocytosis. *Advances in Experimental Medicine and Biology,* 225**,** 189-198.

MAYOR, S. & PAGANO, R. E. 2007. Pathways of clathrin-independent endocytosis. *Nature Reviews Molecular Cell Biology,* 8**,** 603-612.

MCCAFFREY, G. & VALE, R. D. 1989. Identification of a kinesin-like microtubule-based motor protein in *Dictyostelium discoideum*. *The EMBO Journal,* 8**,** 3229-3234.

MCGOLDRICK, C. A., GRUVER, C. & MAY, G. S. 1995. myoA of Aspergillus nidulans encodes an essential myosin I required for secretion and polarized growth. *The Journal of Cell Biology,* 128**,** 577-587.

MCMAHON, H. T. & BOUCROT, E. 2011. Molecular mechanism and physiological functions of clathrin-mediated endocytosis. *Nature,* 12**,** 517-533.

MEHTA, A. D., ROCK, R. S., RIEF, M., SPUDICH, J. A., MOOSEKER, M. S. & CHENEY, R. E. 1999. Myosin-V is a processive actin-based motor. *Nature,* 400**,** 590-593.

MELLMAN, I. 1996. Endocytosis and molecular sorting. *Annual Review of Cell Developmental Biology,* 12**,** 575-625.

MELLMAN, I. & WARREN, G. 2000. The road taken: past and future foundations of membrane traffic. *Cell,* 100**,** 99-112.

MERRIFIELD, C. J., FELDMAN, M. E., WAN, L. & ALMERS, W. 2002. Imaging actin and dynamin recruitment during invagination of single clathrin-coated pits. *Nature Cell Biology,* 4**,** 691-698.

MIACZYNSKA, M., PELKMANS, L. & ZERIAL, M. 2004. Not just a sink: endosomes in control of signal transduction. *Current Opinion in Cell Biology,* 16**,** 400-406.

MICHELOT, A., COSTANZO, M., SARKESHIK, A., BOONE, C., YATES, J. R., 3RD & DRUBIN, D. G. 2010. Reconstitution and protein composition analysis of endocytic actin patches. *Current Biology,* 20**,** 1890-1899.

MOSELEY, J. B. & GOODE, B. L. 2006. The yeast actin cytoskeleton: from cellular function to biochemical mechanism. *Microbiology and Molecular Biology Reviews* 70**,** 605-645.

MOTEGI, F., ARAI, R. & MABUCHI, I. 2001. Identification of two type V myosins in fission yeast, one of which functions in polarized cell growth and moves rapidly in the cell. *Molecular Biology of the Cell,* 12**,** 1367-1380.

MUKHERJEE, S., GHOSH, R. N. & MAXFIELD, F. R. 1997. Endocytosis. *Physiology Reviews,* 77**,** 759-803.

MULHOLLAND, J., KONOPKA, J., SINGER-KRUGER, B., ZERIAL, M. & BOTSTEIN, D. 1999. Visualization of receptor-mediated endocytosis in yeast. *Molecular Biology of the Cell,* 10**,** 799-817.

MULHOLLAND, J., PREUSS, D., MOON, A., WONG, A., DRUBIN, D. & BOTSTEIN, D. 1994. Ultrastructure of the yeast actin cytoskeleton and its association with the plasma membrane. *The Journal of Cell Biology,* 125**,** 381-391.

MULLER, M. J., KLUMPP, S. & LIPOWSKY, R. 2008. Tug-of-war as a cooperative mechanism for bidirectional cargo transport by molecular motors. *Proceedings of the National Academy of Sciences of the United States of America,* 105**,** 4609-4614.

MULLER, P., WEINZIERL, G., BRACHMANN, A., FELDBRUGGE, M. & KAHMANN, R. 2003. Mating and pathogenic development of the smut fungus *Ustilago maydis* are regulated by one mitogen-activated protein kinase cascade. *Eukaryotic Cell,* 2**,** 1187-1199.

MULVIHILL, D. P., EDWARDS, S. R. & HYAMS, J. S. 2006. A critical role for the type V myosin, Myo52, in septum deposition and cell fission during cytokinesis in *Schizosaccharomyces pombe*. *Cell Motility and the Cytoskeleton,* 63**,** 149-161.

MUNN, A. L., STEVENSON, B. J., GELI, M. I. & RIEZMAN, H. 1995. End5, End6, and End7: mutations that cause actin delocalization and block the internalization step of endocytosis in *Saccharomyces cerevisiae*. *Molecular Biology of the Cell,* 6**,** 1721-1742.

NABI, I. R. 1999. The polarization of the motile cell. *Journal of Cell Science,* 112 (Pt 12)**,** 1803-1811.

NABI, I. R. & LE, P. U. 2003. Caveolae/raft-dependent endocytosis. *The Journal of Cell Biology,* 161**,** 673-677.

NAQVI, N. I., ENG, K., GOULD, K. L. & BALASUBRAMANIAN, M. K. 1999. Evidence for F-actin-dependent and-independent mechanisms involved in assembly and stability of the medial actomyosin ring in fission yeast. *The EMBO Journal,* 18**,** 854-862.

NEWPHER, T. M., SMITH, R. P., LEMMON, V. & LEMMON, S. K. 2005. *In vivo* dynamics of clathrin and Its adaptor-dependent recruitment to the actin-based endocytic machinery in yeast. *Developmental Cell,* 9**,** 87-98.

NIELSEN, E., SEVERIN, F., BACKER, J. M., HYMAN, A. A. & ZERIAL, M. 1999. Rab5 regulates motility of early endosomes on microtubules. *Nature Cell Biology,* 1**,** 376-382.

OAKLEY, B. R. 2000. An abundance of tubulins. *Trends in Cell Biology,* 10**,** 537-542.

OAKLEY, B. R. 2004. Tubulins in *Aspergillus nidulans*. *Fungal Genetics and Biology,* 41**,** 420-427.

OAKLEY, C. E. & OAKLEY, B. R. 1989. Identification of gamma-tubulin, a new member of the tubulin superfamily encoded by mipA gene of *Aspergillus nidulans*. *Nature,* 338**,** 662-664.

OBERHOLZER, U., IOUK, T. L., THOMAS, D. Y. & WHITEWAY, M. 2004. Functional characterization of myosin I tail regions in *Candida albicans*. *Eukaryotic Cell,* 3**,** 1272-1286.

OBERHOLZER, U., MARCIL, A., LEBERER, E., THOMAS, D. Y. & WHITEWAY, M. 2002. Myosin I is required for hypha formation in *Candida albicans*. *Eukaryotic Cell,* 1**,** 213-228.

OKADA, Y., YAMAZAKI, H., SEKINE-AIZAWA, Y. & HIROKAWA, N. 1995. The neuron-specific kinesin superfamily protein KIF1A is a unique monomeric motor for anterograde axonal transport of synaptic vesicle precursors. *Cell,* 81**,** 769-780.

OSHEROV, N., YAMASHITA, R. A., CHUNG, Y.-S. & MAY, G. S. 1998. Structural requirements for *in vivo* myosin I function in *Aspergillus nidulans*. *Journal of Biological Chemistry,* 273**,** 27017-27025.

OVERTON, M. C., CHINAULT, S. L. & BLUMER, K. J. 2005. Oligomerization of G-protein-coupled receptors: lessons from the yeast *Saccharomyces cerevisiae*. *Eukaryotic Cell,* 4**,** 1963-1970.

PALMER, K. J., HUGHES, H. & STEPHENS, D. J. 2009. Specificity of cytoplasmic dynein subunits in discrete membrane-trafficking steps. *Molecular Biology of the Cell,* 20**,** 2885-2899.

PANTAZOPOULOU, A. & PEÑALVA, M. A. 2009. Organization and dynamics of the *Aspergillus nidulans* golgi during apical extension and mitosis. *Molecular Biology of the Cell,* 20**,** 4335-4347.

PARK, H., LI, A., CHEN, L. Q., HOUDUSSE, A., SELVIN, P. R. & SWEENEY, H. L. 2007. The unique insert at the end of the myosin VI motor is the sole determinant of directionality. *Proceedings of the National Academy of Sciences of the United States of America,* 104**,** 778-783.

PASCHAL, B. M. & VALLEE, R. B. 1987. Retrograde transport by the microtubule-associated protein MAP 1C. *Nature,* 330**,** 181-183.

PELHAM, R. J. & CHANG, F. 2001. Role of actin polymerization and actin cables in actin-patch movement in *Schizosaccharomyces pombe*. *Nature Cell Biology,* 3**,** 235-244.

PEÑALVA, M. A. 2005. Tracing the endocytic pathway of *Aspergillus nidulans* with FM4-64. *Fungal Genetics and Biology,* 42**,** 963-975.

PIASEK, A. & THYBERG, J. 1980. Effects of colchicine on endocytosis of horseradish peroxidase by rat peritoneal macrophages. *Journal of Cell Science,* 45**,** 59-71.

PLAMANN, M., MINKE, P. F., TINSLEY, J. H. & BRUNO, K. S. 1994. Cytoplasmic dynein and actin-related protein Arp1 are required for normal nuclear distribution in filamentous fungi. *The Journal of Cell Biology,* 127**,** 139-149.

POLLARD, T. D. & WU, J. Q. 2010. Understanding cytokinesis: lessons from fission yeast. *Nature Reviews Molecular Cell Biology,* 11**,** 149-155.

PRAHLAD, V., YOON, M., MOIR, R. D., VALE, R. D. & GOLDMAN, R. D. 1998. Rapid movements of vimentin on microtubule tracks: kinesin-dependent assembly of intermediate filament networks. *The Journal of Cell Biology,* 143**,** 159-170.

PRATTEN, M. K. & LLOYD, J. B. 1979. Effects of temperature, metabolic inhibitors and some other factors on fluid-phase and adsorptive pinocytosis by rat peritoneal macrophages. *Biochemical Journal,* 180**,** 567-571.

PRESCIANOTTO-BASCHONG, C. & RIEZMAN, H. 1998. Morphology of the yeast endocytic pathway. *Molecular Biology of the Cell,* 9**,** 173-189.

PRUYNE, D., EVANGELISTA, M., YANG, C., BI, E., ZIGMOND, S., BRETSCHER, A. & BOONE, C. 2002. Role of formins in actin assembly: nucleation and barbed-end association. *Science,* 297**,** 612-615.

PRUYNE, D. W., SCHOTT, D. H. & BRETSCHER, A. 1998. Tropomyosin-containing actin cables direct the Myo2p-dependent polarized delivery of secretory vesicles in budding yeast. *The Journal of Cell Biology,* 143**,** 1931-1945.

RAMANATHAN, H. N., ZHANG, G. & YE, Y. 2013. Monoubiquitination of EEA1 regulates endosome fusion and trafficking. *Cell Bioscience,* 3**,** 24.

RATHS, S., ROHRER, J., CRAUSAZ, F. & RIEZMAN, H. 1993. End3 and End4: two mutants defective in receptor-mediated and fluid-phase endocytosis in *Saccharomyces cerevisiae*. *The Journal of Cell Biology,* 120**,** 55-65.

RAYMOND, C. K., SIMS, E. H. & OLSON, M. V. 2002. linker-mediated recombinational subcloning of large DNA fragments using yeast. *Genome Research,* 12**,** 190-197.

READ, N. D. 2000. Confocal microscopy of FM4-64 as a tool for analysing endocytosis and vesicle trafficking in living fungal hyphae. *Journal of Microscopy,* 198**,** 246-259.

READ, N. D., FISCHER, S. & PARTON, R. M. 1998. Imaging spitzenkαrper, pH and calcium dynamics in growing fungal hyphae. *Pesticide Science,* 54**,** 179-181.

READ, N. D. & KALKMAN, E. R. 2003. Does endocytosis occur in fungal hyphae? *Fungal Genetics and Biology,* 39**,** 199-203.

REGENFELDER, E., SPELLIG, T., HARTMANN, A., LAUENSTEIN, S., BÖLKER, M. & KAHMANN, R. 1997. G proteins in *Ustilago maydis*: transmission of multiple signals? *The EMBO Journal,* 16**,** 1934-1942.

REYMANN, A. C., BOUJEMAA-PATERSKI, R., MARTIEL, J. L., GUERIN, C., CAO, W., CHIN, H. F., DE LA CRUZ, E. M., THERY, M. & BLANCHOIN, L. 2012. Actin network architecture can determine myosin motor activity. *Science,* 336**,** 1310-1314.

RIEDL, J., CREVENNA, A. H., KESSENBROCK, K., YU, J. H., NEUKIRCHEN, D., BISTA, M., BRADKE, F., JENNE, D., HOLAK, T. A. & WERB, Z. 2008. Lifeact: a versatile marker to visualize F-actin. *Nature Methods,* 5**,** 605-607.

ROBERTSON, A., SMYTHE, E. & AYSCOUGH, K. 2009a. Functions of actin in endocytosis. *Cellular and Molecular Life Sciences,* 66**,** 2049-2065.

ROBERTSON, A. S., SMYTHE, E. & AYSCOUGH, K. R. 2009b. Functions of actin in endocytosis. *Cellular and Molecular Life Sciences,* 66**,** 2049-2065.

ROCA, M. G., KUO, H. C., LICHIUS, A., FREITAG, M. & READ, N. D. 2010. Nuclear dynamics, mitosis, and the cytoskeleton during the early stages of colony initiation in *Neurospora crassa*. *Eukaryotic Cell,* 9**,** 1171-1183.

RODAL, A. A., KOZUBOWSKI, L., GOODE, B. L., DRUBIN, D. G. & HARTWIG, J. H. 2005. Actin and septin ultrastructures at the budding yeast cell cortex. *Molecular Biology of the Cell,* 16**,** 372-384.

RODMAN, J. S., MERCER, R. W. & STAHL, P. D. 1990. Endocytosis and transcytosis. *Current Opinion in Cell Biology,* 2**,** 664-672.

RODRIGUEZ, O. C. & CHENEY, R. E. 2002. Human myosin-Vc is a novel class V myosin expressed in epithelial cells. *Journal of Cell Science,* 115**,** 991-1004.

ROSENBLUTH, J. & WISSIG, S. L. 1964. The distrubution of exogenus ferritin in toad spinal ganglia and the mechanism of its uptake by neurons *The Journal of Cell Biology,* 23**,** 307-325.

ROSSANESE, O. W., REINKE, C. A., BEVIS, B. J., HAMMOND, A. T., SEARS, I. B., O'CONNOR, J. & GLICK, B. S. 2001. A role for actin, Cdc1p, and Myo2p in the inheritance of late golgi elements in *Saccharomyces cerevisiae*. *The Journal of Cell Biology,* 153**,** 47-62.

ROTH, A. F. & DAVIS, N. G. 1996. Ubiquitination of the yeast a-factor receptor. *The Journal of Cell Biology,* 134**,** 661-674.

ROTH, A. F. & DAVIS, N. G. 2000. Ubiquitination of the PEST-like endocytosis signal of the yeast a-factor receptor. *Journal of Biological Chemistry,* 275**,** 8143-8153.

ROTH, A. F., SULLIVAN, D. M. & DAVIS, N. G. 1998. A large PEST-like sequence directs the ubiquitination, endocytosis, and vacuolar degradation of the yeast a-factor receptor. *The Journal of Cell Biology,* 142**,** 949-961.

ROTH, T. F. & PORTER, K. R. 1964. Yolk protein uptake in the oocyte of the mosquito *aedes aegypti*. *The Journal of Cell Biology,* 20**,** 313-332.

ROTHMAN, J. E. & WARREN, G. 1994. Implications of the SNARE hypothesis for intracellular membrane topology and dynamics. *Current Biology,* 4**,** 220-233.

SAKAGAMI, Y., YOSHIDA, M., ISOGAI, A. & SUZUKI, A. 1981. Peptidal sex hormones Inducing conjugation tube formation in compatible mating-type cells of *Tremella mesenterica*. *Science,* 212**,** 1525-1527.

SAMBROOK, J., FRITSCH, E. F. & MANIATIS, T. 1989. *Molecular cloning*, Cold spring harbor laboratory press New York.

SATO, M., SATO, K., FONAREV, P., HUANG, C. J., LIOU, W. & GRANT, B. D. 2005. *Caenorhabditis elegans* RME-6 is a novel regulator of RAB-5 at the clathrin-coated pit. *Nature Cell Biology,* 7**,** 559-569.

SATTERWHITE, L. L. & POLLARD, T. D. 1992. Cytokinesis. *Current Opinion in Cell Biology,* 4**,** 43-52.

SCHANDEL, K. A. & JENNESS, D. D. 1994. Direct evidence for ligand-induced internalization of the yeast alpha-factor pheromone receptor. *Molecular Biology of the cell,* 14**,** 7245-7255.

SCHIEF, W. R. & HOWARD, J. 2001. Conformational changes during kinesin motility. *Current Opinion in Cell Biology,* 13**,** 19-28.

SCHLOSSMAN, D. M., SCHMID, S. L., BRAELL, W. A. & ROTHMAN, J. E. 1984. An enzyme that removes clathrin coats: purification of an uncoating ATPase. *The Journal of Cell Biology,* 99**,** 723-733.

SCHOLEY, J. M., HEUSER, J., YANG, J. T. & GOLDSTEIN, L. S. 1989. Identification of globular mechanochemical heads of kinesin. *Nature,* 338**,** 355-357.

SCHOTT, D. H., COLLINS, R. N. & BRETSCHER, A. 2002. Secretory vesicle transport velocity in living cells depends on the myosin-V lever arm length. *The Journal of Cell Biology,* 156**,** 35-40.

SCHRICK, K., GARVIK, B. & HARTWELL, L. H. 1997. Mating in *Saccharomyces cerevisiae*: the role of the pheromone signal transduction pathway in the chemotropic response to pheromone. *Genetics,* 147**,** 19-32.

SCHUCHARDT, I., ASSMAN, D., THINES, E., SCHUBERTH, C. & STEINBERG, G. 2005. Myosin-V, kinesin-1, and kinesin-3 cooperate in hyphal growth of the fungus *Ustilago maydis*. *Molecular Biology of the Cell,* 16**,** 5191-5201.

SCHUSTER, M., KILARU, S., ASHWIN, P., LIN, C., SEVERS, N. J. & STEINBERG, G. 2011a. Controlled and stochastic retention concentrates dynein at microtubule ends to keep endosomes on track. *The EMBO Journal,* 30**,** 652-664.

SCHUSTER, M., KILARU, S., FINK, G., COLLEMARE, J., ROGER, Y. & STEINBERG, G. 2011b. Kinesin-3 and dynein cooperate in long-range retrograde endosome motility along a nonuniform microtubule array. *Molecular Biology of the Cell,* 22**,** 3645-3657.

SCHUSTER, M., TREITSCHKE, S., KILARU, S., MOLLOY, J., HARMER, N. J. & STEINBERG, G. 2011c. Myosin-5, kinesin-1 and myosin-17 cooperate in secretion of fungal chitin synthase. *The EMBO Journal,* 31**,** 214-227.

SCOTT, M. 2000. Development: The Natural History of Genes Review. *Cell,* 100**,** 27-40.

SEABRA, M. C. & COUDRIER, E. 2004. Rab GTPases and myosin motors in organelle motility. *Traffic,* 5**,** 393-399.

SEILER, S., KIRCHNER, J., HORN, C., KALLIPOLITOU, A., WOEHLKE, G. & SCHLIWA, M. 2000. Cargo binding and regulatory sites in the tail of fungal conventional kinesin. *Nature Cell Biology,* 2**,** 333-338.

SEKIYA-KAWASAKI, M., GROEN, A. C., COPE, M. J. T. V., KAKSONEN, M., WATSON, H. A., ZHANG, C., SHOKAT, K. M., WENDLAND, B., MCDONALD, K. L., MCCAFFERY, J. M. & DRUBIN, D. G. 2003. Dynamic phosphoregulation of the cortical actin cytoskeleton and endocytic machinery revealed by real-time chemical genetic analysis. *The Journal of Cell Biology,* 162**,** 765-772.

SHAW, J. D., CUMMINGS, K. B., HUYER, G., MICHAELIS, S. & WENDLAND, B. 2001. Yeast as a model system for studying endocytosis. *Experimental Cell Research,* 271**,** 1-9.

SHEEMAN, B., CARVALHO, P., SAGOT, I., GEISER, J., KHO, D., HOYT, M. A. & PELLMAN, D. 2003. Determinants of *Saccharomyces cerevisiae* dynein localization and activation: implications for the mechanism of spindle positioning. *Current Biology,* 13**,** 364-372.

SHEFF, D. R., DARO, E. A., HULL, M. & MELLMAN, I. 1999. The receptor recycling pathway contains two distinct populations of early endosomes with different sorting functions. *The Journal of Cell Biology,* 145**,** 123-139.

SHERRILL, C., KHOURI, O., ZEMAN, S. & ROISE, D. 1995. Synthesis and biological activity of fluorescent yeast pheromones. *Biochemistry,* 34**,** 3553-3560.

SINGER, B. & RIEZMAN, H. 1990. Detection of an intermediate compartment involved in transport of alpha-factor from the plasma membrane to the vacuole in yeast. *The Journal of Cell Biology,* 110**,** 1911-22.

SINGER-KRÜGER, B., STENMARK, H., DÜSTERHÖFT, A., PHILIPPSEN, P., YOO, J. S., GALLWITZ, D. & ZERIAL, M. 1994. Role of three rab5-like GTPases, Ypt51p, Ypt52p, and Ypt53p, in the endocytic and vacuolar protein sorting pathways of yeast. *The Journal of Cell Biology,* 125**,** 283-298.

SNETSELAAR, K. M., BÖLKER, M. & KAHMANN, R. 1996. Ustilago maydis mating hyphae orient their growth toward pheromone sources. *Fungal Genetics and Biology,* 20**,** 299-312.

SNETSELAAR, K. M. & MIMS, C. W. 1992. Sporidial fusion and infection of maize seedlings by the smut fungus *Ustilago maydis*. *Mycologia,* 84**,** 193-203.

SNETSELASSR, M., K., MIMS & W., C. 1993. *Infection of maize stigmas by Ustilago maydis : light and electron microscopy,* St. Paul, MN, ETATS-UNIS, American Phytopathological Society.

SOLDATI, T. & SCHLIWA, M. 2006. Powering membrane traffic in endocytosis and recycling. *Nature Reviews Molecular Cell Biology,* 7**,** 897-908.

SOPPINA, V., RAI, A. K., RAMAIYA, A. J., BARAK, P. & MALLIK, R. 2009. Tug-of-war between dissimilar teams of microtubule motors regulates transport and fission of endosomes. *Proceedings of the National Academy of Sciences of the United States of America,* 106**,** 19381-19386.

SPELLIG, T., BÖLKER, M., LOTTSPEICH, F., FRANK, R. W. & KAHMANN, R. 1994. Pheromones trigger filamentous growth in *Ustilago maydis*. *The EMBO Journal,* 13**,** 1620-1627.

STEARNS, T., HOYT, M. A. & BOTSTEIN, D. 1990. Yeast mutants sensitive to antimicrotubule drugs define three genes that affect microtubule function. *Genetics,* 124**,** 251-262.

STEDEN, M., BETZ, R. & DUNTZE, W. 1989. Isolation and characterization of *Saccharomyces cerevisiae* mutants supersensitive to G1 arrest by the mating hormone a-factor. *Molecular Gene Genetics,* 219**,** 439-444.

STEFAN, C. J., PADILLA, S. M., AUDHYA, A. & EMR, S. D. 2005. The phosphoinositide phosphatase Sjl2 Is recruited to cortical actin patches in the control of vesicle formation and fission during endocytosis. *Molecular and Cellular Biology,* 25**,** 2910-2923.

STEINBERG, G. 1997. A kinesin-like mechanoenzyme from the zygomycete *Syncephalastrum racemosum* shares biochemical similarities with conventional kinesin from *Neurospora crassa*. *European Journal of Cell Biology,* 73**,** 124-131.

STEINBERG, G. 2007a. Hyphal growth: a tale of motors, lipids, and the spitzenkorper. *Eukaryotic Cell,* 6**,** 351-360.

STEINBERG, G. 2007b. On the move: endosomes in fungal growth and pathogenicity. *Nature Reviews Microbiology,* 5**,** 309-316.

STEINBERG, G. 2007c. Tracks for traffic: microtubules in the plant pathogen *Ustilago maydis*. *New Phytologist,* 174**,** 721-733.

STEINBERG, G. 2011. Motors in fungal morphogenesis: cooperation versus competition. *Current Opinion in Microbiology,* 14**,** 660-667.

STEINBERG, G. & PEREZ-MARTIN, J. 2008. *Ustilago maydis*, a new fungal model system for cell biology. *Trends in Cell Biology,* 18**,** 61-67.

STEINBERG, G. & SCHLIWA, M. 1996. Characterization of the biophysical and motility properties of kinesin from the fungus *Neurospora crassa*. *Journal of Biological Chemistry,* 271**,** 7516-7521.

STEINBERG, G., SCHLIWA, M., LEHMLER, C., BOLKER, M., KAHMANN, R. & MCINTOSH, J. R. 1998. Kinesin from the plant pathogenic fungus *Ustilago maydis* is involved in vacuole formation and cytoplasmic migration. *Journal of Cell Science,* 111 (Pt 15)**,** 2235-2246.

STEINBERG, G. & SCHUSTER, M. 2011. The dynamic fungal cell. *Fungal Biology Reviews,* 25**,** 14-37.

STEINBERG, G., WEDLICH-SÖLDNER, R., BRILL, M. & SCHULZ, I. 2001. Microtubules in the fungal pathogen *Ustilago maydis* are highly dynamic and determine cell polarity. *Journal of Cell Science,* 114**,** 609-622.

STRAUBE, A., BRILL, M., OAKLEY, B. R., HORIO, T. & STEINBERG, G. 2003. Microtubule organization requires cell cycle-dependent nucleation at dispersed cytoplasmic sites: polar and perinuclear microtubule organizing centers in the plant pathogen *Ustilago maydis*. *Molecular Biology of the Cell,* 14**,** 642-657.

STRAUBE, A., ENARD, W., BERNER, A., WEDLICH-SOLDNER, R., KAHMANN, R. & STEINBERG, G. 2001. A split motor domain in a cytoplasmic dynein. *The EMBO Journal,* 20**,** 5091-5100.

SUEI, S. & GARRILL, A. 2008. An F-actin-depleted zone is present at the hyphal tip of invasive hyphae of *Neurospora crassa*. *Protoplasma,* 232**,** 165-172.

SUELMANN, R. & FISCHER, R. 2000. Mitochondrial movement and morphology depend on an intact actin cytoskeleton in *Aspergillus nidulans*. *Cell Motility and the Cytoskeleton,* 45**,** 42-50.

SUN, Y., KAKSONEN, M., MADDEN, D. T., SCHEKMAN, R. & DRUBIN, D. G. 2005. Interaction of Sla2p's ANTH domain with PtdIns(4,5)P2 Is important for actin-dependent endocytic internalization. *Molecular Biology of the Cell,* 16**,** 717-730.

SUN, Y., MARTIN, A. C. & DRUBIN, D. G. 2006. Endocytic internalization in budding yeast requires coordinated actin nucleation and myosin motor activity. *Developmental Cell,* 11**,** 33-46.

SZABO, Z., TÖNNIS, M., KESSLER, H. & FELDBRÜGGE, M. 2002. Structure-function analysis of lipopeptide pheromones from the plant pathogen *Ustilago maydis*. *Molecular Genetics and Genomics,* 268**,** 362-370.

TAHERI-TALESH, N., HORIO, T., ARAUJO-BAZÁN, L., DOU, X., ESPESO, E. A., PEÑALVA, M. A., OSMANI, S. A. & OAKLEY, B. R. 2008. The tip growth apparatus of *Aspergillus nidulans*. *Molecular Biology of the Cell,* 19**,** 1439-1449.

TAHERI-TALESH, N., XIONG, Y. & OAKLEY, B. R. 2012. The functions of myosin II and myosin V homologs in tip growth and septation in *Aspergillus nidulans*. *PLoS One,* 7**,** 1-14.

TAYLOR, M. J., PERRAIS, D. & MERRIFIELD, C. J. 2011. A high precision survey of the molecular dynamics of mammalian clathrin-mediated endocytosis. *PLoS Biology,* 9.

THOMSEN, K. 2014. *Surface area of ellipsoid* [Online]. www.webformulas.com. Available: http://www.web-formulas.com/Math_Formulas/Geometry_Surface_of_Ellipsoid.aspx.

TOLLIDAY, N., VERPLANK, L. & LI, R. 2002. Rho1 directs formin-mediated actin ring assembly during budding yeast cytokinesis. *Current Biology,* 12**,** 1864-1870.

TORET, C. P. & DRUBIN, D. G. 2006. The budding yeast endocytic pathway. *Journal of Cell Science,* 119**,** 4585-4587.

TORRALBA, S. & HEATH, I. B. 2002. Analysis of three separate probes suggests the absence of endocytosis in *Neurospora crassa* hyphae. *Fungal Genetics and Biology,* 37**,** 221-232.

TORRALBA, S., RAUDASKOSKI, M., PEDREGOSA, A. M. & LABORDA, F. 1998a. Effect of cytochalasin A on apical growth, actin cytoskeleton organization and enzyme secretion in *Aspergillus nidulans*. *Microbiology,* 144 (Pt 1)**,** 45-53.

TORRALBA, S., RAUDASKOSKI, M., PEDREGOSA, A. M. & LABORDA, F. 1998b. Effect of cytochalasin A on apical growth, actin cytoskeleton organization and enzyme secretion in *Aspergillus nidulans*. *Microbiology,* 144**,** 45-53.

TOSHIMA, J. Y., TOSHIMA, J., KAKSONEN, M., MARTIN, A. C., KING, D. S. & DRUBIN, D. G. 2006a. Spatial dynamics of receptor-mediated endocytic trafficking in budding yeast revealed by using fluorescent α factor derivatives. *Proceedings of the National Academy of Sciences of the United States of America,* 103**,** 5793-5798.

TOSHIMA, J. Y., TOSHIMA, J., KAKSONEN, M., MARTIN, A. C., KING, D. S. & DRUBIN, D. G. 2006b. Spatial dynamics of receptor-mediated endocytic trafficking in budding yeast revealed by using fluorescent α-factor derivatives. *Proceedings of the National Academy of Sciences,* 103**,** 5793-5798.

TRAER, C. J., RUTHERFORD, A. C., PALMER, K. J., WASSMER, T., OAKLEY, J., ATTAR, N., CARLTON, J. G., KREMERSKOTHEN, J., STEPHENS, D. J. & CULLEN, P. J. 2007. SNX4 coordinates endosomal sorting of TfnR with dynein-mediated transport into the endocytic recycling compartment. *Nature Cell Biology,* 9**,** 1370-1380.

TRAUB, L. M. 2009. Tickets to ride: selecting cargo for clathrin-regulated internalization. *Nature Reviews Molecular Cell Biology,* 10**,** 583-596.

TROWBRIDGE, I. S., COLLAWN, J. F. & HOPKINS, C. R. 1993. Signal-dependent membrane protein trafficking in the endocytic pathway. *Annual Review of Cell Biology,* 9**,** 129-161.

TSAI, J. W., BREMNER, K. H. & VALLEE, R. B. 2007. Dual subcellular roles for LIS1 and dynein in radial neuronal migration in live brain tissue. *Nature Neuroscience,* 10**,** 970-979.

TSUJIKAWA, M., OMORI, Y., BIYANWILA, J. & MALICKI, J. 2007. Mechanism of positioning the cell nucleus in vertebrate photoreceptors. *Proceedings of the National Academy of Sciences of the United States of America,* 104**,** 14819-14824.

TYNAN, S. H., GEE, M. A. & VALLEE, R. B. 2000. Distinct but overlapping sites within the cytoplasmic dynein heavy chain for dimerization and for intermediate chain and light intermediate chain binding. *Journal of Biological Chemistry,* 275**,** 32769-32774.

UEDA, H., YOKOTA, E., KUTSUNA, N., SHIMADA, T., TAMURA, K., SHIMMEN, T., HASEZAWA, S., DOLJA, V. V. & HARA-NISHIMURA, I. 2010. Myosin-dependent endoplasmic reticulum motility and F-actin

organization in plant cells. *Proceedings of the National Academy of Sciences of the United States of America,* 107**,** 6894-6899.

UNGEWICKELL, E. & BRANTON, D. 1981. Assembly units of clathrin coats. *Nature,* 289**,** 420-422.

UPADHYAY, S. & SHAW, B. D. 2008. The role of actin, fimbrin and endocytosis in growth of hyphae in *Aspergillus nidulans*. *Molecular Microbiology,* 68**,** 690-705.

URBAN, M., KAHMANN, R. & BÖLKER, M. 1996a. The biallelica mating type locus of *Ustilago maydis*: remnants of an additional pheromone gene indicate evolution from a multiallelic ancestor. *Molecular and General Genetics MGG,* 250**,** 414-420.

URBAN, M., KAHMANN, R. & BÖLKER, M. 1996b. Identification of the pheromone response element in *Ustilago maydis*. *Molecular and General Genetics MGG,* 251**,** 31-37.

VALE, R. D. 2003. The molecular motor toolbox for intracellular transport. *Cell,* 112**,** 467-480.

VALE, R. D., REESE, T. S. & SHEETZ, M. P. 1985. Identification of a novel force-generating protein, kinesin, involved in microtubule-based motility. *Cell,* 42**,** 39-50.

VALLEE, R. B., WILLIAMS, J. C., VARMA, D. & BARNHART, L. E. 2004. Dynein: An ancient motor protein involved in multiple modes of transport. *Journal of Neurobiology,* 58**,** 189-200.

VAN DER SLUIJS, P., HULL, M., WEBSTER, P., MÂLE, P., GOUD, B. & MELLMAN, I. 1992. The small GTP-binding protein rab4 controls an early sorting event on the endocytic pathway. *Cell,* 70**,** 729-740.

VAN DER SLUIJS, P., HULL, M., ZAHRAOUI, A., TAVITIAN, A., GOUD, B. & MELLMAN, I. 1991. The small GTP-binding protein rab4 is associated with early endosomes. *Proceedings of the National Academy of Sciences of the United States of America,* 88**,** 6313-6317.

VAVYLONIS, D., WU, J. Q., HAO, S., O'SHAUGHNESSY, B. & POLLARD, T. D. 2008. Assembly mechanism of the contractile ring for cytokinesis by fission yeast. *Science,* 319**,** 97-100.

VICENTE-MANZANARES, M., MA, X., ADELSTEIN, R. S. & HORWITZ, A. R. 2009. Non-muscle myosin II takes centre stage in cell adhesion and migration. *Nature Reviews Molecular Cell Biology,* 10**,** 778-790.

VIDA, T. A. & EMR, S. D. 1995. A new vital stain for visualizing vacuolar membrane dynamics and endocytosis in yeast. *The Journal of Cell Biology,* 128**,** 779-792.

VIDALI, L., MCKENNA, S. T. & HEPLER, P. K. 2001. Actin polymerization is essential for pollen tube growth. *Molecular Biology of the Cell,* 12**,** 2534-2545.

VIDALI, L., ROUNDS, C. M., HEPLER, P. K. & BEZANILLA, M. 2009. Lifeact-mEGFP reveals a dynamic apical F-actin network in tip growing plant cells. *PLoS One,* 4.

WAGNER, W. & HAMMER, J. A., 3RD 2003. Myosin V and the endoplasmic reticulum: the connection grows. *The Journal of Cell Biology,* 163**,** 1193-1196.

WAHL, R., ZAHIRI, A. & KAMPER, J. 2010. The Ustilago maydis b mating type locus controls hyphal proliferation and expression of secreted virulence factors in planta. *Molecular Microbiology,* 75**,** 208-20.

WARNOCK, D. E., HINSHAW, J. E. & SCHMID, S. L. 1996. Dynamin self-assembly stimulates its GTPase activity. *Journal of Biological Chemistry,* 271**,** 22310-22314.

WARRICK, H. M. & SPUDICH, J. A. 1987. Myosin structure and function in cell motility. *Annual Review of Cell Biology,* 3**,** 379-421.

WEBER, I., GRUBER, C. & STEINBERG, G. 2003. A class-V myosin required for mating, hyphal growth, and pathogenicity in the dimorphic plant pathogen *Ustilago maydis*. *The Plant Cell Online,* 15**,** 2826-2842.

WEDLICH-SÖLDNER, R., BÖLKER, M., KAHMANN, R. & STEINBERG, G. 2000. A putative endosomal t-SNARE links exo-and endocytosis in the phytopathogenic fungus *Ustilago maydis*. *The EMBO Journal,* 19**,** 1974-1986.

WEDLICH-SÖLDNER, R., SCHULZ, I., STRAUBE, A. & STEINBERG, G. 2002a. Dynein supports motility of endoplasmic reticulum in the fungus *Ustilago maydis*. *Molecular Biology of the Cell,* 13**,** 965-977.

WEDLICH-SÖLDNER, R., STRAUBE, A., FRIEDRICH, M. W. & STEINBERG, G. 2002b. A balance of KIF1A-like kinesin and dynein organizes early endosomes in the fungus *Ustilago maydis*. *The EMBO Journal,* 21**,** 2946-2957.

WEINBERG, J. & DRUBIN, D. G. 2012. Clathrin-mediated endocytosis in budding yeast. *Trends in Cell Biology,* 22**,** 1-13.

WELLS, A. L., LIN, A. W., CHEN, L. Q., SAFER, D., CAIN, S. M., HASSON, T., CARRAGHER, B. O., MILLIGAN, R. A. & SWEENEY, H. L. 1999. Myosin VI is an actin-based motor that moves backwards. *Nature,* 401**,** 505-508.

WELTE, M. A. 2004. Bidirectional transport along microtubules. *Current Biology,* 14**,** 525-537.

WENDLAND, J., VAILLANCOURT, L. J., HEGNER, J., LENGELER, K. B., LADDISON, K. J., SPECHT, C. A., RAPER, C. A. & KOTHE, E. 1995. The mating-type locus B alpha 1 of *Schizophyllum commune* contains a pheromone receptor gene and putative pheromone genes. *The EMBO Journal,* 14**,** 5271-5278.

WESP, A., HICKE, L., PALECEK, J., LOMBARDI, R., AUST, T., MUNN, A. L. & RIEZMAN, H. 1997. End4p/Sla2p interacts with actin-associated proteins for endocytosis in *Saccharomyces cerevisiae*. *Molecular Biology of the Cell,* 8**,** 2291-2306.

WESSELS, J. 1986. Cell wall synthesis in apical hyphal growth. *International Review of Cytology,* 104**,** 37-79.

WESSELS, J. H., MEINHARDT, F., DUNTZE, W., BETZ, R. & NIENTIEDT, M. 1994. Pheromones in Yeasts. *Growth, Differentiation and Sexuality.* Springer Berlin Heidelberg.

WIEDERKEHR, A., AVARO, S., PRESCIANOTTO-BASCHONG, C., HAGUENAUER-TSAPIS, R. & RIEZMAN, H. 2000. The F-Box Protein Rcy1p Is Involved in Endocytic Membrane Traffic and Recycling Out of an Early Endosome in Saccharomyces cerevisiae. *The Journal of Cell Biology,* 149**,** 397-410.

WILCKE, M., JOHANNES, L., GALLI, T., MAYAU, V., GOUD, B. & SALAMERO, J. 2000. Rab11 regulates the compartmentalization of

early endosomes required for efficient transport from early endosomes to the trans-golgi network. *The Journal of Cell Biology,* 151**,** 1207-1220.

WIN, T. Z., GACHET, Y., MULVIHILL, D. P., MAY, K. M. & HYAMS, J. S. 2001. Two type V myosins with non-overlapping functions in the fission yeast *Schizosaccharomyces pombe*: Myo52 is concerned with growth polarity and cytokinesis, Myo51 is a component of the cytokinetic actin ring. *Journal of Cell Science,* 114**,** 69-79.

WOLFF, M. E. 1996. Burger's Medicinal Chemistry and Drug Discovery. *American Journal of Therapeutics,* 3.

WOLLERT, T., WEISS, D. G., GERDES, H. H. & KUZNETSOV, S. A. 2002. Activation of myosin V-based motility and F-actin-dependent network formation of endoplasmic reticulum during mitosis. *The Journal of Cell Biology,* 159**,** 571-577.

WOO, M., LEE, K. & SONG, K. 2003. *MYO2* is not essential for viability, but is required for polarized growth and dimorphic switches in *Candida albicans*. *FEMS Microbiology Letters,* 218**,** 195-202.

WOOLNER, S. & BEMENT, W. M. 2009. Unconventional myosins acting unconventionally. *Trends in Cell Biology,* 19**,** 245-252.

WOZNIAK, M. J. & ALLAN, V. J. 2006. Cargo selection by specific kinesin light chain 1 isoforms. *The EMBO Journal,* 25**,** 5457-5468.

WOZNIAK, M. J., BOLA, B., BROWNHILL, K., YANG, Y. C., LEVAKOVA, V. & ALLAN, V. J. 2009. Role of kinesin-1 and cytoplasmic dynein in endoplasmic reticulum movement in VERO cells. *Journal of Cell Science,* 122**,** 1979-1989.

WU, J. Q. & POLLARD, T. D. 2005. Counting cytokinesis proteins globally and locally in fission yeast. *Science,* 310**,** 310-314.

WU, X., BOWERS, B., RAO, K., WEI, Q. & HAMMER, J. A., 3RD 1998. Visualization of melanosome dynamics within wild-type and dilute melanocytes suggests a paradigm for myosin V function *In vivo*. *The Journal of Cell Biology,* 143**,** 1899-1918.

WU, X., BOWERS, B., WEI, Q., KOCHER, B. & HAMMER, J. A., 3RD 1997. Myosin V associates with melanosomes in mouse melanocytes: evidence that myosin V is an organelle motor. *Journal of Cell Science,* 110 (Pt 7)**,** 847-859.

WU, X., JUNG, G. & HAMMER JR, J. 2000. Functions of unconventional myosins. *Current Opinion in Cell Biology,* 12**,** 42-51.

WU, X., XIANG, X. & HAMMER, J. A., 3RD 2006. Motor proteins at the microtubule plus-end. *Trends in Cell Biology,* 16**,** 135-143.

XIANG, X., BECKWITH, S. M. & MORRIS, N. R. 1994. Cytoplasmic dynein is involved in nuclear migration in *Aspergillus nidulans*. *Proceedings of the National Academy of Sciences of the United States of America,* 91**,** 2100-2104.

XIANG, X. & PLAMANN, M. 2003. Cytoskeleton and motor proteins in filamentous fungi. *Current Opinion in Microbiology,* 6**,** 628-633.

XIE, J., QIAN, L., WANG, Y., ROSE, C. M., YANG, T., NAKAMURA, T., HAMM-ALVAREZ, S. F. & MIRCHEFF, A. K. 2004. Novel biphasic traffic of endocytosed EGF to recycling and degradative compartments in lacrimal gland acinar cells. *Journal of Cell Physiology,* 199**,** 108-125.

YAMASHIRO, D. J., TYCKO, B., FLUSS, S. R. & MAXFIELD, F. R. 1984. Segregation of transferrin to a mildly acidic (pH 6.5) para-golgi compartment in the recycling pathway. *Cell,* 37**,** 789-800.

YAMASHITA, R. A., OSHEROV, N. & MAY, G. S. 2000. Localization of wild type and mutant class I myosin proteins in *Aspergillus nidulans* using GFP-fusion proteins. *Cell Motility and the Cytoskeleton,* 45**,** 163-172.

YANG, H.-C. & PON, L. A. 2002. Actin cable dynamics in budding yeast. *Proceedings of the National Academy of Sciences of the United States of America,* 99**,** 751-756.

YASUSHI, M. 2003. Polarized distribution of intracellular components by class V myosins in *Saccharomyces cerevisiae*. *International Review of Cytology.* Academic Press.

YOKOYAMA, K., KAJI, H., NISHIMURA, K. & MIYAJI, M. 1990. The role of microfilaments and microtubules in apical growth and dimorphism of *Candida albicans*. *Journal of Genetic Microbiology,* 136**,** 1067-1075.

YONEKAWA, Y., HARADA, A., OKADA, Y., FUNAKOSHI, T., KANAI, Y., TAKEI, Y., TERADA, S., NODA, T. & HIROKAWA, N. 1998. Defect in synaptic vesicle precursor transport and neuronal cell death in KIF1A motor protein-deficient mice. *The Journal of Cell Biology,* 141**,** 431-441.

YOUN, J.-Y., FRIESEN, H., KISHIMOTO, T., HENNE, W. M., KURAT, C. F., YE, W., CECCARELLI, D. F., SICHERI, F., KOHLWEIN, S. D., MCMAHON, H. T. & ANDREWS, B. J. 2010. Dissecting BAR domain function in the yeast amphiphysins Rvs161 and Rvs167 during endocytosis. *Molecular Biology of the Cell,* 21**,** 3054-3069.

ZENG, G., YU, X. & CAI, M. 2001. Regulation of yeast actin cytoskeleton-regulatory complex Pan1p/Sla1p/End3p by serine/threonine kinase Prk1p. *Molecular Biology of the Cell,* 12**,** 3759-3772.

ZHANG, J., LI, S., FISCHER, R. & XIANG, X. 2003. Accumulation of cytoplasmic dynein and dynactin at microtubule plus ends in *Aspergillus nidulans* is kinesin dependent. *Molecular Biology of the Cell,* 14**,** 1479-1488.

ZHANG, J., TAN, K., WU, X., CHEN, G., SUN, J., RECK-PETERSON, S. L., HAMMER, J. A., 3RD & XIANG, X. 2011. Aspergillus myosin-V supports polarized growth in the absence of microtubule-based transport. *PLoS One,* 6.

ZHANG, J., ZHUANG, L., LEE, Y., ABENZA, J. F., PENALVA, M. A. & XIANG, X. 2010. The microtubule plus-end localization of Aspergillus dynein is important for dynein-early-endosome interaction but not for dynein ATPase activation. *Journal of Cell Science,* 123**,** 3596-3604.